Welding Research

SPONSORED BY THE WELDING RESEARCH COUNCIL
OF THE ENGINEERING FOUNDATION

W. SPRAGEN, DIRECTOR

SUPPLEMENT TO THE WELDING JOURNAL, JUNE, 1956

ELECTRICAL AND METALLURGICAL CHARACTERISTICS OF MASH SEAM WELDS

Relationship between mash seam welding variables and resultant characteristics of the weld has been determined through research investigation

BY E. J. FUNK AND M. L. BEGEMAN

Introduction

Mash seam welding produces a weld made in a lap joint, the joint thickness of which is plastically reduced to a considerable extent during the welding operation. The joint is made with a slight overlapping of the metal sheets and welded with circular electrodes, equal mash down occurring in both sheets. The faces of the electrodes are flat and of sufficient width to completely cover the overlap. Since the overlap is only about 1 $^1/_2$ times the stock thickness, preweld tacking, or otherwise rigidly clamping the sheets, is necessary in order to maintain exact overlap during the weld. Good quality welds, having a weld thickness only slightly more than the sheet thickness, can be made by this procedure. In many instances these joints are suitable for industrial application without further finishing.

The three types of seam welds commonly used in industry are illustrated in Fig. 1. The most common type is the simple lap seam weld shown in the upper part of the figure. This weld consists of a series of overlapping spot welds with sufficient overlap of the weld nuggets to provide a pressure tight joint. If the pressure tight quality of the lap seam weld is not required, the individual nuggets may be spaced so as to give a stitch effect. This process is known as roll-spot welding. In the center of the figure, a mash seam weld is shown which is produced by reducing the amount of sheet lapping to a small value. Broad-faced flat electrodes are used which forge the sheets together while welding. This forging action by the electrodes is known as "mash-down" and occurs simultaneously with the fusing of the sheets. Since the joint is covered above and below by the electrodes and from either side by the sheets, any extrusion or spitting from the weld is prevented. Alterations can be made in electrode face contour and the amount of lap increased such that the mash-down takes place on only one side which can later be finished leaving no trace of the joint. This type of mash seam welding, shown in the lower part of the figure, is often referred to as metal finish seam welding and finds application where the product is normally viewed from one side only.

E. J. Funk is Graduate Student, RWMA Fellowship, and **M. L. Begeman** is Professor of Mechanical Engineering, University of Texas, Austin, Tex.

Paper presented at 1956 AWS National Spring Meeting in Buffalo, N. Y., May 7–11.

Welding Variables

The mash seam weld is a combination of two manufacturing processes. First, it is a hot-forming process because the sheets must be plastically deformed in order to reduce the thickening at the joint; and second, it is a welding process because heat and pressure are employed in order to produce coalescence of the two sheets. With this observation in mind, it is convenient to roughly classify the variables involved in mash seam welding into two major groups: (1) those associated with the forging of the sheets, and (2) those associated with the fusion of the sheets. It is difficult to make a suitable classification of the variables involved as they are all inter-related, but it is believed that this classification will be proved by the experimental results.

The forging variables are the factors which influence the final thickness and appearance of the joint. Among these factors, the amount of material that must be redistributed is of particular significance and it follows that the initial overlapping of the sheets determines this quantity. The second item which influences the forging action is the electrode force which is employed to effect a plastic redistribution of the metal in the joint.

Principally, the fusion variables influence the amount of heat employed in making the weld. All of the heat generated in an electrical-resistance welding process is the result of a current passing through the resistance of the welding circuit. The current magnitude obviously becomes one of the most signi-

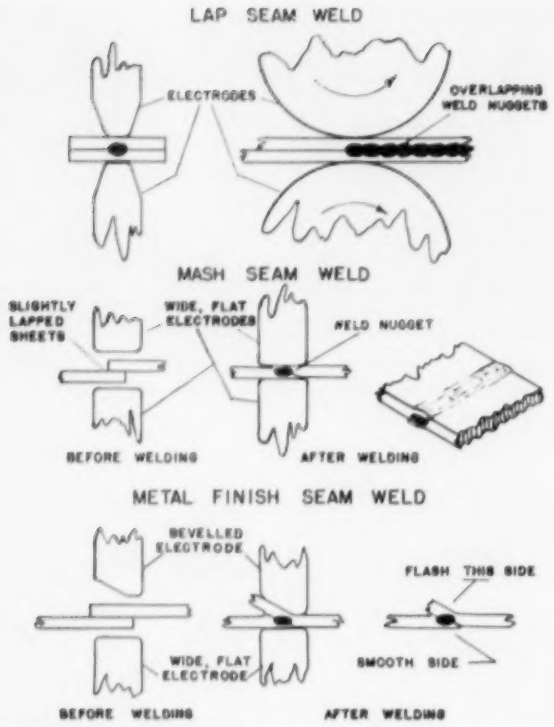

Fig. 1 Types of seam welds

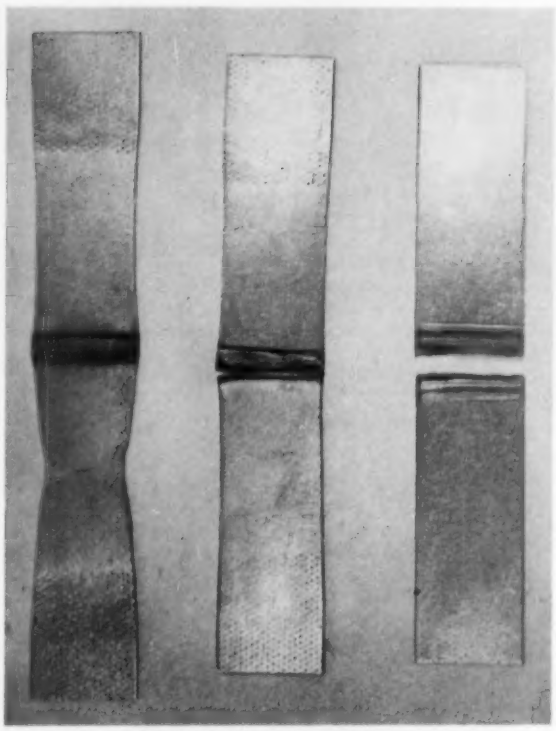

Fig. 2 Typical failures of tensile specimens

ficant factors in controlling the amount of heat generated in the weld. A second variable is the resistance of the welding circuit. There are three sources of resistance to be considered: first, the contact resistance between the electrodes and the surfaces of the materials being welded; second, the electrical resistance of the materials being welded, and third, the contact resistance at the interface of the weldments. The heat, due to resistance offered at the surface, is kept at a minimum by the use of copper-alloy electrodes and is dissipated by flooding the electrodes and weld area with water. The heat, resulting from the electrical resistance of the materials, is a constant depending on the material being welded and its thickness. The contact resistance offered at the interface of the weldments is not constant and its actual value depends mainly on the surface conditions and the intimacy with which the surfaces contact each other which is controlled by the electrode force. The third variable which influences the magnitude of the heat in the weld is time. Time in mash seam welding is controlled by the speed of rotation of the electrodes, and the amount of heat generated is decreased with an increase in welding speed.

Materials and Equipment

The material used in this investigation was low carbon, pickled and oiled, hot-rolled, rimmed steel commonly designated as SAE 1010. The three thicknesses used were of the following analysis:

Thickness, in.	*C*, %	*Mn*, %	*P*, %	*S*, %
0.031	0.08	0.39	0.008	0.029
0.050	0.07	0.41	0.012	0.037
0.078	0.08	0.39	0.010	0.034

All welding was performed on a 250-kva circular seam welder designed for operation on 440-v, single-phase, 60-cycle, alternating current and intended to be capable of handling a maximum short circuit secondary current of 40,600 amp at a secondary transformer potential of 7.85 v. The machine was equipped with a thyratron welding control which features two size C ignitron power tubes. During the first part of the investigation a knurl-drive system for rotating the electrodes was used because it allowed the use of the maximum face width of the electrodes. Friction drive was not used since it would have necessitated beveling the outer edges of the electrodes to accommodate the friction-drive rolls which would have resulted in an undesirable face width reduction. However, it was found that the knurl marks left in the surface of the electrode yielded an undesirable duplication of these marks on the weld to the extent that its usefulness was questionable if surface appearance was important. To eliminate this defect a roller chain drive to rotate the electrodes was installed on the machine. This proved satisfactory and allowed a speed variation of from 55 ipm to 300 ipm depending on the size of the pulley used on the drive motor. All electrodes were 10 in. in diam, $^1/_2$ in. thick and made from RWMA Class III forged copper alloy. Adjacent to the electrodes a specimen guide bar was provided to position and guide the specimens as they were being welded.

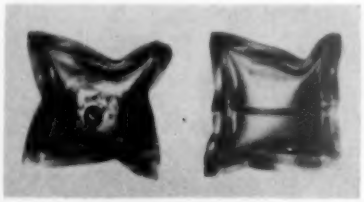

Fig. 3 Appearance of pillow specimens after failure

The amount of overlap used in making the mash weld was controlled by first accurately positioning the sheets to be welded and then tacking them with a light spot weld. A 75-kva spot welder with an appropriate fixture to position the specimen and gage the amount of overlap was used for this purpose.

The principal physical test used in the investigation was a simple tension test. The original weldments in all cases consisted of two sheets $2^3/_4$ x 15 in. in length and the tensile specimens were

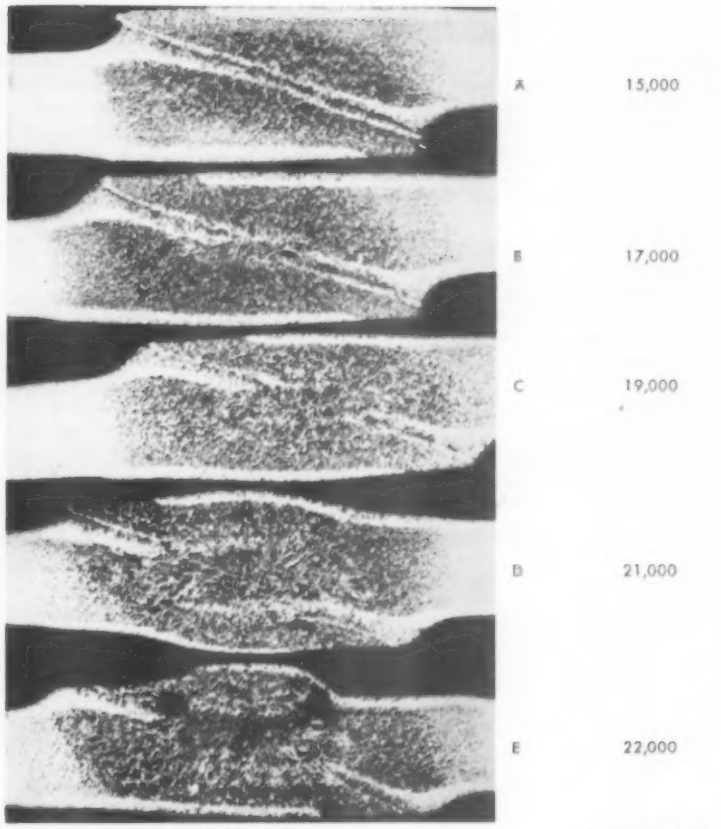

Fig. 4 Macrographs of mash seam welds made with 0.078-in. low-carbon steel at various current magnitudes. Electrode force 2500 lb, welding speed 55 ipm, and initial overlap 125%. Magnification X12 (Reduced by 25% upon reproduction)

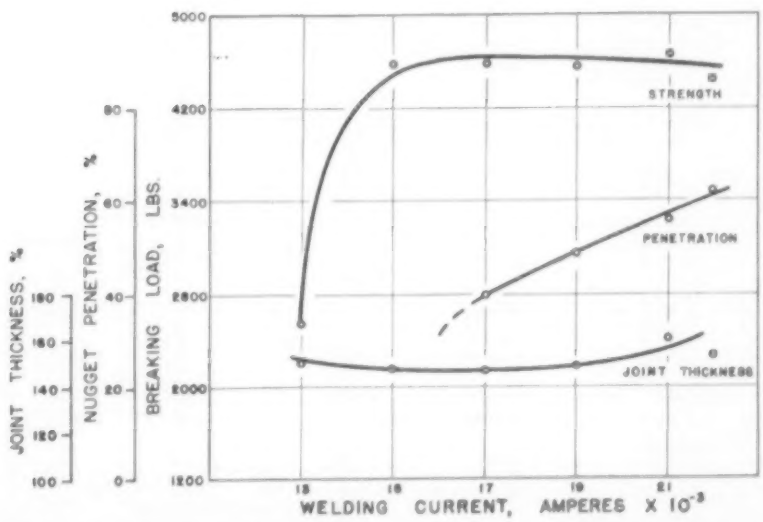

Fig. 5 Weld characteristics in 0.078-in. low-carbon steel as a function of current. Electrode force 2500 lb, welding speed 55 ipm, and an initial overlap of 125%

cut from the finished weld so as to give a strip 1 in. wide and approximately $5^1/_2$ in. long. Several specimens shown in Fig. 2 are intended to depict the various types of failure which were encountered. The specimen at the left side of the picture represents the most desirable type of failure and was the most common in occurrence. The type of failure shown at the right illustrates a very poor weld. Failures such as shown by the center specimen were seldom encountered—they appear to be caused by a stress concentration at one edge due to misalignment.

The other physical test used was the conventional hydrostatic pillow test in which a mash seam welded specimen was lap welded around the edges of a 6- x 6-in. sheet. The weldment was subjected to hydrostatic pressure until failure appeared, after which it had the appearance shown in Fig. 3. The most common type of failure occurred at an inside edge of the lap seam weld in the vicinity of the corners where the stresses due to bending were greatest—only occasionally would a mash seam weld open up. Failures at the inside edge showed some correlation with the tensile tests in which the weld withstood the load and rupture occurred either above or below the weld. Other than indicating that the joint was leak tight, the pillow test was of little use. Tensile tests were much simpler to conduct and proved to be a better test of weld quality.

Procedure

All specimens were wire brushed and wiped down with cleaning solvent prior to tack welding. This was done in order to hold the contact resistance at as constant a value as possible. After surface treatment, the specimens were tack welded so as to retain the proper amount of overlap while being mash welded.

Before an organized procedure of investigation could be embarked upon, a number of welds were made without taking data and by varying the machine settings over a wide range until, in the judgment of the operator, the process appeared to produce good welds. This served as a basis for selecting the initial overlap and the welding speed.

After the assumptions regarding speed and overlap had been made, a detailed and precise investigation was made to determine the electrode force and current magnitude that would produce the best weld. The current was allowed to vary over a wide range for several values of electrode force and these samples were then subjected to metallurgical investigation and physical testing which furnished information necessary to making a selection.

Once the electrode force and current had been determined, then the effect of varying the degree of overlap and

speed was studied. These samples were subsequently subjected to metallurgical investigation and physical testing and their effects determined. This procedure was followed for each of the three thicknesses investigated.

Weld Characteristics

The curves which follow attempt to show the relation of the weld characteristics to each of the major seam welding variables involved.

The strength or relative load-carrying quality of the weld is plotted as the breaking load of a 1-in. tensile test specimen. The actual load-carrying capacity of the joint would be very difficult to measure, but the manner in which the tensile specimen failed can be taken as a reasonable basis for evaluating the quality of the joint. Although the method of failure is not plotted, it correlates nicely with the value of the breaking load. The lower values of breaking load indicate that the failure occurred in the weld and the higher values indicate that failure occurred elsewhere in the sheet.

The nugget penetration is taken as the ratio of the thickness of the zone which exhibits a columnar dendritic structure to the thickness of the joint. Penetration indicates the nature of the heating conditions employed in making the weld and, to some extent, the load-carrying performance which can be expected.

The joint thickness is an indication of the surface condition of the weld and the amount of mash down which has been accomplished. It is expressed as the ratio of final joint thickness to initial sheet thickness.

Effect of Welding Current

Figure 4 shows a series of macrographs of mash seam welds made in 0.078-in. low-carbon steel, showing the effect of current magnitude on weld appearance with other variables held constant. The effect of insufficient heating is shown at A—in this case the weld is a solid phase bond along the entire length of the joint line and the sheared edges can readily be recognized by the absence of the white band of ferrite, characteristic of rimmed steels. Weld B, made at a current increase of 2000 amp, shows the presence of a small weld nugget located at the center of the joint line. Further increase of current in Weld C shows both an increased nugget size and improved edge contour. The columnar, dendritic structure is an indication that melting has occurred and the ferrite band has been diffused with the surrounding metal. The lower two macrographs show the result of overheating. This is indicated by an increase in final joint thickness resulting from the inability of the weld to cool while under the influence of the electrode force. In all cases the nuggets are aligned with the upper and lower surfaces of the joint and not with the joint line indicating that they were formed after the plastic deformation occurred.

In Fig. 5 weld characteristics are plotted as a function of current for mash seam welds in 0.078-in. steel using the same welding variables as indicated in Fig. 4. The curves indicate that strength becomes questionable below 17,000 amp because of a lack of penetration, and tensile failure occurs in the weld at a current of 13,000 amp. The joint appears to be slightly thicker at extremely low values of current, no doubt, because the metal was not hot enough to allow the maximum deformation to occur. The current magnitude has little effect on joint thickness until the range of overheating is approached and then thickness increases.

Figure 6 shows weld characteristics plotted as a function of current for mash seam welds in 0.050-in. steel. The behavior in the range investigated indicates that the welds all exhibited good strength and nearly uniform joint thickness. The sudden rise in joint thickness at a current of 22,000 amp indicates that overheating was present and any increase in current beyond that point would likely have resulted in damage to the electrodes.

Weld characteristics are plotted in Fig. 7 as a function of current for mash seam welds in 0.031-in. low-carbon steel. The strength of welds made at current values lower than 11,000 amp becomes questionable because of a lack of measurable penetration, and weld

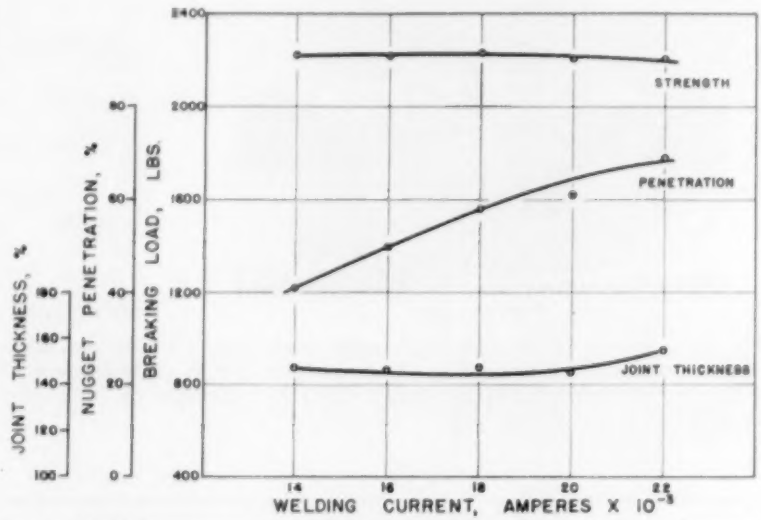

Fig. 6 Weld characteristics in 0.050-in. low-carbon steel as a function of current. Electrode force 1500 lb, welding speed 80 ipm, and an initial overlap of 150%

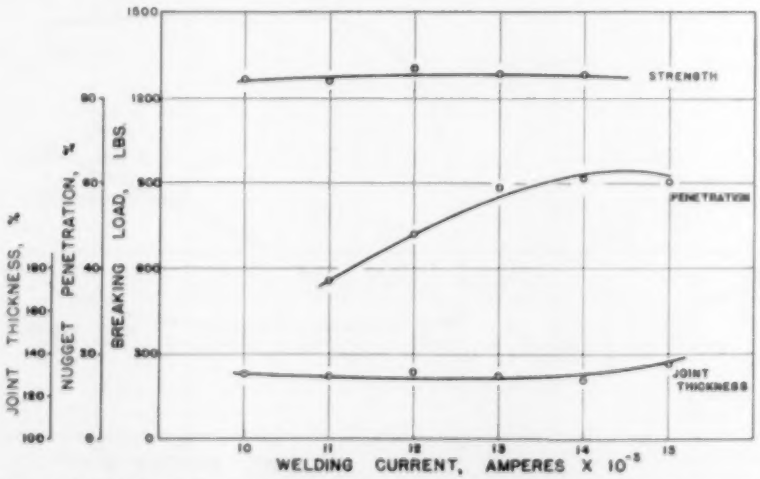

Fig. 7 Weld characteristics in 0.031-in. low-carbon steel as a function of current. Electrode force 900 lb, welding speed 130 ipm, and an initial overlap of 150%

quality at or above 15,000 amp will be impaired as a result of overheating.

Effect of Electrode Force

The macrographs shown in Fig. 8 indicate the effect of electrode force on mash seam welds made in 0.031-in. steel while holding all other variables constant. Study of these macrographs reveals that increasing electrode force reduces the resulting thickness of the weld and decreases the magnitude of the heating effects. One can account for the reduction in joint thickness because a greater force was available to redistribute the same amount of metal. The decrease in heat apparently generated in the weld requires consideration of several factors. First, the contact resistance between the two sheets was, no doubt, reduced as a result of the higher force; thus causing a decrease in heat available from that source. Second, assuming that plastic deformation occurs before sufficient heat is generated to form the nugget, the area of the electrodes in contact with the sheets is greatly increased as soon as mash down occurs, and current density is correspondingly decreased. This results in a reduction of the heat available due to the resistivity of the metal. A third factor involves an improved condition for heat transfer to the electrodes which obviously accompanies an increase in electrode force. This makes for a more efficient dissipation of the heat as it is generated and results in cooler weld conditions.

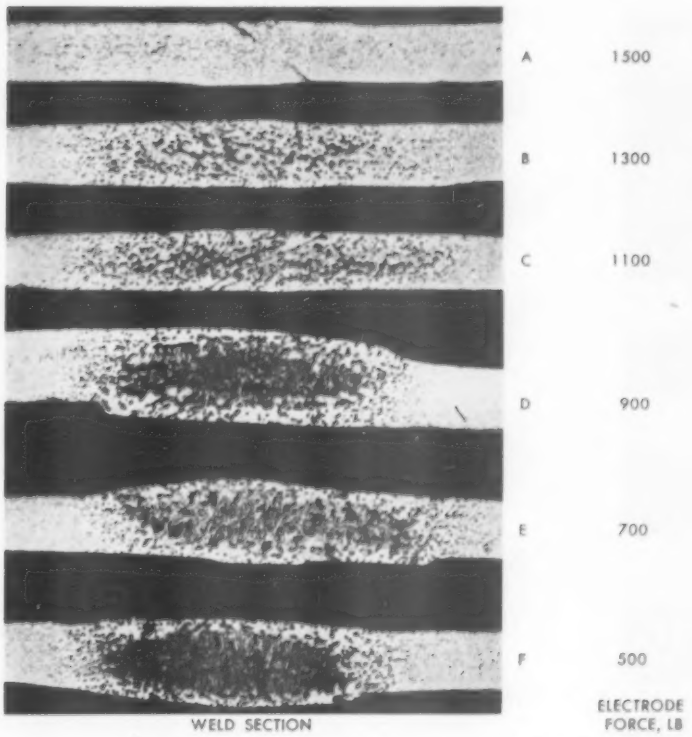

Fig. 8 Macrographs of mash seam welds made with 0.031-in. low-carbon steel at various electrode forces. Current 13,000 amp, welding speed 130 imp, and an initial overlap at 150%. Magnification X20 (Reduced by 25% upon reproduction)

The weld characteristics for the macrographs shown in the previous figure are plotted in Fig. 9. These curves indicate that the effect of electrode force is significant as weld strength and penetrations fall off rapidly above 1100 lb. The welds made at low values of electrode force become objectionable as a result of increased joint thickness. Electrode forces over the range of 900 to 1900 lb were checked for 0.050-in. steel, and forces from 1500 to 3000 lb were checked for the 0.078-in. steel, the results of which may be seen in the two weld characteristic curves included in the Appendix (see Figs. 17 and 18). The weld characteristics obtained for both thicknesses were similar to those shown in Fig. 9; that is, the penetration and joint thickness decreased as electrode force increased. In both cases the strength was not appreciably affected over the range investigated.

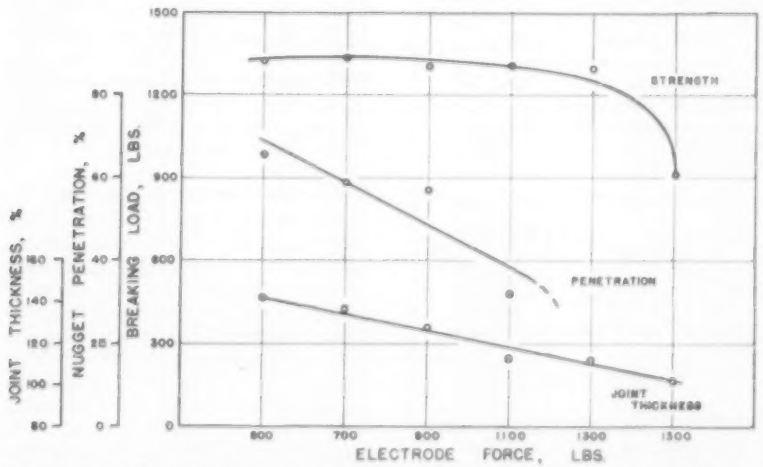

Fig. 9 The effect of electrode force on mash seam welds made in 0.031-in. low-carbon steel. Current 13,000 amp, welding speed 130 ipm, and initial overlap 150%

Effect of Initial Overlap

Figure 10 shows the effect of varying the initial overlap used in making mash seam welds with 0.031-in. steel. Examination of the figure will reveal that increasing the initial overlap results in weld joints that are thicker and appear to have been made under higher heat conditions. The thickness variation can be attributed to the fact that the amount of overlap determines the amount of metal that must be plastically redistributed when mash-down occurs. The variation in heating effects is thought to result from a combination of two factors. First, the smaller contact area of a specimen having a low percentage overlap causes an increase in current density. This results in rapid heating of the metal in the vicinity of the contact area to a state of

plasticity which allows mash-down to occur very quickly. If mash-down occurs permaturely, then the condition of greater electrode contact area, with its associated lower current density and improved heat dissipation characteristics, prevents sufficient heat from being generated to properly effect the weld.

Figure 11 shows a curve of weld characteristics plotted as a function of initial overlap for mash seam welds made in 0.031-in. low-carbon steel. A study of the curves reveals that joint thickness can be reduced along with penetration until an overlap of 80% is reached without affecting the strength of the joint. Further decreases in overlap below 80% result in weld joints of inferior strength. Similar trends were found to exist in varying the overlap for 0.050- and 0.078-in. steels. In both cases an overlap of around 60% was the lowest value that could be used without detrimental effect on the strength of the joint. It should also be noted that a small overlap is difficult to clamp or hold uniformly. Some overlap tolerance must be provided and, if the overlap is too small, a poor weld will result. The values of from 125–150% are conservative and should result in good welds (see Figs. 19 and 20, Appendix, for 0.050- and 0.078-in. weld characteristic curves).

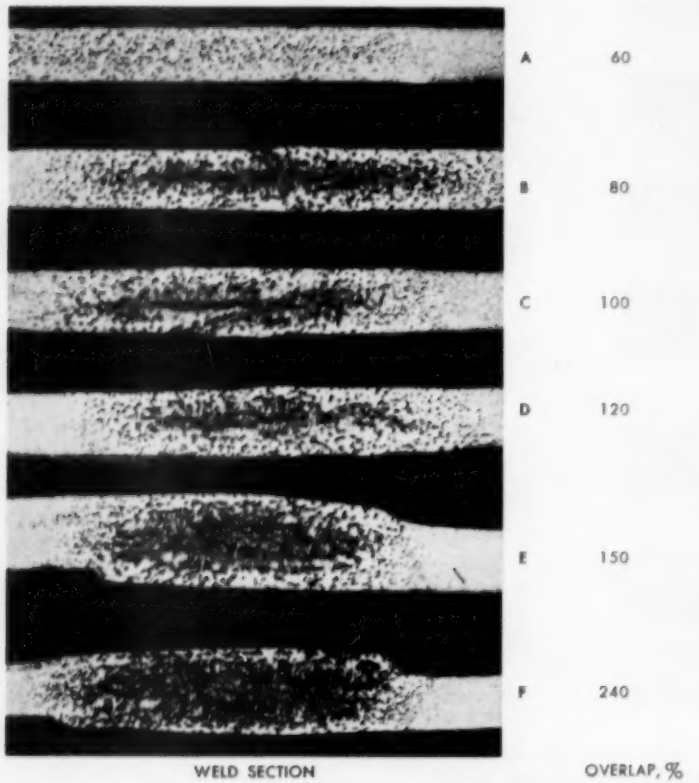

Fig. 10 Effect of initial overlap on welds made with 0.031-in. steel. Electrode force 900 lb, current 13,000 amp, and welding speed 130 ipm. Magnification X20 (Reduced by 25% upon reproduction)

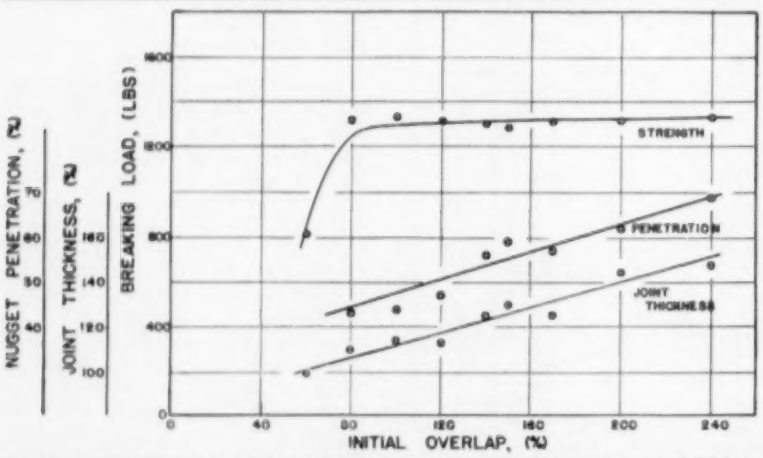

Fig. 11 The effect of initial overlap on mash seam welds made with 0.031-in. low-carbon steel. Electrode force 900 lb, current 13,000 amp, and welding speed 130 ipm

Effect of Welding Speed

Figure 12 shows a series of cross and longitudinal macrograph sections which were made with 0.050-in. low-carbon steel welded at various speeds. Both longitudinal and cross sections are presented to show that weld penetration remains consistent along the length of the weld for each of the speeds. Close observation of the various macrographs will reveal that very little difference can be observed as a result of speed variation. Some of the points on the curve shown in Fig. 13 correspond to welds shown in Fig. 12. The speed of welding appears to have little influence on weld strength and thickness and causes only a slight change in penetration. The change in penetration can be attributed to the fact that so long as the circuit resistance and current magnitude remain constant, the rate of heat generation remains the same, but the amount of heat generated depends upon the duration of the heating period. Therefore, the longer the material remains between the electrodes the larger the amount of heat generated and in turn the greater the measurable penetration.

Welding speeds were investigated for 0.031-in. steel in the range of from 100 to 160 ipm, and for 0.078-in. steel in the range of from 55 to 75 ipm. The same trend appeared in both thickness as was illustrated in the curves for the 0.031-in. steel (Figs. 21 and 22, Appendix, for 0.031- and 0.078-in. curves).

Metallurgical Characteristics of Welds

The various macrographs shown in this paper were made from selected specimens prepared under different welding conditions. In all welds made under suitable welding conditions, the characteristic weld nugget in spot and seam welding was in evidence. This nugget, dendritic in structure, is made up of resolidified metal and surrounded by a layer of recrystallized metal. The structure shown is low-carbon martensite produced by flood cooling during the welding operation. The small dark areas surrounding the nugget are also

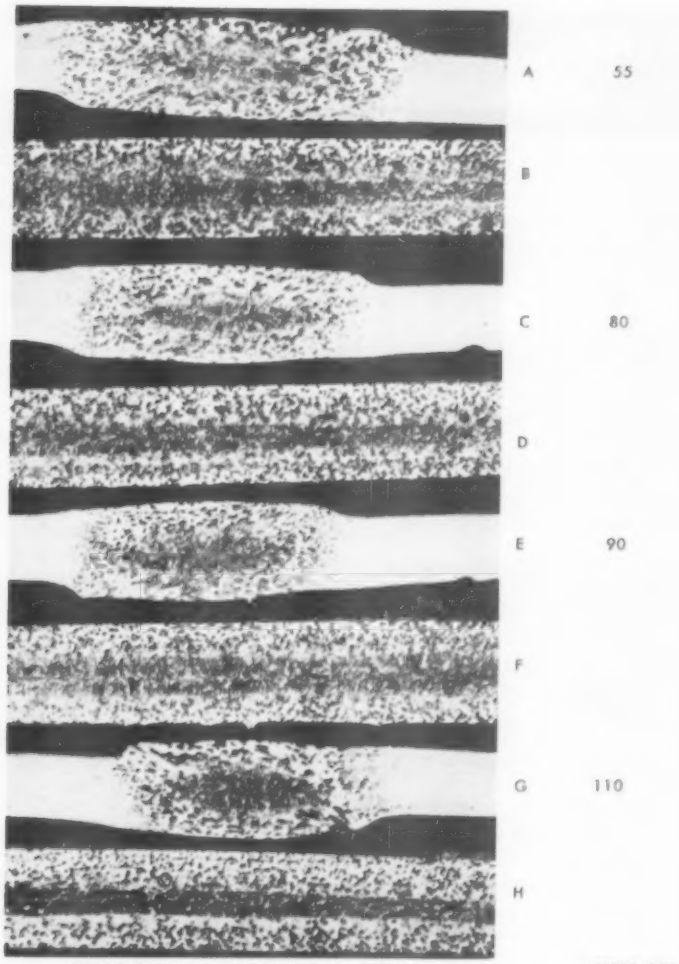

Fig. 12 Longitudinal and cross section of mash seam welds made with 0.050-in. steel at various speeds. Current 19,000 amp, electrode force 1500 lb, and initial overlap at 150%. Magnification X12.5 (Reduced by 25% upon reproduction)

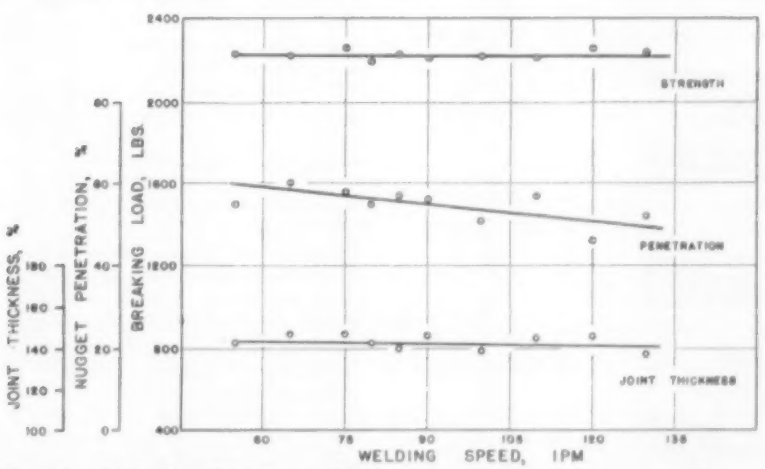

Fig. 13 Weld characteristics in 0.050-in. low-carbon steel as a function of welding speed. Welding current 16,000 amp, electrode force 1500 lb, and initial overlap 150%

made up of martensite with a higher carbon content.

Figure 14 shows the result of a microhardness study made in a mash seam weld of 0.031-in. low-carbon steel. This weld was made using the recommended values, namely, current 13,000 amp, electrode force 900 lb, overlap 150%, and at a speed of 130 ipm. The curve indicates that there was a definite hardness increase within the nugget area. The Knoop hardness number obtained corresponds closely to 35 Rockwell C which, according to some authorities is the maximum hardness that can be obtained in steel of the carbon content involved in this investigation. The base metal hardness is approximately 61 Rockwell B.

Defects Encountered in Mash Seam Welding

Mash seam welds are subject to two types of defects. One type concerns the bonding at the edge of the joint line and is peculiar to mash seam welding. The second is porosity of the weld nugget which is common to other forms of resistance welding. Edge defects, which occur in the pressure weld or solid phase bonding zone, are cracking or burning. They are believed to be largely the result of improper heating which could have been caused by the presence of spot tack welds. Welds in which porosity was noted most often were made at either very high values of current or at high welding speeds. Since the nature of resistance weld nuggets is such that there is a tendency to have high shrinkage stresses at their center, it seems logical to conclude that for sound welds the nugget size should not be any larger than necessary to provide good penetration. Also, if the weld is allowed to cool partially while still under the influence of electrode force, any cavities present will be forged together.

Since most of the detrimental defects encountered in the mash seam welds were found to be in the vicinity of the spot tack welds, a study was made to determine the effect of spot tacking procedure on resulting mash weld quality. A number of 0.031-in. specimens were prepared each having spot tack welds made at different values of heat. Three current values were used in making the spot welds, one at 60% heat which resulted in a mild solid phase bonding, one at 70% heat which removed all traces of the joint line and caused some bulging of the sheared edges, and one at 90% heat which caused considerable deformation of the sheets accompanied by some porosity. Mash weld specimens having tack welds made under the low-heat setting were unharmed by the spot tack weld while those made under high-heat conditions resulted in defective edge conditions in the seam. In order to determine the seriousness of

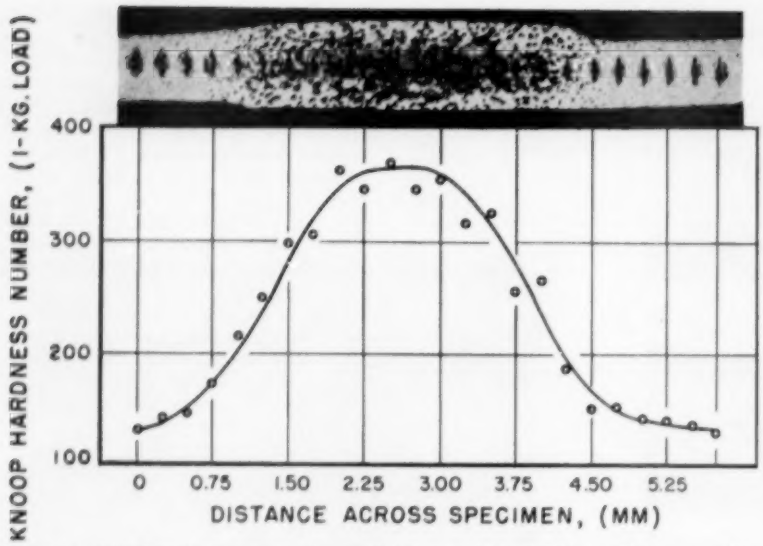

Fig. 14 Microhardness survey of a mash seam weld in 0.031-in. thick low-carbon steel. Electrode force 900 lb, current 13,000 amp, overlap 150%, and welding speed 130 ipm. Magnification X22 (Reduced by $^1/_3$ upon reproduction)

THICKNESS (INCHES) SEE NOTE 1	INITIAL OVERLAP (PER CENT OF SHEET THICKNESS) SEE NOTE 2	WELDING SPEED (INCHES PER MIN)	CURRENT (AMPERES) SEE NOTE 3	ELECTRODE FORCE (POUNDS) SEE NOTES 4 & 5
.031	150	130	13,000	900
.050	150	80	16,000	1500
.078	125	55	19,000	2500

1. LOW CARBON STEEL.
2. INTENDED TO PRODUCE WELDS HAVING EQUAL MASH-DOWN ON BOTH SIDES.
3. PARTIAL WAVE CONTINUOUS CURRENT.
4. RWMA CLASS III. ALLOY.
5. ELECTRODE GEOMETRY:
10-INCH DIAMETER.
UPPER & LOWER ELECTRODES ALIKE.

Fig. 15 Recommended machine settings for mash seam welding thickness of 0.031, 0.050 and 0.078-in. low-carbon steel

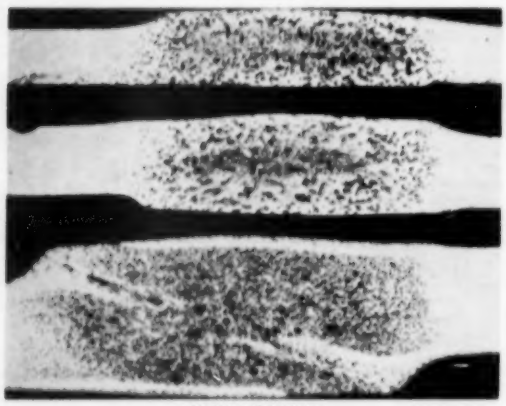

Fig. 16 Mash seam welds made under recommended conditions indicated in Fig. 15. X19 (Reduced by $^1/_2$ upon reproduction)

edge defects a number of specimens were porcelain enameled and the conditions of the enamel covering the weld joint was examined for blow holes and blistering. A study of the specimens revealed that defects caused by the stronger tack welds resulted in unsatisfactory enameling and that the weaker tack welds yielded seam welds of the best enameling quality.

Conclusions

On the basis of the data presented in this report the following conclusions concerning the relationship of the mash seam welding variables and the characteristics of the weld appear to be justified:

1. The final thickness of the joint is determined by the amount of initial overlapping of the sheets and by the magnitude of the electrode force.
2. The strength of the joint depends upon whether or not sufficient heat was generated during welding to produce a well-defined nugget.
3. The four ways in which the heat, generated during the mash seam welding process, may be increased are: (*a*) increase the magnitude of the welding current, (*b*) decrease the magnitude of the electrode force, (*c*) increase the initial overlap of the sheets, and (*d*) reduce the magnitude of the welding speed.
4. Internal defects in mash seam welds are the result of an overheated weld cooling without the beneficial influence of the electrode force.
5. The internal defects can be reduced to a minimum by means of establishing a balance between the current, electrode force, and welding speed such that the joint is not in an overheated condition as it passes from beneath the electrodes.
6. The welding speed is limited by the rate at which the heat, generated in making the joint, can be dissipated.
7. Spot tack welds are to blame for most of the surface defects encountered in mash seam welding.
8. The spot tack weld should be as light as possible but strong enough to maintain the desired overlap during the mash seam welding operation.

Recommended Mash Seam Welding Schedules

Figure 15 gives recommended machine settings for mash seam welding three thicknesses of low-carbon steel. As a result of the widely differing applications of mash seam welded joints, it is for all practical purposes impossible to recommend any one single set of machine settings that will answer the requirements for every case. The schedules shown are intended to represent the mid-points of the range in which satisfactory results can be obtained under the conditions indi

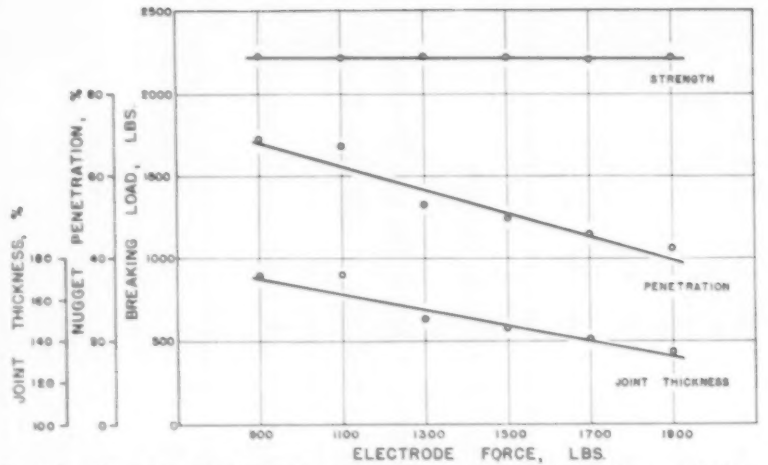

Fig. 17 The effect of electrode force on mash seam welds made in 0.050-in. low-carbon steel. Current 16,000 amp, welding speed 80 ipm, and initial overlap 150%

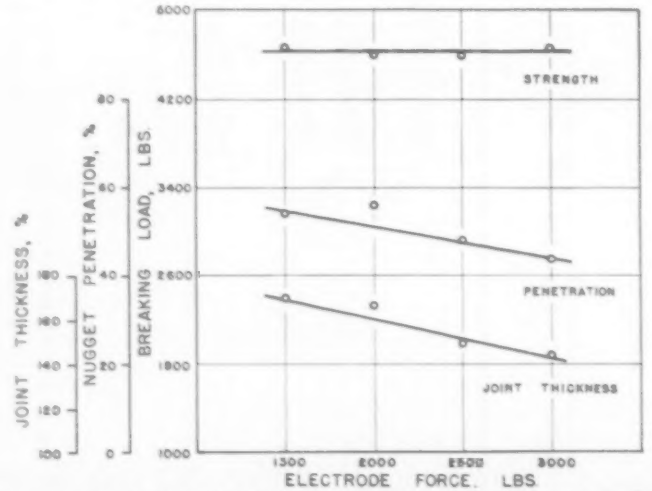

Fig. 18 The effect of electrode force on mash seam welds made in 0.078-in. low-carbon steel. Current 19,000 amp, welding speed 55 ipm, and initial overlap 125%

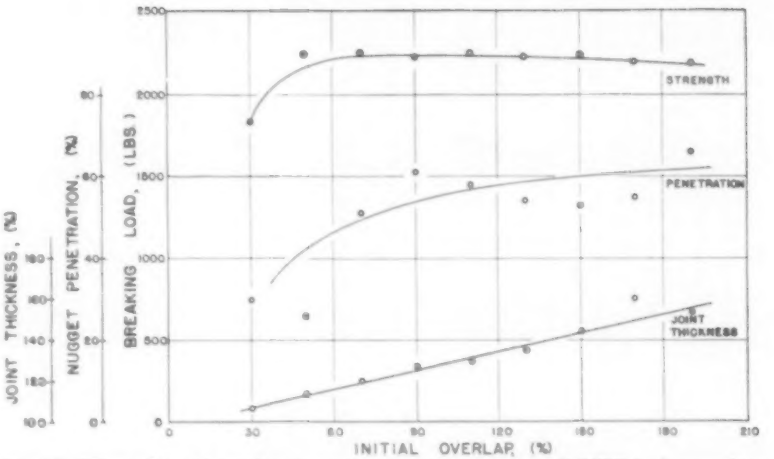

Fig. 19 Effect of initial overlap on mash seam welds made in 0.0500-in. low-carbon steel. Electrode force 1500 lb, current 16,000 amp, and welding speed 80 ipm

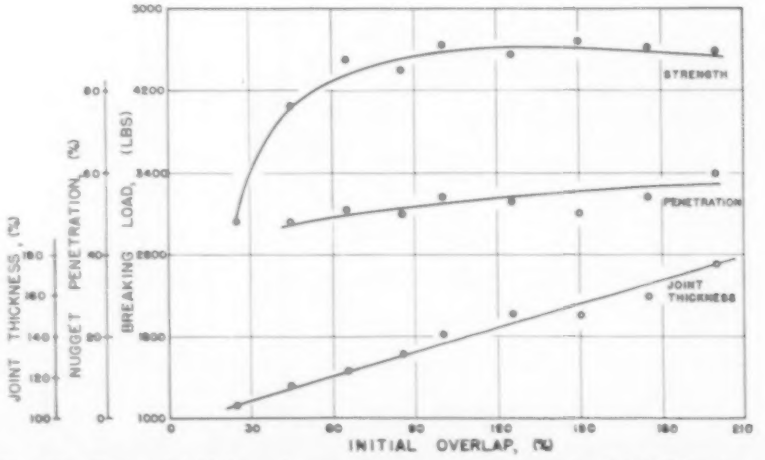

Fig. 20 Effect of initial overlap on mash seam welds made in 0.078-in. low-carbon steel. Electrode force 2500 lb, current 19,000 amp, and welding speed 55 ipm

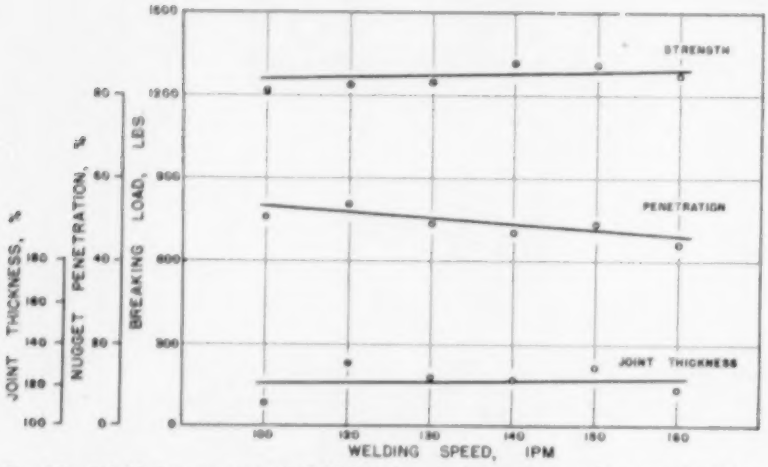

Fig. 21 Weld characteristics in 0.031-in. low-carbon steel as a function of welding speed. Welding current 13,000 amp, electrode force 900 lb, and initial overlap 150%

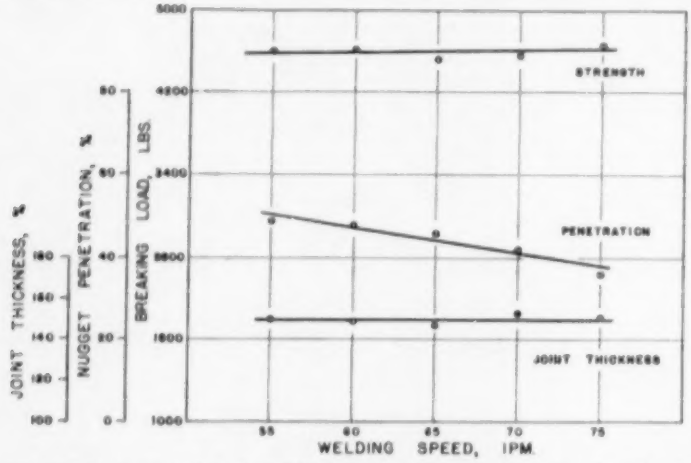

Fig. 22 Weld characteristics in 0.078-in. low-carbon steel as a function of welding speed. Welding current 19,000 amp, electrode force 2500 lb, and initial overlap 125%

cated. The type of joints that can be obtained under these so-called recommended conditions are shown in Fig. 16. The macrographs show that the welds have approximately 50% penetration which indicates that the joints would be strong when subjected to a load and pressure tight if made in container assemblies. In addition the surfaces are free from spikes or feathers which would interfere with painting and finishing and there are no cracks at the joint line edges to prevent satisfactory porcelain enameling. Information presented in the form of conclusions and curves may be used to modify the recommended schedules to suit the needs of a specific application.

APPENDIX

Because of the large number of illustrations, some curves were omitted in this report. It is felt that these curves should be made available to those interested since the weld characteristics plotted cannot be adequately described by words. Therefore the six curves shown in Figs. 17 through 22, all mentioned in the text material, are included without further comment.

Acknowledgment

The authors extend their appreciation to the Resistance Welder Manufacturers Association and to the Welding Research Council for sponsoring this investigation. Also, they wish to thank the United States Steel Corp. for supplying the sheet steel, and P. R. Mallory and Co., Inc., for supplying the needed electrodes.

Welding Research Council Bulletin No. 26

Investigation of the Influence of Deoxidation and Chemical Composition on Notched-Bar Properties of Ship Plate Steel

by F. W. Boulger, R. H. Frazier and C. H. Lorig, Battelle Memorial Institute

Results of an investigation of some 400 heats of steel to investigate the effects of variations in composition and deoxidation practice on the fracture characteristics of a ship plate steel.

This Bulletin is priced at $1.00 a copy. Copies may be ordered through the American Welding Society, 33 W. 39th St., New York 18, N.Y.

EVALUATION OF THE SIGNIFICANCE OF CHARPY TESTS FOR QUENCHED AND TEMPERED STEELS

High-strength steels tested to determine the critical fracture transition temperatures at which welded structures, loaded in the presence of sharp, crack-like defects, may initiate or propagate brittle fractures

BY P. P. PUZAK AND W. S. PELLINI

ABSTRACT. Crack-starter tests of various high-strength steels have been conducted to determine the critical fracture transition temperatures at which welded structures, loaded in the presence of sharp, crack-like defects, may initiate or propagate brittle fractures. The test procedures establish three critical fracture transition temperatures related to the specific loading conditions required to initiate and propagate brittle fractures. The temperature interval of change from the state of complete ductility (even under conditions of severe plastic deformation) to nil ductility (such that brittle fracture initiation is possible upon reaching incipient yielding in the vicinity of crack defects) is shown to be approximately 100° F for all of the steels investigated. This interval was determined to be in the −200 to −100° F temperature range for the steels of highest notch ductility, and in the +100 to +200° F range for the steels of lowest notch ductility.

Correlation studies of Charpy V and keyhole transition curves are presented. It is concluded that keyhole curves deviate greatly from Charpy V curves for materials of this type. The nil ductility transition temperature in high-strength steels is generally related to the 20/30 ft-lb temperature of the Charpy V energy transition curve. Fracture propagation is possible through elastic loaded material to temperatures corresponding to relatively high positions on the Charpy V transition curve; however, complete resistance to brittle fracture (shear tearing only) is obtained at temperatures related to the "upper-shelf" of the curve.

A discussion is presented relative to the use of the critical fracture transition concept in design.

Introduction

The brittle fractures of wartime merchant ships and other large welded structures resulted in extensive investigations of the factors which contribute to such failures. It is now recognized that brittle failure is a function of various probabilities related to notch ductility properties of the steel, presence of sharp flaws, temperature of service, design features, and loading conditions. Various approaches may be taken to reduce or eliminate the probability of brittle fracture; these include:

(*a*) Improving the notch ductility of the steel to provide for ductile behavior despite the presence of sharp-notch flaws.

(*b*) Designing to eliminate all regions of plastic flow; recognizing that brittle fractures cannot be initiated if the stress level in the general area of the notch remains within the elastic range.

(*c*) Elimination of sharp-notch flaws which may be developed during fabrication.

Items (*b*) and (*c*), if achieved, eliminate the need for notch-ductile steel; however, it is not realistic to rely on such achievement for the case of complex structures fabricated by welding. Thus, if the service is critical, it is necessary to use steels which permit deviations from perfect design and perfect fabrication, that is, to use steels which permit flow in the presence of the crack-like flaws developed in welded structures. Approach (*a*) may be used to reduce probabilities of fracture to zero while approaches (*b*) and (*c*), in practice, lower the probabilities to values which may be acceptable depending on the relative critical nature of the structure.

It should be recognized that approaches (*b*) and (*c*) are not applicable to all types of service. They are applicable only to service of structures which are expected to operate under nominal elastic loads (merchant ships, pressure vessels, etc.) but are not applicable to service of structures which may possibly be subjected to plastic loading in service. For example, a ship hull dimpled by an accidental collision with another ship or by explosions may be expected to be deformed and to develop crack flaws in weld regions at points of connections. This will be discussed further in the sections to follow.

In order to arrive at a decision relative to the notch ductility required in a steel to prevent the initiation and propagation of brittle fractures in service, it is necessary to develop information as to the result of loading the steel in the presence of sharp-crack defects. This view is pessimistic only to the extent that sharp cracks are assumed to be present; such pessimism is warranted for large welded structures. The fracture behavior of the steel, which may be related to various types of loading encountered in service, is categorized as falling into one of several possible types:

Type 1—Brittle failure developed immediately on exceeding the yield point, i.e., without appreciable prior deformation.

Type 2—Brittle failure developed following extensive deformation, i.e., fracture initiation that must be "forced" by plastic loading.

Type 3—Ductile failure by shear, following severe deformation.

All ferritic steels may be made to change from Type 3 to Type 2 to Type 1 behavior by lowering temperature.

Following a design decision as to the type of loading which is expected in service, it is essential to consider whether the specific steels under consideration are of Types 1, 2 or 3 at the lowest temperature of service. At this point, factors of economy and the critical nature of the service required,

P. P. Puzak and W. S. Pellini are associated with Metallurgy Division, Naval Research Laboratory, Washington, D. C.

Paper presented at ASME Metals Engineering Division Conference held in conjunction with 1956 AWS National Spring Meeting, May 7–11, Buffalo, N. Y.

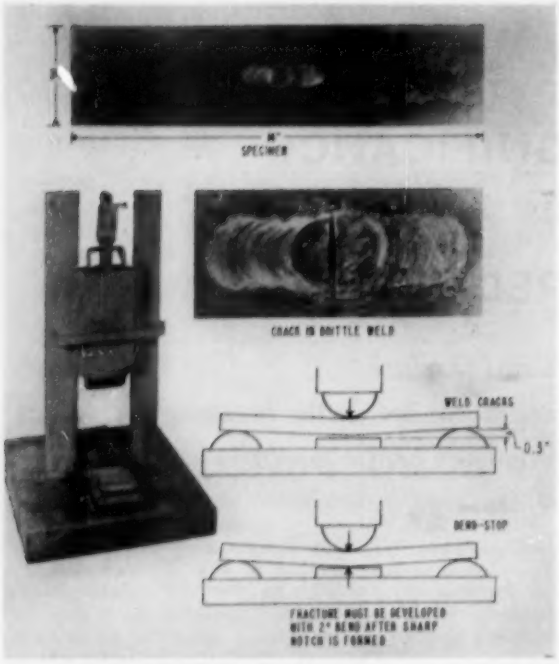

Fig. 1 Drop-weight test method

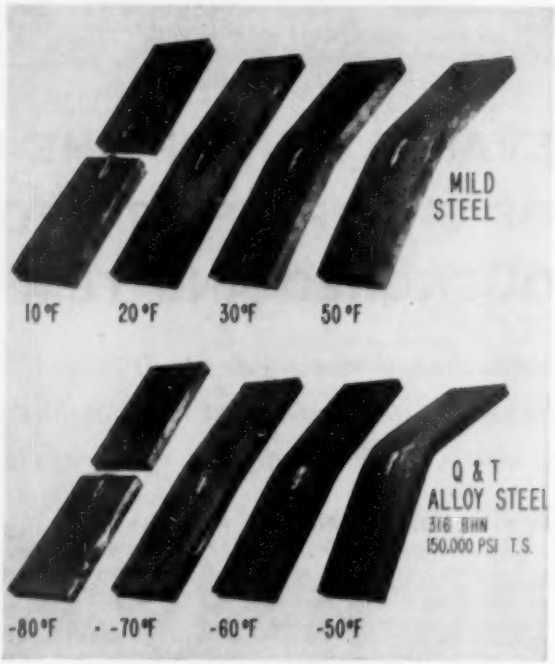

Fig. 2 Drop-weight test results indicating sharp drop in ductility to nil values with decreasing temperature. The deformed specimens represent nonstandard tests made without the stop to illustrate ductility at the respective temperatures

should determine whether Type 1 steel is adequate and permissible, or if Types 2 or 3 are required.

Extensive series of drop-weight and explosion crack-starter tests have been conducted by this Laboratory with the aim of defining the behavior of conventional mild steels in the presence of sharp flaws.[1-4] The significance of the sharp-flaw evaluation method was validated by tests of ship-fracture steels. The tests correctly predicted the failure of the steels at the temperatures of fracture and differentiated between fracture source (Type 1) and fracture propagation (Type 2 with respect to initiation) steels. Briefly, the major fraction of semikilled and rimmed steels of wartime manufacture were indicated to be of fracture initiation type below 50° F and of fracture propagation type below 100° F. Correlation with the National Bureau of Standards' Charpy V data for ship-fracture steels provided further corroboration of the significance to service performance of the crack-starter tests. For the subject steels, fracture initiation in conventional service was indicated to be possible at temperatures below the Charpy V 10 ft-lb transition temperature and fracture propagation below the temperatures of the Charpy V 25 ft-lb transition temperature.

As the result of further drop-weight tests, it was found that fully killed mild steels, high-tensile steels (HTS), quenched and tempered steels, and other types did not conform to the 10 ft-lb rule established for the semikilled and rimmed ship-fracture steels. A302 steel was indicated by drop-weight test to be of nil ductility type to temperatures as high as the Charpy V 30 ft-lb transition. The drop-weight test indications for A302 were corroborated by the initiation of a fracture in a pressure vessel at a temperature of Charpy V 20 ft-lb. A further corroboration obtained for the case of HTS will be described later.

Current trends to higher stresses and lower weight call for the use of high-strength steels in welded construction. The added features of use in arctic climates or in low-temperature chemical processing demand the utmost of low-temperature notch ductility for these steels. This paper provides a summary of tests of the performance of various high-strength steels when loaded in the presence of ultrasharp cracks. It is the purpose of these continuing studies, as well as the aim of the presentation of this report, to develop the following information:

(1) The temperature ranges in which specific types of steel become highly sensitive to the presence of crack-like defects and brittle-fracture becomes a possibility.

(2) The procedures by which Charpy V data may be utilized to define the critical fracture transition temperatures for specific steels.

Concept of Critical Fracture Transition Temperatures

It is not within the scope of this report to discuss fracture mechanics, but it is essential to discuss briefly the significance of the critical fracture transition temperature concept as it relates to the performance of ferritic steels in the presence of a sharp crack. In the absence of notches, even mild steels may be deformed severely without fracturing at temperatures as low as −80° F, as indicated by explosion-bulge tests. For welded structures, the concept of inherent flaws is quite realistic; accordingly, it is necessary to consider the fracture behavior of the steels in the presence of sharp, crack-like flaws as the practical case in service.

Crack-starter tests, in which specimen loading is accomplished either by the impact of a drop weight or by explosion,* have been developed at

* Crack-starter tests evaluate the fracture characteristics of specimens which are loaded in the presence of the sharpest possible type of notch—a cleavage crack. Crack-starter test specimens feature a bead-on-plate of a highly brittle, hard-surfacing type weld. The sole purpose of this brittle weld is to function as a "crack-starter." Upon loading of the specimen, the weld cracks, thus, introducing a cleavage crack into the steel being tested. Crack-starter tests of 3½ x 14 in. x plate thickness specimens, loaded by the impact of a falling weight, with conditions adjusted so as to obtain only incipient yielding, are described as drop-weight tests. Crack-starter tests of 14 x 14 in. x plate thickness specimens which are placed over a circular die, and loaded by the action of an offset explosive charge, are termed explosion crack-starter tests.

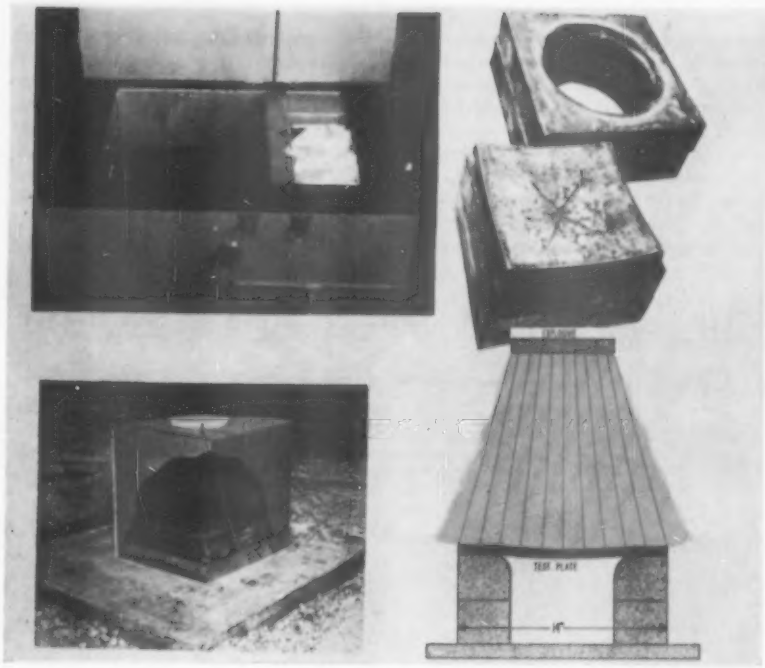

Fig. 3 Explosion crack-starter test method. *(Top left)* Test plate in refrigeration cabinet; *(top right)* plate positioned over die; *(bottom left)* explosive wafer positioned over test plate by means of cardboard box; *(bottom right)* schematic of test

NRL for the determination of critical fracture transition temperatures of steels in the presence of ultra-sharp cracks. The crack-starter tests are aimed at defining three critical temperatures, as follows:

(1) The temperature below which the steel loses all ability to deform in the presence of a sharp crack (i.e., nil ductility, % elongation = 0).

(2) The temperature below which brittle fractures will run through elastically loaded material (fracture transition for elastic loading).

(3) The temperature above which only shear tearing is possible, irrespective of severity of plastic loading (fracture transition for plastic loading).

The drop-weight test (Fig. 1) is a laboratory method for defining the temperature of nil ductility (% elongation = 0). The significance of this test is illustrated in Fig. 2 by the sharp fall in ductility, with temperature, to essentially zero values. The explosion crack-starter test (Fig. 3) is a field method of determining the fracture propagation characteristics of the steel when fracture initiation is "forced." Figure 4*A* illustrates a typical test series for a mild-steel ship plate. At 20° F the steel breaks flat, indicating nil ductility (same temperature as would be indicated by drop-weight test), i.e., the absence of "forcing" for initiation. In the range of 40 to 60° F, "forcing" is required to initiate the fracture as indicated by bulging; however, the fracture continues through the elastically loaded edge regions. This indicates that once started at a position of forcing, the fracture will continue through material that is under elastic loads. In the range of 80 to 120° F, fracture occurs only in the plastically deformed center material. This indicates that propagation will be restricted to material that has been embrittled by plastic loading (cold work). At 140° F and higher temperatures, only shear tearing is possible; that is, the metal is completely ductile. If extra-heavy explosive charges are used for tests at temperatures above 140° F, deep bulges are produced with shear tears radiating from the crack-starter weld, Fig. 4*B*.

The changing performance of steels with increasing temperature will be defined in terms of the three critical fracture transition temperatures. The steel of Fig. 4*A* will serve to illustrate the significance of the terms as follows:

(1) *NDT (nil ductility transition)*. Below this temperature (20° F of Fig. 4*A*) the steel does not deform prior to fracturing, i.e., fracture occurs immediately on reaching the yield point. The fractures propagate easily through elastic-load regions.

(2) *FTE (fracture transition for elastic loading)*. Below this temperature (70° F, midspan of T-S range of Fig. 4*A*) fractures propagate through elastic-

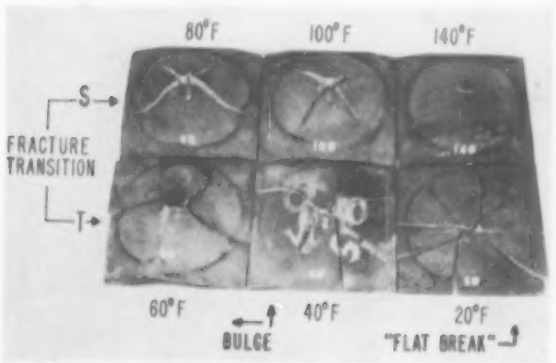

Fig. 4*A* Explosion crack-starter test series of a typical ABS-A type ship-plate steel depicting: *(a)* nil ductility transition at 20° F (flat break); *(b)* fracture transition for elastic loading at 70° F (mid-point of through to stop, T-S range); *(c)* fracture transition for plastic loading (crack refusal at 140° F)

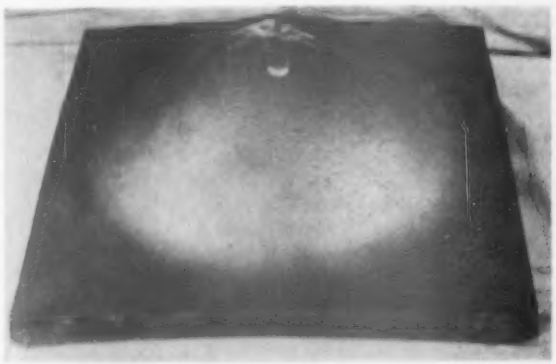

Fig. 4*B* Illustrating failure by shear at temperatures above 140° F for a typical ABS-A type ship plate. Extra heavy charge used to develop deep bulge

load regions while above this temperature fractures propagate only through plastic-load regions. At the FTE temperature, considerable "forcing" (great deal of plastic deformation) is required to initiate fracture. As the temperature is lowered to approach the NDT temperature the amount of "forcing" required falls off rapidly.

(3) *FTP (fracture transition for plastic loading).* Above this temperature (140° F of Fig. 4*A*) brittle fractures cannot propagate even through material which is plastically deformed severely by high over-stressing.

The results of the sharp-crack tests, defined in terms of the three critical fracture transition temperatures, provide a guide in the use of steels for various conditions of anticipated loading, as indicated in Fig. 5.

(A) *Case of General Service.* In such service, all portions of the structure remain within elastic loads, except for corners, cutouts, etc., where minute amounts of yielding (shakedown) may occur. If fracture initiation is to occur, it must be as the result of the steel being unable to deform even slightly in the presence of a sharp crack. Such behavior requires that the steel be at or below the NDT temperature; accordingly, the subject temperature is critical to this case of loading. Above this temperature, "forcing" is required to initiate failure, indicating that there is a large margin of safety in design; below this temperature, design is critical and must not permit yielding to develop at crack-flaw positions.

(B) *Case of Accident in Service.* Accident is defined as a condition such that a local region of a structure is deformed by collision, impact, etc. This provides the "forcing" required to initiate the fracture at temperatures above the NDT. Once initiated, the fractures will propagate through adjacent material which is under nominal elastic loads if the temperature is below the FTE, or will stop at the edge of the deformation region if the temperature is above the FTE. It is interesting to note that FTE as determined by the explosion tests is in good agreement with the sharp rise from low stresses to yield-point loading in the stress for fracture vs. temperature curve of the Robertson test[5] (Critical Arrest Temperature, CAT), and that of the Esso Research and Engineering Co. (Esso Brittle Temperature, EBT).[6] This agreement was established by mutual tests of the same steels of the ship plate type. The significance of the FTE in design is that below this temperature propagation of brittle fracture through the elastic-load regions of a structure is a possibility, provided a "forced" start is obtained; above this temperature, this possibility need not be considered. An example may be made of a ship hull dented by collision—if the steel is above its critical FTE temperature, the fracture will be contained in the dented region; but if it is below its critical FTE temperature, continued propagation is possible outside of the dented region.

(C) *Case of Severe Military Service.* The severe military service case is defined as the ultimate in loading such that the structure is deformed over a large area (action of explosion on ship hull, for example). This case provides the utmost of forcing, and propagation is through deformed material. If propagation of brittle fracture must absolutely be prevented even in the case of such drastic loading, it is necessary that the material be above the FTP temperature. This case also covers the condition of severe fabrication operations (cold forming of weldments, etc.).

In a broad sense, the behavior of the

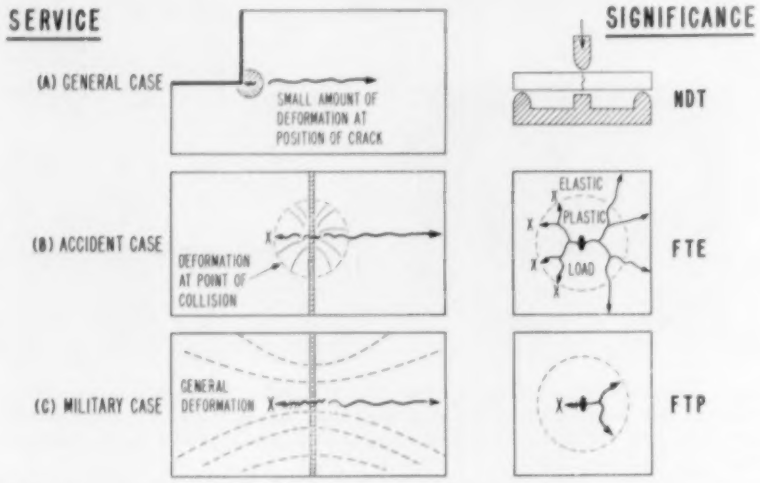

Fig. 5 Significance of crack-starter test results relative to specific service applications. The "X" mark side represents condition for material above the respective transition temperatures; the other side represents conditions for material below the respective transitions

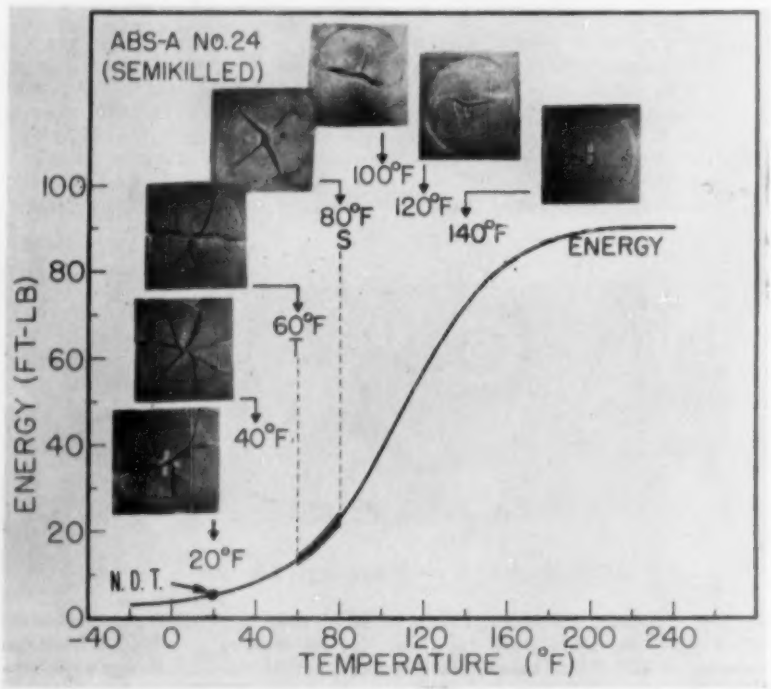

Fig. 6 General relationships of crack-starter test results of ABS-A type semikilled mild steel to Charpy V energy transition curve

steel in the described sharp-crack tests indicates temperature ranges of possible "penalty by failure" if certain conditions of loading are imposed. Design and service determine the conditions of loading while notches and temperature determine the response of the steel to the imposed conditions. The critical fracture transition temperature concept described above establishes three points on the temperature scale at which, as temperature is lowered or raised, major changes in the fracture characteristics of the steel are indicated.

The temperature intervals between the NDT, FTE and FTP transition temperatures have been found to be remarkably similar for all material which have been tested by the authors to date. These include mild steels, high-strength steels, cast steels, nodular irons, malleable irons, 12% Cr steels, etc. In these tests, the FTE temperature taken as the midpoint of the T-S range (see Fig. 4*A*) in the explosion crack-starter test was found to be commonly at 30 to 50° F above the NDT temperature established by the drop-weight test. The FTP temperature as indicated by complete refusal to fracture in the explosion test was found to be commonly at 100 ± 20° F above the NDT temperature. Because of this common relationship it is possible to establish the NDT temperature by the use of the relatively simple drop-weight test and then to predict the FTE and FTP temperatures within relatively narrow temperature ranges.

Providing allowance is made for the fact that the relationships depend on the type of steel under consideration, Charpy V transition curves may also be used to predict the three critical fracture transition temperatures. The general relationship established for the semikilled and rimmed mild steels of the same type as those involved in ship fractures (steels of relatively low manganese and high carbon content) is illustrated in Fig. 6. This type of steel was tested in quantity (33 separate steels) and it was established that the 10 ft-lb temperature provided a safe "fix" for the NDT temperature (usual correlations 5 to 8 ft-lb and never higher than 10 ft-lb). Similarly the 20 ft-lb temperature provided a good "fix" for FTE temperature. A common Charpy V impact value for correlation to FTP temperature was not observed because of the varying maximum energy shelves obtained in these steels. In all cases, however, FTP performance was reached at temperatures equivalent to the upper portion of the Charpy V impact curve where the curve bends into the maximum energy shelf. Charpy V specimens fractured at these temperatures generally reveal almost total shear in the fracture surfaces.

It is interesting to note that the correlations based on NDT and FTE temperatures are in exact agreement with ship fracture data.[7] In all cases, the source plates of ship fractures had less than 11 ft-lb (maximum 11, average 5–8) Charpy V energy when broken at the temperature of service fracture initiation. Through plates (those which sustained the propagation of fractures started in source plates) had a maximum of 19 ft-lb at the fracture temperature.

The general relationships of the NDT temperature and Charpy V values for these and other types of steels are summarized in Table 1. It is apparent that significantly higher values of Charpy V energy than those cited above (10 and 20 ft-lb) should be used for NDT and FTE correlations not only for the high strength steels, but also the mild steels which are characterized by higher states of deoxidation or by higher manganese contents than the ship fracture mild steels. The reason for these variations in correlation is not known; however, the following should be noted:

(1) The shapes of Charpy V curves vary with type of steel. The ship fracture type described above are characterized by "long sloping tails" in the 30 to 5 ft-lb range, while the improved mild steels and the high-strength steels show more rapidly rising curves in this range.[8] That is, the Charpy curves *per se* show differences in shape when comparison is made between various types of steels.

(2) Differences in Charpy V energy should not be confused with differences in temperature between any given

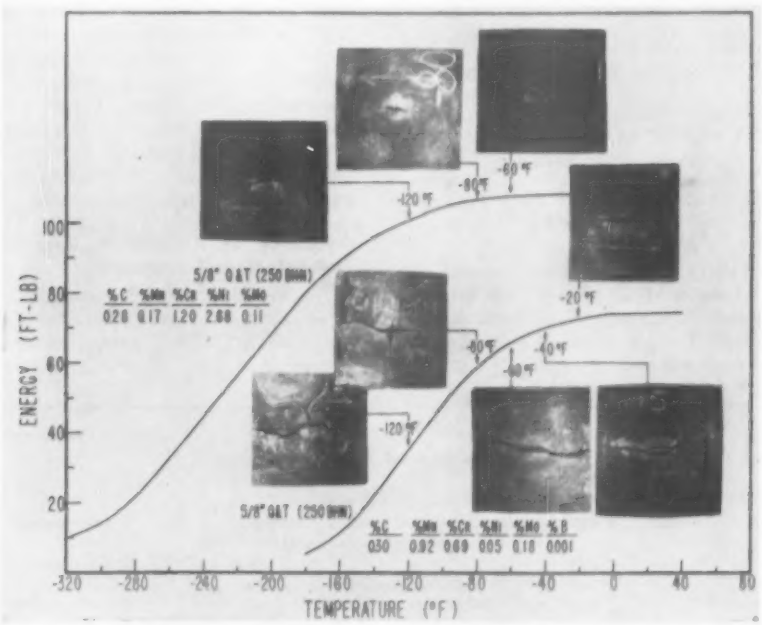

Fig. 7 Relationship of explosion crack-starter tests to Charpy V curves of 5/8-in. "K" (*top*, steel No. 1) and 5/8-in. "X" steel (*bottom*, steel No. 8)

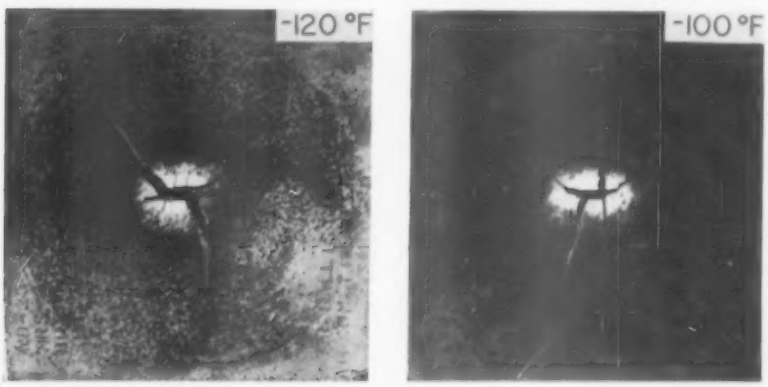

Fig. 8 Crack-starter tests of 1-in. "K" prime plate (steel No. 6). Fractures are ductile tears by high-energy blast

Table 1

Steel	*Observed range of Charpy V correlation with NDT, ft-lb*	*Average "fix" (usual value), ft-lb*	*Conservative "fix" (high end of range), ft-lb*
Rimmed mild steel[a]	3 to 7	5	7
Semikilled mild steel, A-7 or equivalent[b]	5 to 10	7	10
AB8-B	7 to 32	11	15[c]
Fully killed mild steel (Norm. AB8-C)	15 to 24	17	20[d]
High-tensile steel (Norm. HT8)	13 to 45	23	30[e]
A-302	11 to 30	20	30[f]
Quenched and tempered steel (250 BHN)	20 to 45	25	35
Quenched and tempered steel (375 BHN)	11 to 16	13	15[g]
12% Cr steel	10 to 30	15	20[h]
Nodular and malleable iron	3 to 8	5	8[i]

[a] Includes 7 ship fracture steels.
[b] Includes 11 ship fracture steels.
[c] Of 17 steels tested, only 3 cases observed to be higher than 15 ft-lb.
[d] Of 7 steels tested, only one case above 20 ft-lb.
[e] Only two steels involving steep Charpy V curves observed to be higher than 30 ft-lb. In the steep portion on these curves, a change of 10° F may result in a large change in ft-lb position.
[f] Of 15 steels tested, four cases observed to be 25 ft-lb or higher.
[g] High-hardness steels usually display Charpy V curves which do not rise to high maximum values in Charpy V tests.
[i] Of 28 steels tested, only two cases above 21 ft-lb.
[h] Approximately 50 test groups, no exceptions.

values of Charpy energy. For example, the temperature difference between 15 and 30 ft-lb for a steel of steeply rising Charpy V curve may be 15 to 20° F while the difference between 5 and 10 ft-lb for a steel characterized by a long tail may be of same order.

Detailed analysis of the data for all steels indicates that, irrespective of the range of values indicated in Table 1, the NDT temperature defined by the drop-weight test always falls within a range of 30° F about the Charpy V temperature indicated as the average fix value of Table 1.

As the type of steel changes, the use of Charpy V curve values to define the FTE and FTP temperatures is difficult because of the varying slopes of the curves and the different maximum values of energy which are obtained. The most direct method is to establish the NDT temperature by the described fix procedure and then to add a "ΔT" temperature correction to establish the approximate FTE and FTP temperatures. The addition of 30 to 40° F to the NDT to establish the FTE gives excellent results. Similarly, the addition of 80 to 100° F to establish the FTP is a safe procedure. Explosion crack-starter results indicate that the correct temperature normally will be within these ranges.

Materials

The high-strength materials reported herein varied in thickness from $^1/_2$ to 1 in. with the exception of ASTM A302 which represented material 2$^1/_2$ to 4$^1/_2$ in. thick. Table 2 lists the code, type, thickness, and chemical analyses of the test materials. The basic groups are as follows:

Steel	*Type*	*No. of heats tested*
K (Code)	A Standard Navy quenched and tempered steel of Krupp type	7
HY-80	A low-carbon variety of Krupp steel	1
"X" (Code)	Proprietary quenched and tempered steel	9 (10 plates)
"Y" (Code)	Proprietary low-carbon quenched and tempered steel	2 (5 plates)
HT8	Standard Navy high-tensile steel	20
A302	Commercial Mn-Mo high-tensile steel	9 (15 samples)
A203 Gr D	Commercial low-carbon 3$^1/_2$ % Ni steel	2

In addition to tests of as-received material, certain of these steels were reheat-treated, to check on the development of improved properties or as a check on temper-embrittlement susceptibilities, as pertinent to the steel in question.

Crack-Starter Test Results for K Steel

The Krupp-type steel (Mil-S-20154) represents a relatively high-alloy steel (nominal analysis 3.25% Ni, 1.25% Cr, 0.28% C) which has been used as a structural steel for applications involving relatively high-strength levels (100,000 psi minimum yield strength and 250–280 BHN).

Because of limitations of equipment, it has not been practical to conduct explosion crack-starter tests at temperatures below −120° F. Figures 7 and 8 illustrate K steel performance which indicate resistance to brittle fracture at −100 to −120° F. Drop-weight tests of this material developed NDT in the range of −170 to −200° F. By interpolation, the FTE should be located in the range of −130 to −160° F.

It should be noted that not all of the K material investigated was of this high quality. Figure 9 illustrates production material with −80 to −120° NDT. Explosion tests of the −120° F NDT, K steel located the FTE at approximately −70° F and the FTP at approximately −20° F. The −80° F NDT material was not available in sufficient quantity for explosion tests; however, the FTE is predicted to be in the range of −40 to −30° F and the FTP in the range of 0 to 20° F. It is interesting to note that the −80° F NDT steel was shifted to −170° F NDT on full reheat-treatment and the −120° F NDT steel was shifted to −200° F. Equivalent shifts were developed by the Charpy V curves of the steels. These data were interpreted to signify temper-embrittlement damage developed during or following the commercial tempering treatment.

Response of K Steel to Temper-Embrittlement Treatments

It is well known that K material may be embrittled by slow cooling through the 1150 to 750° F range following tempering at 1200° F or by reheating into this range.[9,10] The degree of embrittlement is a function of the time the steel remains in the embrittlement temperature range either by virtue of slow cooling or holding, and of the chemical composition. Increasing Ni, Cr, and Mn contents promote susceptibility to temper brittleness while additions of Mo have a counteracting effect. The temperature of most rapid embrittlement is approximately 950° F. Temper embrittlement is detectable only by notch-toughness tests; no measureable changes occur in tensile properties or hardness. Temper brittleness is believed to be due to a precipitate at the grain boundaries of an unknown compound, probably a carbide, but still not identified. The reaction is reversible, in that heating to temperatures slightly

Table 2—Data on Test Materials

Code No.	Steel type	Thickness in.	Chemical analysis C, %	Mn, %	Si, %	Cr, %	Ni, %	Mo, %	V, %	Ti, %
1	K	5/8	0.28	0.17	0.07	1.20	2.68	0.11	0.005	...
2	K	3/4	0.32	0.29	0.10	1.36	3.28	0.03	0.07	0.00
3	K	3/4	0.30	0.29	0.24	1.30	3.12	0.00	0.01	...
4	K (cast)	3/4	0.25	0.15	0.14	1.55	2.96	0.20	...	...
5	K	1	0.29	0.29	0.12	1.40	2.84	0.07	0.017	...
6	K	1	0.24	0.22	0.14	1.41	3.20	0.04	0.003	...
7	K	1	0.27	0.22	0.10	1.24	2.80	0.10	0.00	0.00
8	"X"	5/8	0.30	0.92	0.61	0.69	0.05	0.18	0.005	...
9	"X"	5/8	0.31	1.00	0.52	0.77	0.06	0.20	...	...
10	"X"	5/8	0.31	1.43	0.55	1.52	0.08	0.42	0.06	0.005
11	"X"	5/8	0.33	1.46	0.55	1.47	0.06	0.32	0.04	0.01
12	"X"	5/8	0.33	1.26	0.55	1.63	0.05	0.18	0.06	0.005
13	"X"	5/8	0.24	1.55	0.19	0.08	0.03	0.87	0.04	0.001
14	"X"	5/8	0.29	1.65	0.20	0.10	0.05	0.83	0.04	0.001
15	"X"	5/8	0.29	1.55	0.17	0.19	0.07	0.88	0.03	0.001
16	"X"	5/8	0.30	1.56	0.19	0.16	0.07	0.32	0.04	0.001
17	HY-80	1	0.15	0.26	0.26	1.00	2.21	0.23	0.00	0.00
18	"Y"	1/2	0.14	0.97	0.26	0.50	0.88	0.50	0.09	...
19	"Y"	1	0.17	0.90	0.18	0.61	0.91	0.46	0.06	...
20	HTS	1	0.15	1.24	0.24	0.06	0.16	0.01	0.01	0.01
21	HTS	1	0.15	0.95	0.22	0.15	0.11	0.01	0.02	0.01
22	HTS	1	0.16	1.33	0.26	0.26	0.05	...	0.01	0.05
23	HTS	3/4	0.17	1.21	0.26	0.12	0.12	...	0.12	...
24	HTS	1	0.11	1.17	0.30	0.13	0.13	0.04	0.06	0.02
25	HTS	1	0.13	0.94	0.27	0.03	0.13	0.03	0.06	0.03
26	HTS	1	0.16	0.97	0.26	0.10	0.20	0.04	0.08	0.03
27	HTS	1 3/16	0.16	0.98	0.24	0.10	0.20	0.04	0.06	0.04
28	HTS	1	0.14	1.06	0.21	0.10	0.13	0.04	0.08	0.05
29	HTS	1	0.15	1.02	0.30	0.20	0.07	0.03	0.12	0.05
30	HTS	1	0.14	1.10	0.28	0.06	0.05	0.03	0.10	0.05
31	HTS	1	0.13	1.23	0.31	0.14	0.05	0.03	0.13	0.02
32	HTS	1	0.13	1.05	0.23	0.06	0.03	0.03	0.10	...
33	HTS	1	...	...	...	...	...	...	...	...
34	HTS	1	...	...	...	...	...	...	...	...
35	HTS	1	...	...	...	...	...	...	...	...
36	HTS	1 1/4	0.15	1.37	0.26	0.10	0.22	0.01	0.04	...
37	HTS	1 1/4	0.15	1.24	0.24	0.10	0.12	0.01	0.04	...
38	HTS	1 1/4	0.14	1.13	0.34	0.10	0.08	0.01	0.04	...
39	HTS	1 1/4	0.16	1.17	0.25	0.17	0.15	0.01	0.04	...
40	A302	3	0.19	1.24	0.29	0.23	0.08	0.51	...	...
41	A302	2 1/2	0.29	1.25	0.27	0.14	0.13	0.50	...	...
42	A302	4 1/2	0.19	1.34	0.32	0.12	0.13	0.50	...	...
43	A302	2 1/2	0.20	1.19	0.18	0.12	0.22	0.56	...	...
44	A302	3 1/16	0.24	1.41	0.29	0.12	0.07	0.52	...	...
45	A302	3 1/2	0.26	1.43	0.29	0.05	0.07	0.52	...	...
46	A302	2 3/8	0.27	1.43	0.29	0.08	0.07	0.52	...	...
47	A302	2 3/8	0.26	1.41	0.27	0.07	0.08	0.52	...	...
48	A302	2 1/2	0.20	1.41	0.27	0.05	0.10	0.52	...	...
49	A203G-D	1/2	0.12	0.72	0.29	0.19	3.40	0.03	...	...
50	A203G-D	1	0.13	0.60	0.20	0.05	3.40	0.03	...	...

over the precipitation range (1200 or 1250° F) and fast cooling restores notch ductility.

Figure 10 presents a comparison of properly heat-treated 3/4-in. K steel (water-quenched from 1200° F tempering temperature) with material that was temper-embrittled as the result of slow cooling (air) from the tempering temperature, and material that was reheat-treated for 4 hr at 950° F. It may be seen that the damage resulting from air cooling is sufficient to raise the FTE to approximately −60° F and the FTP to approximately −20° F. The severe temper embrittlement resulting from 4-hr reheating times at 950° F raised the FTE and FTP to over +100° F. It should not be interpreted that all K plates should perform in this fashion since the extent of temper embrittlement which may be developed differs considerably for various K plates depending on composition. The significant feature being demonstrated here is that the Charpy V curves fully predict the extent of embrittlement developed by these treatments.

Crack-Starter Tests of Cast K Steel

It has been demonstrated for mild steels that cast and rolled steels behave exactly the same in the crack-starter test if their Charpy V transition ranges are developed over the same temperature range.[11] That is, Charpy V curves have exactly the same significance for cast or rolled steels. This point is demonstrated also for quenched and tempered steels (Fig. 11) by comparsion of crack-starter tests of cast and rolled K plates. This comparison is of interest for the evaluations of castings by Charpy V tests.

Crack-Starter Tests of "X" Steel

"X" steel represents relatively low-alloy commercial steels containing boron and zirconium. Metallurgical and hardenability characteristics of the nominal composition are such as to develop through-hardening easily when heat treated in section sizes up to approximately 1/2 in. thickness. Requirements for the conservation of critical alloy materials in times of emergency make the investigation of notch-ductility characteristics of this and similar low-alloy steels of particular interest.

The ultimate strength level obtained in fully hardened alloy steels is, of course, varied in heat treating by

tempering at different temperatures. The notch-ductility characteristics which are developed at a particular strength level, however, may vary from steel to steel. Consequently, various "X" type plates were tested after heat treatment to two strength levels. On the basis of two plates heat treated to a strength level comparable to that obtained in fully tempered K steel (250-280 BHN and 100,000 psi minimum ys) this material is indicated to have an NDT of approximately −100° F; an FTE of −50° F; and an FTP of approximately 0° F. The explosion crack-starter test results for one of these steels are shown in Fig. 7 (*bottom*).

In order to provide data on such steels heat treated to strength levels higher than that considered above for conventional structural applications, "X" type material was tested after heat treating to hardnesses of about 360 BHN (approximately 160,000 psi ys). Figure 12 presents the results of drop-weight and Charpy V tests made of plates taken from various heats of such material heat treated to this strength level. It is pertinent to note the relatively low-maximum energy shelves obtained in Charpy V tests (all heats displaying less than 30 ft-lb maximum energy shelf). Such a reduction in maximum energy is characteristic of relatively high hardness quenched and tempered steels. The experience gained in crack-starter tests of steels which display low-maximum Charpy V energy shelves has indicated that FTP relationships are still applicable; i.e., only shear fractures are developed at temperatures higher that that at which Charpy V specimens display 100% shear in fracture appearance. However, steels displaying exceedingly low-Charpy V energy shelves (e.g., 15 to 20 ft-lb) absorb less energy when rupturing in a shear fashion than that absorbed by the shear tearing of a similar steel which displays a high-Charpy V energy shelf (e.g., 80 to 100 ft-lb). Thus, for steels of a similar strength level, the application of sufficient energy to produce ductile tearing at temperatures above the FTP should result in somewhat longer ruptures in the steel characterized by a low-Charpy V energy level. The test results on "X" type steel heat treated to 360 BHN indicate that the NDT may vary from −20 to −100° F. Accordingly, it is estimated that the FTE could vary from +20 to −60° F and the FTP from +60 to −20° F.

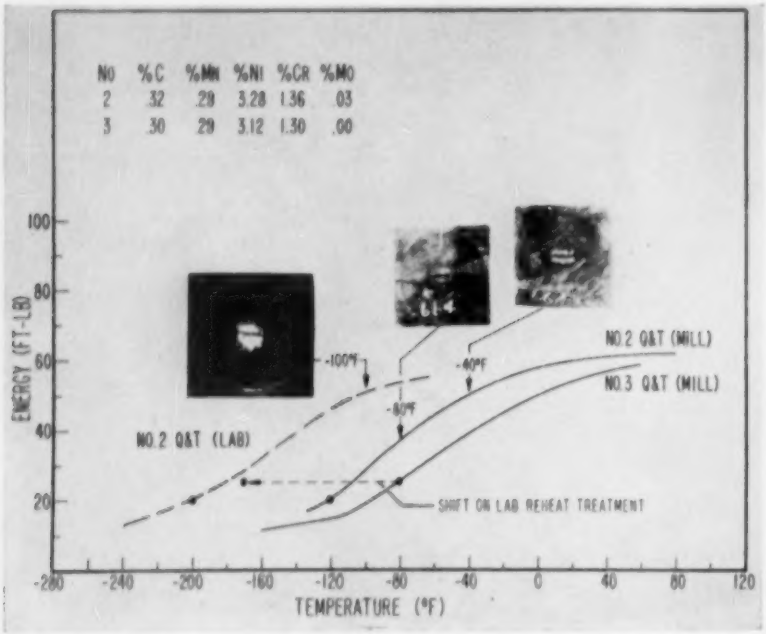

Fig. 9 Improvement of poor quality K-steel by reheat treatment. Note shift in nil ductility transition by approximately 100° F upon laboratory reheat treatments. Solid dots represent nil ductility transition temperatures and their relations to Charpy V energy

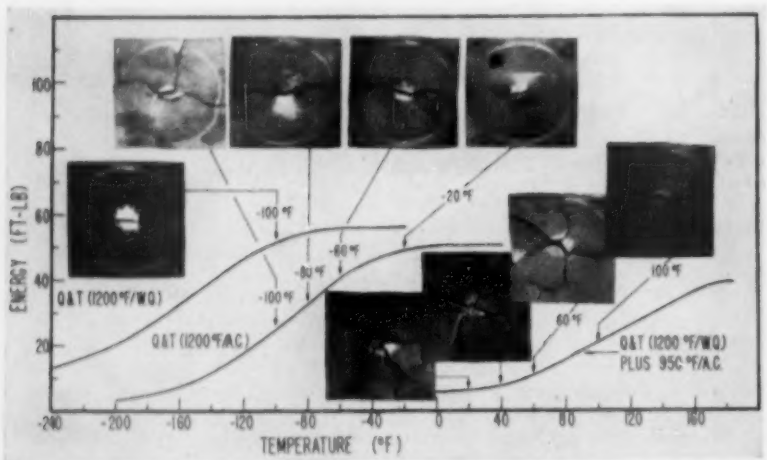

Fig. 10 Explosion crack-starter and Charpy V test results for $^3/_4$-in. "K" (steel No. 2) depicting optimum notch toughness when water quenched from tempering temperature (1200° F/WQ); moderate temper embrittlement as the result of air cooling (C1200° F/A.); and severe temper embrittlement resulting from reheating to 950° F (1200° F/WQ plus 950° F/AC)

Crack-Starter Tests of HY-80

A material equivalent to a low-carbon K steel (nominal analysis 2.25% Ni, 1.10% Cr, 0.20% Mo, 0.16% C) specified for certain structural applications (Mil-S-16216, 80,000–95,000 psi ys) is commonly termed HY-80. Figure 13 and Table 3 present the results of drop-weight and explosion crack-starter tests of HY-80 material as-received from the mill in comparison to material reheated for 4 hr at 950° F followed by water quenching. Since the maximum rate of temper embrittlement occurs at approximately 950° F, the data, as suggested by the high Mo content, are interpreted to indicate that HY-80 is not susceptible to temper embrittlement. In the as-received and reheated conditions the fracture characteristics of the HY-80 plate are as follows: NDT, −130° F; FTE, −90° F; FTP, −40° F.

Figure 13 illustrates that the temperature of transition in the fracture properties of this steel are predicted correctly by the Charpy V transition curves.

Crack-Starter Tests of "Y" Steel

"Y" steel represents a commercial high-yield strength, boron-treated material containing less than 1% of Ni, Mo, Cr, etc., considered for use for structural applications. In the fully quenched and tempered condition (1700° F/WQ + 1200° F temper), strength levels and hardnesses are obtained comparable to those developed in fully tempered K steel (250 BHN, 100,000 psi minimum ys). Crack-starter test results completed for 1/2 and 1 in. thick "Y" steel are summarized in Fig. 14 and Table 3. Four plates of the 1/2 in. thick steel were drop-weight tested to evaluate processing variables (cross rolling vs. straight-away rolling) and specimen orientation (transverse vs. longitudinal). No significant differences were observed due to these variables. The transition features of the crack-starter tests and Charpy V tests for the 1/2-in. plate were equivalent to those of a 1-in. plate from a separate heat. The NDT ranged from −80 to −90° F; the FTE −50° F; and the FTP from approximately 0 to −20° F. The differences in maximum Charpy V energy shelf observed for the two thicknesses is not significant to brittle-fracture characteristics; this fact has been demonstrated repeatedly for a great variety of materials. The transition range is always the important criterion of the Charpy V test.

On the basis of tests of limited data for only one plate (Table 3) "Y" material is believed not to be susceptible to temper embrittlement since reheating for 4 hr at 950° F did not result in shifting the NDT of material from the 1/2-in. plate. These observations corroborate the claims of the manufacturer.

Crack-Starter Tests of HTS

The material conventionally used for Navy structural applications involving moderately high strengths is a high-Mn steel termed HTS (Mil-S-16113 Grade HT, 88,000 psi maximum ts, and 47,000 psi minimum ys). Because of improvements in notch ductility, material 1/2 in. and thicker is specified to be furnished in the normalized rather than the as-rolled condition. Table 4 summarizes the crack-starter test results for normalized HTS plates. Steel No. 36 to 39 represent 1 1/4 in. thick plates obtained from an underwater test of a welded structure.

The material removed from a structure subjected to underwater explosion tests represents another example of "service-failures" which corroborates the predictions made as the result of crack-starter test data. After appreciable deformation was developed in the structure, a 39-in. brittle fracture, confined entirely to the plastically deformed region dimpled by the explosion, was obtained in one of the plates (No. 38). Drop-weight tests of material from this plate indicated a NDT of −10° F. The water temperature was 60° F, at which temperature propagation confined to plastic load-regions would be predicted by the crack-starter test critical fracture transition concepts.

Table 3—Brittle-Fracture Characteristics of HY-80 and "Y" Steels

Code No.	*Type*	*Thickness, in.*	*Tempering treatment*	*Hardness, BHN*	*NDT, ° F*
17	HY-80	1	Mill	201	−130
17	HY-80	1	Mill + 950° F/WQ	207	−130
18A	"Y"	1/2	Mill	262	− 80
18B	"Y"	1/2	Mill	269	− 80
18C	"Y"	1/2	Mill	255	− 90
18D	"Y"	1/2	Mill	267	− 90
18E	"Y"	1/2	Mill + 950° F/WQ	262	−100
19	"Y"	1	Mill	262	− 80

The range of quality observed in a survey of these steels is indicated in Fig. 15. One of the steels which exhibited the best performance in crack-starter tests (NDT, −60° F) is shown in comparison to two steels exhibiting the poorest performance (NDT, +10° F and +40° F). As shown in Table 4, these poor steels were reheat-treated under optimum laboratory conditions to check the effectiveness of the mill-normalizing operation. Although an improvement was obtained in one of the steels (NDT of 40° F shifted to −20° F) the others remained unchanged. The resulting improvement developed in the one steel by reheat-treating suggests that this steel was not mill-normalized.

Crack-Starter Tests of Heavy Section A302

Existing boiler-code specifications limit the design for pressure vessels to stress values of a maximum of one-fourth ultimate strength (ts) of the material employed. Although such limitations approach a design factor of 2.5 based on ys for the carbon steels normally used, code requirements do not permit pressure-vessel design on the basis of such a factor. If permitted, such practices would afford the opportunity for the optimum utilization of high-strength steels possessing a higher ts/ys ratio than the carbon steels. Vessels of high-strength steels have been built, however, for specialized applications with design factors of 2.5 and, technically, not

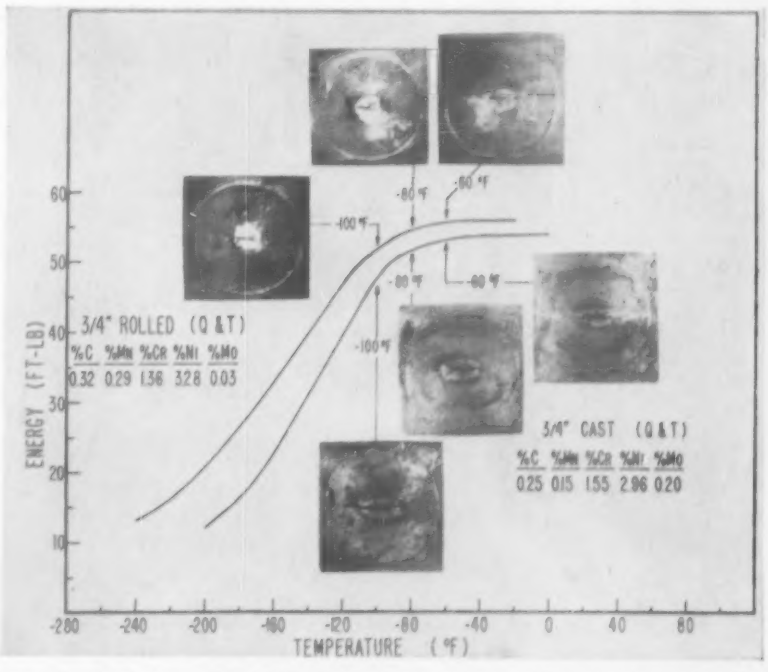

Fig. 11 Explosion crack-starter and Charpy V test results indicating equivalent performance of properly heat-treated cast K-steel (No. 4) and rolled K-steel

complying to the code. For reasons of economy and the greatest net return from the use of high-strength materials, the special pressure vessels have been constructed of ASTM-A302 material (80,000 psi minimum ts, 50,000 psi minimum ys).

During the past year, brittle-fracture failures of two such vessels constructed of heavy wall thickness A302 material have been experienced. The first of these brittle failures occurred during hydrostatic proof testing of the fabricated vessel at a temperature between 55 and 60° F (Fig. 16). The second occurred at an identical temperature range in a partially fabricated vessel as the result of residual welding stresses developed during the welding of the manway reinforcement. Charpy V tests of steel taken from these two "service-failure" vessels corroborated the predictions made from drop-weight tests of these steels with reference to possible initiation of brittle fracture (NDT) at temperatures corresponding to the 20 ft-lb Charpy V temperature.[1] Drop-weight tests of these two failure steels indicated an NDT of 70° F for the first, and 100° F for the second failed vessel.

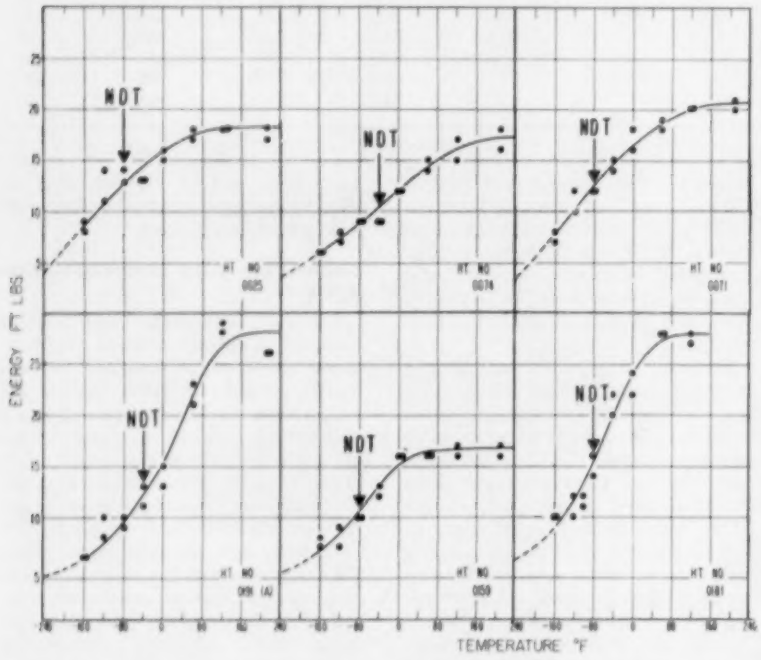

Fig. 12 Charpy V and drop-weight test results of high-hardness "X" material (steel No. 10, *upper left corner*, to No. 15, *lower right corner*)

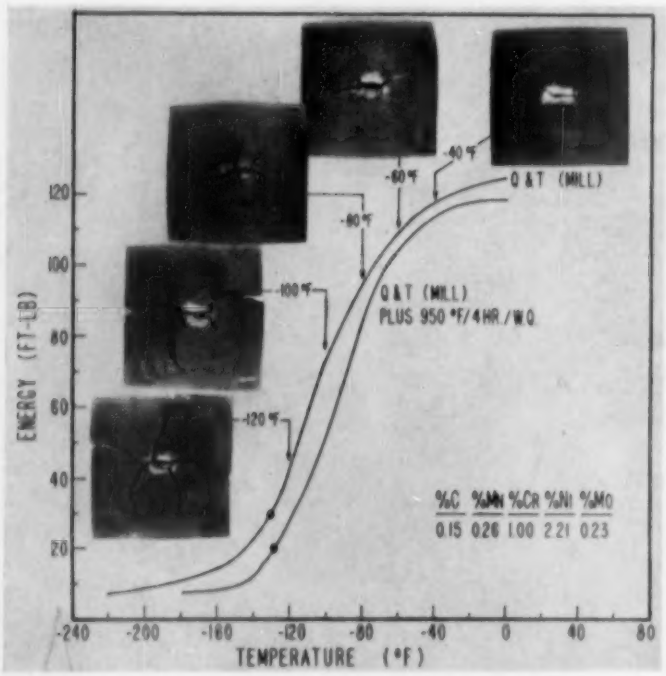

Fig. 13 Charpy V and crack-starter test results (explosion and drop-weight) for HY-80 (steel No. 17) as received from the mill and after a 4-hr reheating period at 950° F

For the development of optimum strength properties in A302 material, a heat treatment consisting of normalizing and tempering is required. Because of questions related to the heat treatment of the steel involved in the initial failure, drop-weight tests were made of heavy-section A302 material after several different types of heat treatments. Table 5 lists pertinent data relative to the tests performed on the various A302 heats. Figure 17 represents a graphical summary of these tests. The Charpy V curve and related drop-weight temperature position (heavy dot superimposed upon the V curve) are shown for the 3 in. thick (initial failure under hydrostatic testing) and $2^1/_2$ in. thick (second failure due to residual stresses) A302 steels. In appropriate locations of Charpy V energy and drop-weight temperature, the NDT results of the other steels are shown by the heavy dots and, the Charpy V curves for these steels have been eliminated for purposes of clarity. An average Charpy V energy of approximately 20 ft-lb and a range of 10 to 30 ft-lb appears to delineate the potential range of NDT characteristics for these A302 materials. That is, 30 ft-lb should be used as a minimum value for a safe fix for the NDT.

For Naval applications such as air pressure vessels within interior holds of ships (minimum estimated service temperature of 40° F), new material is required to meet impact specifications of 30 ft-lb minimum at 10° F. This provides a safety factor of 30° F based on NDT and 40° F lowest operating temperature. The dashed curve of Fig. 17 represents the authors' estimation of the minimum acceptable heat under the new specification. Material of this nature (or better) should preclude the possibility of brittle fracture initiation under normal service conditions as stated above.

For the "accident case" (Fig. 5) there is a small probability of failure

Table 4—Brittle-Fracture Characteristics of HTS Steel

Code No.	Thickness, in.	Normalized	NDT, ° F	FTE, ° F
20	1	Lab.	−40	−10
21	1	Lab.	−40	−10
22	1	Lab.	−50	−10
23	3/4	Mill	−60	−20*
24	1	Lab.	0	40*
25	1	Lab.	−20	20*
26	1	Lab.	−20	20*
27	1 3/16	Lab.	−40	0*
28	1	Lab.	−20	20*
29	1	Mill	0	30*
29	1	Lab.	0	40*
30	1	Mill	40	90
30	1	Lab.	−20	20*
31	1	Mill	10	70
31	1	Lab.	10	50*
32	1	Mill	−20	10
32	1	Lab.	−20	20*
33	1	Mill	0	50
34	1	Mill	0	40*
35	1	Mill	−20	20*
36	1 1/4	Mill	−50	−10
37	1 1/4	Mill	−40	10
38†	1 1/4	Mill	−10	30
39	1 1/4	Mill	−10	30*

* Values deduced by "ΔT" correction.

† This plate developed brittle fracture contained entirely within plastic deformation region in underwater explosion tests in 60° F water.

at 40° F since a 0° F, NDT material (minimum accepted) should have an FTE in the range of 30 to 50° F. The probability is considered reasonably small because it would be necessary to have a combination of:

(1) A crack flaw
(2) Minimum quality material
(3) 40°/50° F operating temperature
(4) "Accident" loading at the crack position

Thus, the 30° F safety factor based on the NDT provides for additional safety involving the possibility of accident in service.

NDT Evaluations of A203 Grade D Material

A low-carbon, 3 1/2% nickel steel frequently used for pressure vessels, valves, fittings or pressure lines is covered by ASTM-A203 Grade D Specifications. Under SA300, this material is specified for low-temperature service for temperatures down to −150° F providing average Charpy keyhole impact values of 15 ft-lb are obtained. Commercial material from two heats of A203 (1/2-in. plate and 1-in. bar stock) was obtained for drop-weight and Charpy tests.

The 1/2-in. plate of 3 1/2% Ni steel (No. 49) was furnished in the normalized and tempered condition, however, the 1-in. 3 1/2% Ni bar stock (No. 50) was furnished only in the normalized condition. Figure 18 and Table 6 present the results of Charpy and drop-weight tests of the A203 material in the as-received condition. NDT values of −190° F and −130° F were obtained respectively for the 1/2-in. plate and 1-in. bar stock. Tempering and testing additional sections from steel No. 50 revealed no change in NDT (−130° F) or in the Charpy V transition curve.

In Fig. 18, the conventional keyhole scatterband data are lacking for steel No. 49 since no tests were conducted at intermediate temperatures between −260° F and −320° F (keyhole values of 21, 24, 26 and 27 ft-lb were obtained for −260° F and 5, 6, 8 and 9 ft-lb for −320° F tests). On the basis of existing practices for unfired pressure vessels (15 ft-lb minimum keyhole impact value at lowest service temperature) steel No. 49 would meet approval for use at −260° F (70° F below NDT of −190° F) and steel No. 50 for use at −220° F (90° F below NDT of −130° F). The 20 ft-lb Charpy V temperatures, however, are indicated by these data to be the approximate "fix" for the NDT. It is seen that the use of such a criterion (20 ft-lb V) for these steels would permit the use of steel No. 49 (NDT of −190° F) but not the use of steel No. 50 (NDT of −130° F) for service at temperatures of −150° F.

Comparison of Charpy V and Keyhole Data for Quenched and Tempered Steels

As the result of studies involving various notch-bend specimens, the Charpy V energy transition curve is considered by most research investigators to provide the most significant and practical method of correlation to service performance of welded structures. The keyhole test, however, is still used extensively in many industrial as well as ASME Specifications for pur-

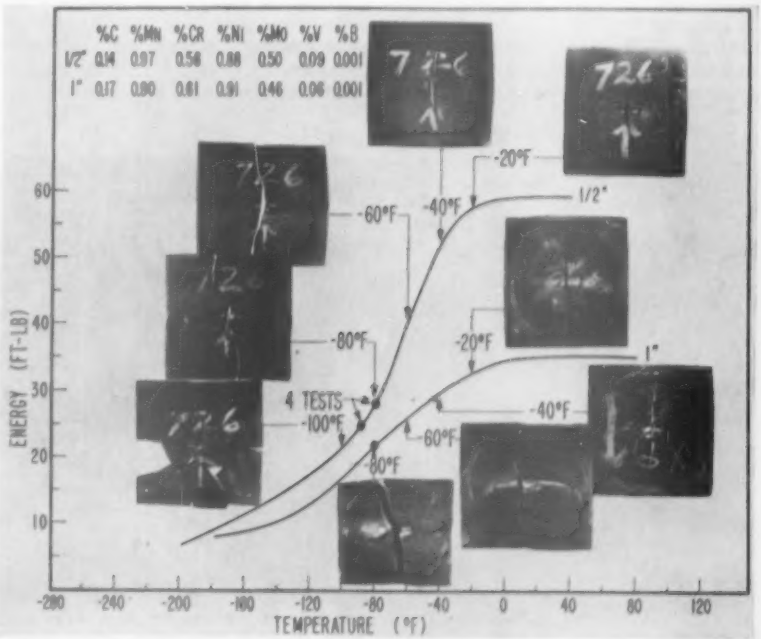

Fig. 14 Charpy V and crack-starter test results (explosion and drop-weight) for 1/2- (No. 18) and 1-in. (No. 19) "Y" steels

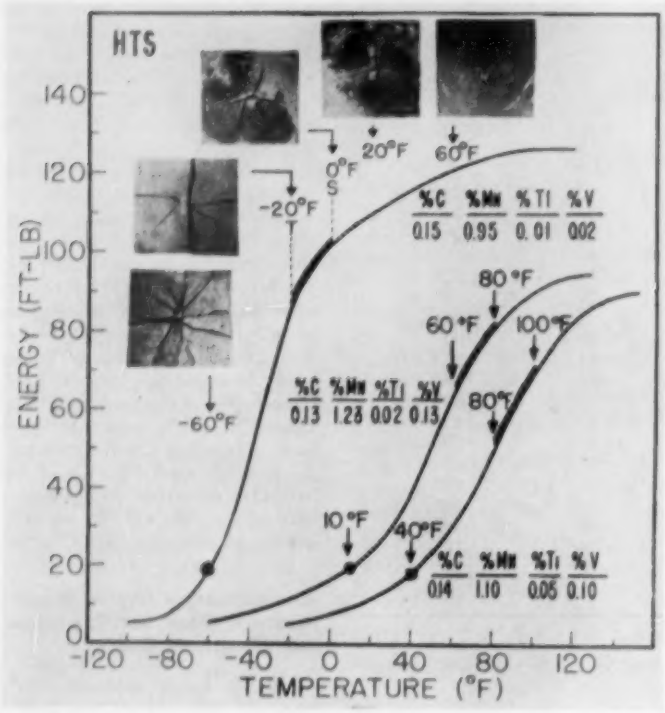

Fig. 15 Charpy V and crack-starter test results indicating probable range in quality expected for mill-normalized HTS plates (steel No. 21, *top*; No. 31, *center*; No. 30, *bottom*)

poses of specifying notch-ductility requirements. It has been demonstrated[2] that the empirical relationships existing between keyhole and V curves for the rimmed and semikilled ship plate steels do not hold for other types of medium steels; e.g., fully killed, high-manganese medium steels. For this investigation, it was considered of interest to establish the interrelationships existing between V and keyhole curves for the quenched and tempered steels.

The empirical correlation established between V and keyhole curves for the ship steels has been based upon the temperature differential observed between the 10 ft-lb V and the keyhole midspan temperatures (approximately 20° F separation). A great number of the quenched and tempered steels, however, develop "secondary shelves" in the lower portion of the Charpy V curve which preclude the determination of such a relationship. Figure 19 summarizes the significant features of V and keyhole curves as related to NDT for quenched and tempered steels. For steel No. 9 (Fig. 19, *top*), it is noted that the Charpy V curve maintains an average fracture energy of approximately 20 ft-lb over a range of 100° F (24 ft-lb at −120° F and 18 ft-lb at −220° F). The NDT as determined by drop-weight tests occurs approximately at the beginning of this "secondary shelf." The keyhole curve for this steel drops off only slightly in this range, and does not develop the scatterband-zone to temperatures as low as −220° F. Such behavior has been observed for numerous quenched and tempered steels. For such steels, it becomes apparent that one must be cognizant of the complete transition curve, and that impact values obtained at only one temperature may be highly misleading as to the actual notch-toughness of the steel in question.

It has long been recognized that temper embrittlement is more readily revealed by Charpy V than by keyhole tests. The possible errors introduced by specifying keyhole values at single temperatures, are illustrated by the test results (Fig. 19, *center* and *bottom*) for K steel No. 3 described previously in Fig. 9. The laboratory reheat treatment of the mill quenched and tempered steel resulted in an improvement of approximately 100° F in both the NDT and Charpy V transitions. On the basis of the keyhole midspan transition temperatures, however, an improvement of approximately 50° F is observed (−200

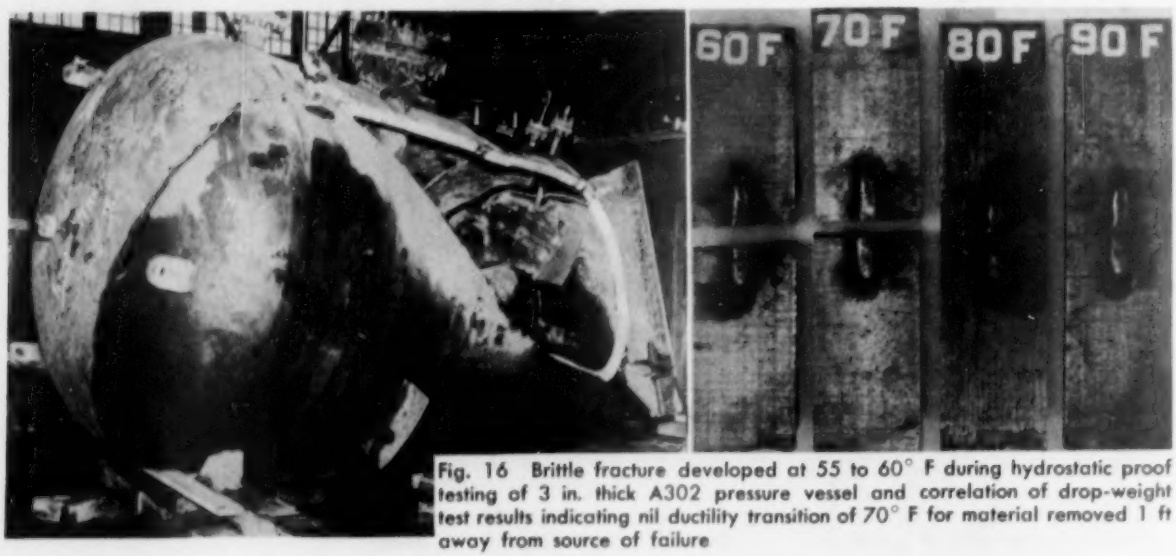

Fig. 16 Brittle fracture developed at 55 to 60° F during hydrostatic proof testing of 3 in. thick A302 pressure vessel and correlation of drop-weight test results indicating nil ductility transition of 70° F for material removed 1 ft away from source of failure

to −255° F) to be due to the laboratory reheat treatment. More importantly, at the significant temperature of interest for these two steels, −80° F (at which temperature fracture initiation is possible in the temper-embrittled steel but not in the laboratory reheat-treated steel) the average keyhole impact values are higher by 3 ft-lb for the temper-embrittled steel than for the reheat-treated steel. In addition, for the temperature range between −80 and −160° F, the keyhole data indicate the temper-embrittled steel to be more notch tough than the laboratory reheat-treated steel. For any criterion of reference based upon Charpy V tests (energy absorption, fracture appearance, etc.) it is obvious that these two steels are evaluated in the same order as that established by NDT determinations.

Comparison of Quenched and Tempered and Normalizing Heat Treatments of Alloy Steels

It is well known that the optimum combination of mechanical properties and notch ductility is obtained in alloy steels by quench and tempering heat-treating procedures aimed at developing low-temperature transformation structures. It is of interest to compare properties obtained by normalizing alloy steels with properties resulting from conventional quenching and tempering treatments. Tables 7 and 8 present data on cast steels obtained in the course of investigations of steels considered for possible use as ship propellers.[12] It is apparent that although the strength properties developed by these two heat treatments are roughly equivalent, the NDT of the quenched and tempered condition is greatly superior (−70 to −100° F) to that of the normalized and tempered condition (+40 to +60° F). Thus, the use of the normalizing heat treatment results in fracture initiation characteristics equivalent to those of plain-carbon steels. The primary purpose of alloy additions to steels is the effect they exert on hardenability as related to microstructure. By retarding high-temperature transformation, alloying elements facilitate the development of low-temperature transformation products desirable for high notch ductility. Depending on the type and amount of alloy present, or on the section size treated, normalizing heat treatments tend to vitiate the effect for which the alloy was intended.

Conclusions

Tests were conducted at various temperatures to determine the fracture characteristics of high-strength structural steels when loaded beyond the yield point in the presence of a sharp-crack defect. The sharp-crack defect was introduced by means of the brittle crack-starter weld method developed at the Naval Research Laboratory.[1] Two test methods described as the drop-weight and explosion crack-starter tests were utilized to evaluate the fracture characteristics of the high-strength steels.

In the drop-weight test, loading is accomplished by dropping a weight which impacts at midspan of a $3^1/_2$ x 14 in. x plate thickness specimen supported on a 12-in. span. A stop is placed under the specimen to limit the specimen deformation to minute amounts which may be described as "incipient yielding." Thus, this test determines the temperature below which yielding is not possible in the presence of a sharp-crack and fracture results. In the explosion crack-starter test, a plate 14 x 14 in. x plate thickness is placed over a circular die and loaded by explosion of an offset charge. This test indicates the degree of "forcing" required to initiate fracture (at temperatures above the drop-weight test transition) by the amount of bulging developed prior to fracture. In addition the explosion crack-starter test develops information concerning fracture propagation by establishing the temperatures at which brittle fractures propagate through the lightly loaded edge-regions (indicative of ability to propagate through elastic-load regions) or are

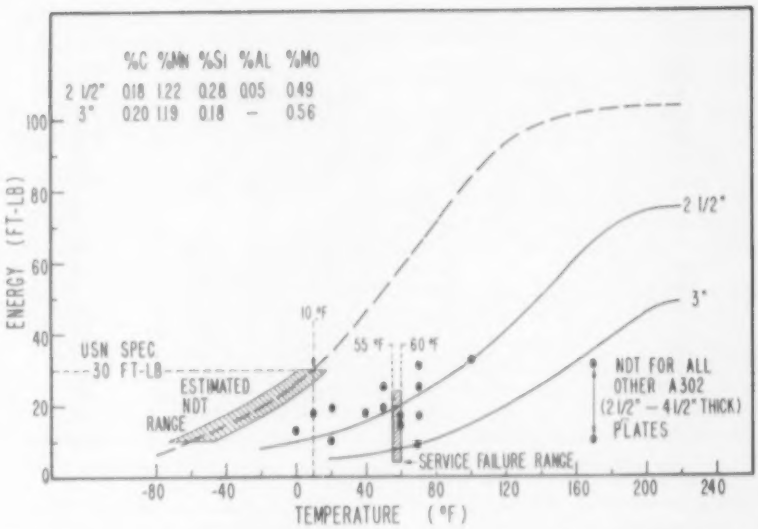

Fig. 17 Charpy V and drop-weight test results of heavy section A302 steels. Initiation of brittle fractures occurred at service temperatures of 55 to 60° F for 3- (No. 40) and $2^1/_2$-in. (No. 43) steels

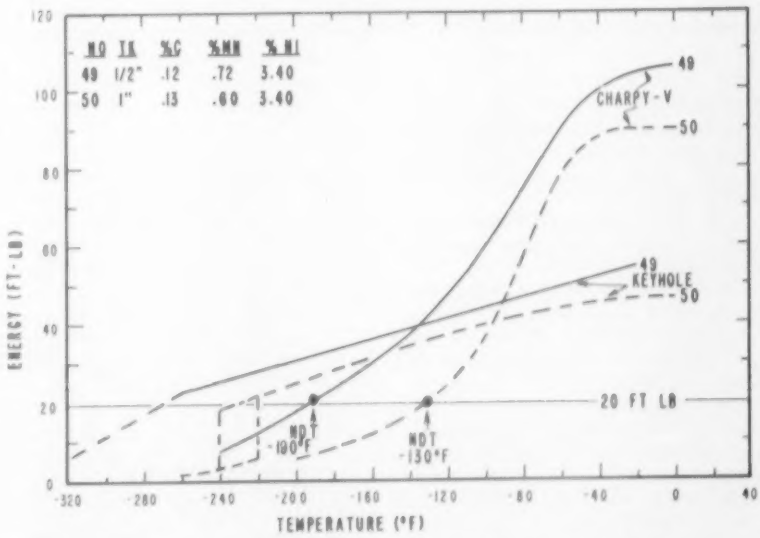

Fig. 18 Charpy and drop-weight test results of A203 Grade D steels

Table 5—Brittle-Fracture Characteristics of A302

Code No.	Thickness, in.	Heat treatment	NDT, °F
40*	3	Ann. (1650° F) + Temp. (1150° F)	70
40	...	Ann. (1650° F)	10
40	...	Norm. (1650° F)	40
40	...	Norm. (1650° F) + Temp. (1175° F)	30
41	2 1/2	Ann. (1650° F)	20
41	...	Norm. (1650° F)	70
41	...	Norm. (1650° F) + Temp. (1150° F)	50
41	...	Norm. (1650° F) + Temp. (1250° F)	20
42	4 1/2	Norm. (1650° F) + Temp. (1225° F)	0
43*	2 9/16	Norm. (1700° F) + Temp. (1150° F)	100
44	3 1/16	Norm. (1700° F) + Temp. (1150° F)	60
45	3 1/2	Norm. (1700° F) + Temp. (1150° F)	70
46	2 9/8	Norm. (1700° F) + Temp. (1150° F)	60
47	2 9/8	Norm. (1700° F) + Temp. (1150° F)	70
48	2 1/2	Norm. (1650° F) + Temp. (1150° F)	50

* Samples from failed tanks (55 to 60° F failures); material within 1 ft of source point.

Table 6—Brittle-Fracture Characteristics of A203 Grade D Steels

Code No.	Type	Thickness, in.	Heat treatment	NDT, °F
49	A203D	1/2	Norm. (1580° F) + Temp. (1200° F)	−190
50	A203D	1	Norm. (1650° F)	−130
50	A203D	1	Norm. (1650° F) + Temp. (1200° F)	−130

restricted to the cold-worked (bulged) center regions. The utmost of resistance to fracture is also indicated in this test by the development only of short, ductile shear tears.

The test procedures define three critical fracture transition temperatures, as follows:

(1) *NDT (nil ductility transition)*. Below this temperature the steels show no ability to exceed yield-point loading, i.e., % elongation in the presence of a sharp crack is nil.

(2) *FTE (fracture transition for elastic loading)*. Above the NDT temperature the steels show notch ductility to the extent that relatively large amounts of deformation may be applied *before* fracture initiation occurs. The amount of prefracture deformation increases rapidly from the NDT temperature to the NDT plus 30/50° F temperature. While fracture initiation is difficult in this range (requires forcing by plastic loading) propagation is "easy" as indicated by the fact that the fractures continue through the lightly loaded edge-regions supported by the die. For all steels tested, the FTE temperature is located approximately 40° F above the NDT temperature and marks the temperature above which fracture propagation becomes difficult and the fractures remain entirely within the central bulge regions, i.e., in the regions that are embrittled by cold work developed by bulge deformation. The FTE temperature correlates with the Robertson and Esso test transitions which mark the temperature above which fracture propagation through elastic-load regions is not possible.

(3) *FTP (fracture transition for plastic loading)*. This temperature, located for all steels approximately 100° F above the NDT and 60° F above the FTE, marks the temperature above which the explosion test may tear the steel by shear but cannot develop brittle fracture. This temperature represents a point of absolute ductility irrespective of the severity of loading.

In recognition of this behavior, the various steels are characterized by the development of transitions from complete ductility to nil ductility over a range of temperatures defined by three points of critical change in fracture characteristics—FTP, FTE and NDT, as described.

The following table summarizes the critical fracture transition temperatures of various high-strength steels. In the case of steels which were tested in quantity, the values represent average performance (A); tests of a limited number of steels are indicated as (L). A special case is made for A302 casualty material from failed pressure vessels and minimum quality material falling under a new Navy specification. Values for ship plate obtained from wartime

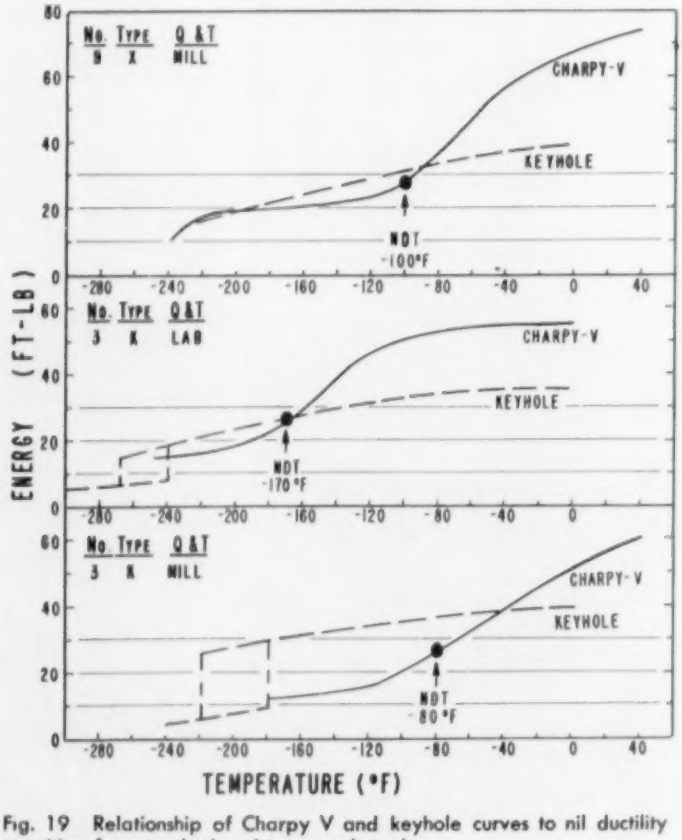

Fig. 19 Relationship of Charpy V and keyhole curves to nil ductility transition for quenched and tempered steels

ships and from wartime stock are also included for comparison purposes. These latter steels (of semikilled or rimmed variety) varied in thickness from $^5/_8$ to $1^1/_2$ in., and approximately 33 ship-plate steels were tested.[2,3]

region. Above the FTP temperature, it is possible only to tear the steel in a ductile manner.

For the high-strength steels, the NDT temperature is generally related to the 20/30 ft-lb temperature of the Charpy

Steel	*NDT, ° F*	*FTE, ° F*	*FTP, ° F*
K	−180 (A)	−140 (A)	−100 (A)
HY-80	−130 (L)	− 90 (L)	− 40 (L)
X* (250 BHN)	−100 (L)	− 50 (L)	− 10 (L)
Y†	− 90 (L)	− 50 (L)	− 10 (L)
HTS (norm.)	− 20 (A)	+ 30 (A)	+ 80 (A)
A302 (casualty I)	+ 70	+120 (P)	+170 (P)
A302 (casualty II)	+100	+150 (P)	+200 (P)
A302 (new spec. min quality)	+ 10	+ 60 (P)	+100 (P)
AB8-C (norm.)	− 20 (L)	+ 20 (L)	+ 80 (L)
A203D	−130/−190 (L)	−90/−150 (L)	−30/−90 (L)
Ship plate of ship fracture type	+20/30 (A)	+ 70 (A)	+140 (A)

NOTES: (A) Average; (L) Limited tests; (P) Predicted values.

* "X" Commercial quenched and tempered steel; 0.30% C, 1.00% Mn, 0.50% Si, 0.75% Cr, + B + Zr.

† "Y" Commercial quenched and tempered steel; 0.15% C, 0.90% Mn, 0.20% Si, 0.50% Cr, 0.90% Ni, 0.50% Mo, 0.05% V.

It is interpreted that if sharp cracks are present in structures, a possibility of fracture initiation exists when minute amounts of yielding in the vicinity of the cracks are developed at temperatures below the NDT transition. In the range of temperatures between NDT and FTE transitions, severe plastic deformation must be developed in the structure to initiate fracture; when initiated, however, fracture propagation is possible in regions outside of the location of "forcing." At temperatures in the FTE to FTP range, very severe plastic loading is needed to initiate fracture and the fractures may run only in the plastic deformation

V energy transition curve. Some of these steels do not reach relatively high maximum energies; as an example, steels of relatively high hardness which ordinarily have a maximum Charpy V energy of 30 ft-lb or less, are characterized by NDT temperatures related to the 10/15 ft-lb Charpy V temperature. The procedures by which Charpy V data may be utilized for the approximation of the three critical fracture transition curves have been presented. The determination of the NDT temperature by drop-weight tests makes it possible to estimate the FTE and FTP temperatures to within relatively narrow temperature ranges. Because of the tendency of quenched and tempered steels to develop "secondary shelves" in the 15 to 20 ft-lb regions, single temperature determinations of Charpy V impact energies are not adequate, and may be highly misleading with respect to the notch ductility of the steel. The NDT temperature generally occurs near the beginning of these "secondary shelves." For service correlation purposes, it is preferable to establish the complete Charpy V energy transition curve.

The high-strength steels have been shown to deviate greatly from the empirical relationship for Charpy keyhole midspan and Charpy V 10 ft-lb temperature established for the mild steels. In addition, experience has indicated that it was exceedingly difficult to establish the keyhole midspan temperature for steels which require testing at temperatures of −220 to −300° F in order to establish the position of the scatterband range. Single temperature keyhole energy determinations are highly misleading and may result in considerable error with respect to the estimation of notch toughness of these steels. For example, it has been shown that single temperature keyhole tests in the temperature range of possible initiation of brittle fracture may, in fact, indicate a temper-embrittled steel to be more notch-tough than the same steel heat treated to optimum toughness and properties. For service correlation purposes, Charpy V energy transition curves are preferred.

It should be appreciated that production steels have a quality range; a range of 60° F in NDT is not unusual. The wartime ship-fracture steels (18 investigated) showed at least such a spread (0° F for the best and 60° F for the worst). Examples of greater spreads have been encountered in other types. Thus, the data presented herein are considered to provide a guide as to the probable tolerance of the various steels with respect to specific temperatures and to various types of anticipated loadings. For certain applications where the steels may be of borderline quality for the intended service (A302 for example) rigid notch-ductility specifications may be necessary to achieve close control. On the other hand, for steels such as K type, which are expected to have critical fracture transitions far below the intended service temperatures, simplified procedures which determine whether proper heat treatment was applied may be used for control or check. This, for example, would be the case for a quenched and tempered steel of general −160° F NDT type which is to be used only at atmospheric temperatures.

Table 7—Chemical Analysis

Heat	*C%*	*Mn %*	*Si %*	*Cr %*	*Ni %*	*Mo %*	*V %*
D50	0.25	0.76	0.81	0.70	1.02	0.28	0.06
NRL D40 (A90 steel)	0.19	0.68	0.44	1.41	—	0.41	—
Commercial (A90 steel)	0.16	0.65	0.47	1.30	0.45	0.51	—

Table 8—Results of Heat Treatment

Heat	*Section,* in.*	*Heat treatment†*	*Ys, kips/ in.²*	*Ts, kips/ in.²*	*RA, %*	*EL, %*	*NDT, ° F*
D50	4	WQ & Temp. (1)	82	104	45	21	− 70
	1	WQ & Temp. (1)	88	108	50	22	− 80
	4	Norm. & Temp. (2)	91	111	48	20	+ 60
D40	1	Norm. & Temp. (3)	75	96	59	21	+ 40
(A90 steel)	1	OQ & Temp. (4)	94	110	46	19	−100
Commercial (A90 steel)	4	Norm. & Temp. (5)	—	—	—	—	+ 40

* Plates 4 x 14 x 14 in. and 1 x 14 x 14 in. D40 and D50 NRL Cast Heat numbers. Commercial, represents material obtained from a commercial foundry.

† (1) 1650° F, AC, 1550° F, WQ, 1250° F, FC. (2) 1650° F, AC, 1550° F, AC, 1250° F, AC. (3) 1700° F, AC, 1225° F, FC. (4) 1700° F, OQ, 1225° F, AC. (5) 1675° F, FC, 1750° F, AC, 1150° F, FC.

Acknowledgment

The authors acknowledge the support

and interest in this investigation by T. Griffin of Code 582, Bureau of Ships.

References

1. Puzak, P. P., Eschbacher, E. W., and Pellini, W. S., "Initiation and Propagation of Brittle Fracture in Structural Steels," THE WELDING JOURNAL, **31** (12), Research Suppl., 561-s to 581-s (1952).

2. Puzak, P. P., Schuster, M. E., and Pellini, W. S., "Applicability of Charpy Test Data," *Ibid.*, **33** (9), Research Suppl., 433-s to 441-s (1954).

3. Puzak, P. P., Schuster, M. E., and Pellini, W. S., "Crack-Starter Tests of Ship Fracture and Project Steels," *Ibid.*, **33** (10), Research Suppl., 481-s to 495-s (1954).

4. Pellini, W. S., "The Evaluation of the Significance of Charpy Tests," ASTM Symposium on Effect of Temperature on the Brittle Behavior of Metals with Particular Reference to Low Temperatures, Atlantic City, N. J. (June 28–30, 1953). (Special Tech. Pub. No. 158) Philadelphia, *American Society for Testing Materials*, 1954.

5. Robertson, T. S., "Propagation of Brittle Fracture in Steel," *The Journal of the Iron and Steel Inst.*, **175** (December 1953).

6. Feeley, F. J., Northup, M. S., Kleppe, S. R., and Gensamer, M., "Studies on the Brittle Failure of Tankage Steel Plates," THE WELDING JOURNAL, **34** (12), Research Suppl., 596-s to 607-s (1955).

7. Williams, M. L., "Investigation of Fractured Steel Plates Removed from Welded Ships," Ship Structure Committee Report, Ser. No. NBS-3 (June 1951).

8. Puzak, P. P., and Pellini, W. S., "Evaluation of Notch Bend Specimens," THE WELDING JOURNAL, **33** (4), Research Suppl., 187-s to 192-s (1954).

9. Pellini, W. S., and Queneau, B. R., "Development of Temper Brittleness in Alloy Steels," *Trans. ASM* **39**, 139–161 (1947).

10. Pellini, W. S., and Eschbacher, E. W., "Investigation of the Performance of 1 In. STS Weldments of G260 and 25–20 Types," NRL Memorandum Report No. 191 (July 1953).

11. Pellini, W. S., Brandt, F. A., and Layne, E. E., "Performance of Cast and Rolled Steels in Relation to the Problem of Brittle Fracture," *Trans. AFS* LXI: 243–262 (1953).

12. Brandt, F. A., Bishop, H. F., and Pellini, W. S., "Martensitic (Type 410) Stainless Steel for Propellers," NRL Memorandum Report No. 376 (September 1954).

RESEARCH NEWS

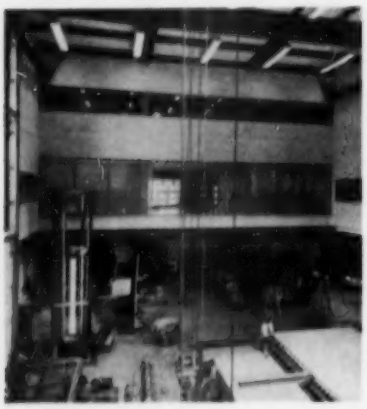

Large Test Chamber Erected by Cornell

A hangar-sized test chamber on the Cornell University campus in Ithaca, N. Y., is giving university engineers a better tool for finding out how structures and materials react to the stresses and strains of actual use.

The unusual facility is designed to act as a huge testing machine, capable of pulling, squeezing, bending and twisting structures as big as a medium-sized house. Its ability to put a structure to three-dimensional tests is said to give it an advantage over conventional testing devices of its range.

Although tests so far have been limited to comparatively simple structures, the chamber can handle full-scale bridge and airplane components and other units of similar size.

Filling a wing of Thurston Hall, the chamber soars 40 ft from a floor that is 55 by 60 ft in area. Forces and loads can be applied from ceiling, floor and side walls in all sorts of combinations and up to many thousands of pounds. A 40 by 90 ft lower ceilinged part of the same testing area offers additional space for such work.

The big test bay is the realization of a desire of S. C. Hollister, Cornell's dean of engineering, "to simulate the real performance of engineering structures and devices under the complex conditions of actual use."

One current project is an experimental study of a full-scale pressure vessel being conducted by Prof. E. T. Cranch to confirm calculations made by Prof. P. P. Bijlaard at Cornell under a contract with the Welding Research Council.

Internal forces are created by pressurized oil within the tank. External forces and couples are applied to various pipe attachments. The strains in the neighborhood of the pipes are measured with electrical strain gages.

Rugged as well as versatile—some have likened it to a torture chamber—the hall is floored with 18 in. of reinforced concrete that can withstand a load of 100,000 psf. The center portion of the floor, about 20 ft square, is concrete down to bedrock and can take any conceivable load.

Twenty-seven steel anchors to bedrock can take an upward pull of 200,000 lb apiece. Steel columns, supporting a crane and the roof, will withstand forces of three-quarters of a million pounds each.

Yet to be installed is a box-shaped girder spanning the width of the room and adjustable to any height. This will allow loads to be applied at any number of locations on large structures.

The test wing has more conventional apparatus too: a 400,000-lb universal testing machine that can test beams up to 40 ft long, a device for testing columns up to 17 ft tall, two movable testing machines of 100,000-lb capacity for use anywhere in the chamber and in any direction, four fatigue-testing units and many special devices designed by the Cornell staff for unusual testing problems.

Carbon Content Determination

A new device, utilizing the elementary chemical fact that carbon and oxygen have a strong natural affinity for each other, is now being used at U. S. Steel's Research Center in Monroeville, Pa., to measure within 5/10,000 of a per cent the carbon content of low-carbon steels.

The apparatus was designed and developed by research personnel of U. S. Steel in answer to the growing need for closer control of carbon in steels where this element is a decisive factor in quality and performance.

The new equipment is used only in the analysis of steels where accuracy greater than that provided by standard equipment is required, usually in the range below 0.03% carbon. The device consists principally of a force-pump together with a mercury diffusion pump to create a vacuum in the system, an oxygen purifier, a combustion chamber, freezing chambers and a measuring system.

Absolutely pure oxygen is essential to accurate analysis. The gas is cleaned in a system consisting of two liquid-nitrogen traps, separated by a catalyst of asbestos on which palladium chloride has been dissolved and then baked. Oxygen from a tank is admitted into

the catalyst chamber which is heated to about 400° C. Here, any hydrocarbons contained in the oxygen are converted to carbon dioxide and water.

The oxygen is recirculated about three times by moving the liquid-nitrogen traps from one side of the

(*Continued on page 297-s*)

SOME DYNAMIC MECHANICAL PROPERTIES OF HEAT-TREATED LOW-ALLOY WELD DEPOSITS

Results of investigation indicate that nickel-molybdenum-vanadium (AWS E10015-16) deposits are of good quality, have excellent ductility and show exceptional endurance limits under cycles of reversed stress

BY E. H. FRANKS AND W. H. WOODING

ABSTRACT. The mechanical properties including impact and fatigue strengths have been determined and are illustrated for low-alloy nickel-molybdenum-vanadium (E100XX) weld deposits in the as-welded, stress-relieved, quenched and tempered and annealed conditions.

The results obtained indicate that the AWS E10015-16 (Ni-Mo-V) deposits are of good quality, have excellent ductility and show exceptional endurance limits under cycles of reversed stress in both the as-welded and heat-treated conditions. In this respect, it is concluded that the AWS E10015-16 (Ni-Mo-V) type electrodes offer considerable promise for use in engineering applications, particularly where fatigue properties are of prime importance.

In view of the favorable results obtained in various heat-treated conditions, the use of this type weld deposit in commercial applications are presented as evidence of the potential use of the electrode.

Introduction

Recently developed arc-welding electrodes suitable for the fusion welding of low-alloy steels have been well received by industry. These electrodes are of the low-hydrogen type and deposit good quality low-alloy steel weld metal of high strength combined with exceptional ductility. Presently, the greater demand for these electrodes is in structural fabrication where considerable advantage is being taken of the excellent mechanical properties of the weld deposits.

One electrode of this type which has met with considerable success in the welding of low-alloy steels is the nickel-molybdenum-vanadium steel (AWS E10015-16) electrode. This is a heavy mineral-covered electrode, the coating of which is relatively free of hydrogen and hydrogen-producing compounds such as water. The absence of water also permits transfer across the arc of such alloys as manganese, silicon and vanadium without material loss through oxidation. The electrode deposits weld metal having a strength level in excess of 100,000 psi and the resulting weldments show excellent performance in a variety of tests including impact. This electrode is finding wide acceptance for the welding of low-alloy steel structures, particularly where a high degree of restraint is encountered.

Presently, this electrode is finding limited application in the construction and repair of machinery. It would appear that this restricted use is due in part to the fact that relatively little information is available concerning the performance of such weldments under cyclic loading particularly after heat treatment.

AWS E10015-16 (Ni-Mo-V) Electrode

When the nickel-molybdenum-vanadium steel (AWS E10015-16) electrodes were first introduced to industry, they represented an effort to produce high-strength weld metal suitable for the fabrication of low-alloy steel under high restraint. The aim chemistry of the weld deposit approximated 1.75% nickel, 0.60% molybdenum and 0.15% vanadium. This composition produced weld metal having a tensile strength in excess of 100,000 psi with good ductility and impact properties in the as-welded condition. However, when weldments were subjected to thermal stress relief treatments, there was pronounced degradation of the impact properties of the weld metal. As a result, the use of the electrode was primarily restricted to those applications where post-thermal treatments were not required.

In an endeavor to determine the cause for the adverse effect of thermal stress-relief treatments, the chemistry of the weld deposit was further investigated. This investigation was conducted using a group comprising several lots of electrodes in which the molybdenum content was progressively decreased while the strength level of the deposit was maintained by adjustment of alloys other than molybdenum and vanadium. Each lot of electrodes was used to deposit two circular restrained groove (Navy Patch) weld assemblies using the procedure described in Military Specification MIL-E-18038(SHIPS). One assembly of each lot was tested in the as-welded condition while the second assembly was given a thermal stress-relief treatment at 1150° F prior to sectioning for test. The results of these tests, together with partial chemistry of the respective weld pads, are given in Table 1.

As indicated in Table 1, the impact properties at 0° F after thermal stress-relief treatment improve with progressive reduction in the molybdenum content. Below 0.35% molybdenum, the impact properties after thermal stress relief closely approximate those in the as-welded condition. In view of these results, the chemical composition requirements were revised and a new range established to designate nickel-molybdenum-vanadium steel (AWS E10015-16) electrodes capable of depositing weld metal suitable for post-thermal treatments. The revised chemistry requirements are presented in Table 2.

The electrodes under consideration in this investigation are of the modified type. Prior to use, they were subjected to test in accordance with the requirements of Military Specification MIL-E-18038(SHIPS) for Type MIL 10015 electrodes and found to be in strict conformity therewith. The weld-deposit chemistry determined for an undiluted

E. H. Franks is Supervisory Welding Engineer and W. H. Wooding is Superintendent, Metals Section, Industrial Test Laboratory, Philadelphia Naval Shipyard, Philadelphia, Pa.

This paper represents the personal opinions of the authors and in no way reflects the official attitude of the Department of the Navy.

Paper presented at AWS 1956 National Spring Meeting in Buffalo, N. Y., May 7-11, 1956.

Table 1—Impact Properties of Various Nickel-Molybdenum-Vanadium Steel Weld Deposits As-Welded and Stress-Relieved

ELECTRODE LOT DESIGNATION (1)	A	B	C	D	E	F
CHEMICAL COMPOSITION (2)						
CARBON	0.06	0.05	0.07	0.04	0.06	0.05
MANGANESE	0.78	0.55	0.74	0.48	0.80	0.80
SILICON	0.31	0.50	0.34	0.12	0.40	0.37
NICKEL	1.68	1.70	1.67	1.44	1.58	1.52
CHROMIUM	0.05	0.14	0.05	0.05	0.07	0.05
VANADIUM	0.08	0.12	0.09	0.08	0.14	0.13
MOLYBDENUM	0.79	0.64	0.46	0.46	0.27	0.30
IMPACT PROPERTIES - FT. LBS. AT 0° F. (3)						
AS WELDED	26	30	34	28	28	32
	30	34	40	32	38	34
	30	34	32	32	32	32
	32	34	42	36	34	32
AVER.	30	33	37	32	33	33
STRESS RELIEVED (4)	14	23	26	22	24	28
	4	6	22	18	24	32
	6	14	12	24	26	30
	4	5	22	22	24	32
AVER.	7	12	21	22	25	31

NOTES (1) ALL ELECTRODES 3/16" DIAMETER DEPOSITED AT 21-23 ARC VOLTS, 225 AMPERES DCRP.
(2) OBTAINED FROM UNDILUTED WELD PADS.
(3) CHARPY KEYHOLE SPECIMENS OBTAINED FROM CIRCULAR RESTRAINED GROOVE (NAVY PATCH 4-1/2" DIA.) WELD. PREHEAT AND INTERPASS TEMP. 100°F. MAX.
(4) STRESS RELIEF TREATMENT - HEATED AT 100°F. MAX. PER HOUR TO 1150°F, HELD FOR 2 HOURS AND FURNACE COOLED AT 100°F. MAX. PER HOUR TO BELOW 500°F.

Table 2—Chemical Composition and Mechanical Properties of Weld Metal E-10015 (Ni-Mo-V) Electrode (1)

		COMPOSITION - % (2)									
		C	Mn	P	S	Si	Ni	Cr	V	Mo	WATER(3) CONTENT
RANGE	MIN	–	0.75	–	–	0.05	1.40	–	–	–	–
	MAX	0.10	1.10	0.030	0.040	0.60	1.80	0.15	0.20	0.35	0.40
ELECTRODE "G"		0.06	0.75	0.009	0.028	0.37	1.76	0.06	0.11	0.35	0.28

TENSILE PROPERTIES (4)				
	YIELD STRENGTH POUNDS PER SQUARE INCH	TENSILE STRENGTH POUNDS PER SQUARE INCH	ELONGATION % IN 2"	REDUCTION IN AREA %
AS WELDED	97,000	106,000	24	61

IMPACT PROPERTIES - FT. LBS. AT 0°F. (6)		
	UNRESTRAINED (7)	RESTRAINED (8)
AS WELDED	36, 36, 31, AVE. 34	–
STRESS RELIEVED (5)	28, 28, 26, AVE. 28	30, 32, 30, 28, AVE 30

NOTES - (1) ALL ELECTRODES 5/16" DIA. DEPOSITED AT 21-23 ARC VOLTS, 225 AMPS. DCRP.
(2) OBTAINED FROM UNDILUTED WELD PADS.
(3) TOTAL WATER CONTENT AT 2400°F.
(4) ALL WELD METAL TENSILE (0.505") PROPERTIES OBTAINED FROM UNRESTRAINED WELD ASSEMBLY. PREHEAT AND INTERPASS TEMPERATURE 100°F.
(5) STRESS RELIEF TREATMENT - HEATED AT 100°F. MAX. PER HOUR TO 1150°F. HELD FOR 2 HOURS AND FURNACE COOLED AT 100°F. MAX. PER HOUR TO BELOW 500°F.
(6) CHARPY KEYHOLE SPECIMENS
(7) OBTAINED FROM UNRESTRAINED TENSILE ASSEMBLY. PREHEAT AND INTERPASS TEMPERATURE 100°F.
(8) OBTAINED FROM CIRCULAR RESTRAINED GROOVE (NAVY PATCH 4-1/2" DIA.) WELD PREHEAT AND INTERPASS TEMPERATURE 100°F.

weld pad sample is presented in Table 2. The tensile properties determined using 0.505-in. diam all-weld-metal tension specimens in the as-welded condition are likewise presented in Table 2. Also included in this table are the results of impact tests of samples taken from a circular restrained groove (Navy Patch) weld assembly which had been given a thermal stress-relief treatment prior to sectioning. For additional information, unrestrained impact test results also were obtained using specimens taken from the above tensile test weld assemblies and are included in this table. It is to be pointed out that these impact test results were obtained using Charpy keyhole-type specimens.

Dynamic Mechanical Properties

In view of the satisfactory reaction to thermal stress-relief treatment a study was made of the impact and fatigue characteristics of AWS E10015 (Ni-Mo-V) welds after various post-thermal treatments. Weldments were prepared using nickel-chromium-molybdenum steel plate. Upon completion of welding, various assemblies were subjected to a full-anneal treatment, a temper-anneal treatment (stress relief) and a liquid-quench and temper treatment. After heat treatment, the assemblies were sectioned and subjected to several tests. In addition, similar assemblies also were prepared and subjected to test without the benefit of any post-thermal treatment. Four identical assemblies were prepared, one for each condition. Each assembly consisted of a single-vee butt weld deposited in nickel-chromium-molybdenum steel plate 12 x 12 x 1 in. of the following composition: C 0.17%, Mn 0.27%, P 0.008%, S 0.039%, Si 0.17%, Ni 2.33%, Cr 1.03% and Mo 0.19%. All welding was performed using $^{3}/_{16}$-in. diam electrodes at 100° F preheat and interpass temperature. Upon completion of weld, the backing strap and the reinforcement were removed from each assembly prior to X-ray examination and heat treatment. One assembly was stress relieved by heating to 1150° F, holding at temperature for 2 hr and furnace cooling to below 500° F. A second assembly was annealed by holding 1 hr at 1650° F followed by furnace cooling. The third assembly was heated to 1650° F, held for 1 hr at temperature, quenched in water to room temperature and immediately tempered for 1 hr at 1050° F followed by air cooling to room temperature. The fourth assembly remained in the as-welded condition. All assemblies were heat treated intact in order to obtain a uniform mass effect.

Upon completion of heat treatment, approximately 16 Charpy V notch impact specimens were machined from each assembly. The impact specimens were oriented with the notch normal to

the plate surface at the centerline of the weld deposit. Triplicate specimens were tested at the several temperatures and average values were used to construct the curves presented in Fig. 1.

The all-weld-metal fatigue properties of the AWS E10015 (Ni-Mo-V) deposits were obtained from two cladded single-vee butt weld assemblies using 12 - x 24 - x 1-in. medium-carbon steel base material. The weld-groove scarfs were clad with a layer of weld metal and the butt welds were deposited using $^{3}/_{16}$-in. diam electrode at 100° F preheat and interpass temperature. Upon completion, the backing strap and the reinforcement were removed from each assembly prior to X-ray examination and heat treatment. One assembly was stress relieved using the same procedure as described for the impact assemblies, while the second assembly remained in the as-welded condition. After heat treatment, five R.R. Moore-type rotating beam fatigue test specimens were obtained from each assembly as shown in Fig. 2. The test section of each specimen was hand finished in a lathe with 400-grit abrasive paper. Testing was conducted in an R.R. Moore rotating beam fatigue machine at speeds of 1750 and 3500 rpm. The data obtained are presented in Table 3 and illustrated in the *S–N* diagram, Fig. 3.

The transverse fatigue properties were obtained from four single-vee butt weld assemblies similar to those described above for the impact tests. These butt welds also were deposited and heat treated in the same manner as the impact assemblies. Upon completion of heat treatment each assembly was machined into ten transverse R.R. Moore-type rotating beam specimens with the center of the reduced section located at the centerline of the weld deposit as shown in Fig. 2. Machining, finishing and testing of the specimens followed the procedure described above for all-weld-metal fatigue specimens. The data obtained are presented in Table 3 and illustrated in the *S–N* diagram, Fig. 4.

To provide supplemental test data, the all-weld-metal tensile properties were determined for the various conditions of heat treatment. Assemblies approximately 12 x 10 x 1-in. were prepared using medium-carbon steel base material. The weld groove scarfs were clad with a layer of weld metal and then assembled to provide a single-vee groove having a root opening of $^{1}/_{2}$ in. and an included angle of 45°. The assemblies were welded and heat treated in the same manner as those prepared for the all-weld-metal fatigue test specimens. After heat treatment, all-weld-metal 0.505-in. diam tension specimens were obtained from the center of the deposits and subjected to test. In addition, one transverse 0.505-in. diam tensile specimen was machined from each welded impact assembly. The physical properties obtained for the all-weld-metal and transverse 0.505-in. diam tensile specimens are given in Table 4.

The results of the various tests have been summarized and those observations considered pertinent to this investigation are presented in Table 5.

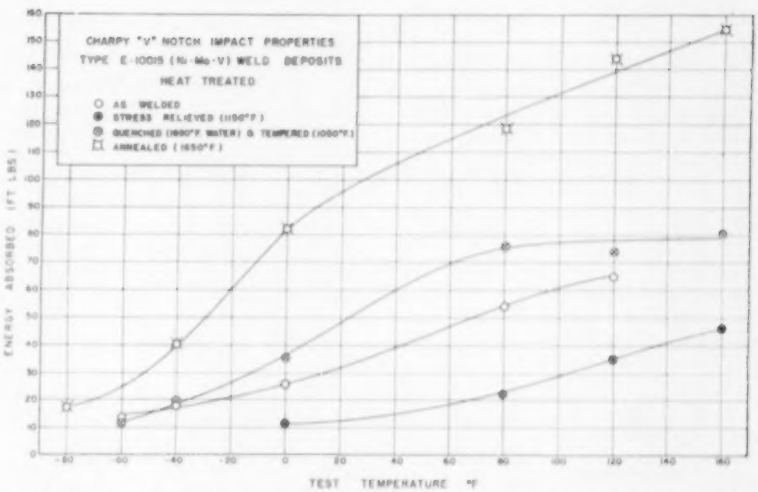

Fig. 1 Charpy V-notch impact properties of type E-10015 (Ni-Mo-V) weld deposits after heat treatment

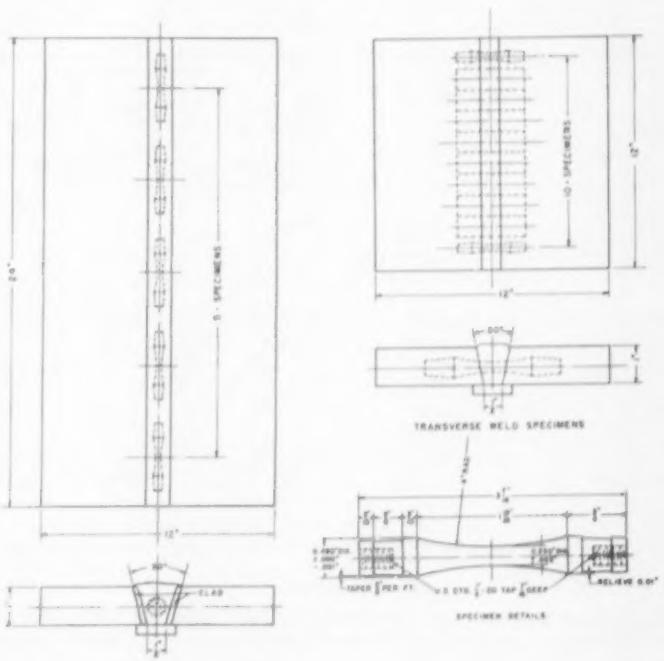

Fig. 2 Rotating beam fatigue test specimen

Discussion

The Charpy V notch impact results presented in Fig. 1 are somewhat discouraging in that at 0° F the as-welded and stress-relieved values are lower than the Charpy keyhole results presented in Table 2. The data would indicate that in the stress-relieved condition, the temperature of transition from ductile to brittle failure is above 0° F. However, it should be noted that, for both the as-welded and stress-relieved conditions, there is but a gradual reduction in energy absorbed with lowering of temperature. Though not shown in Fig. 1, additional tests conducted at temperature above 160° F continued to show a gradual rise in energy

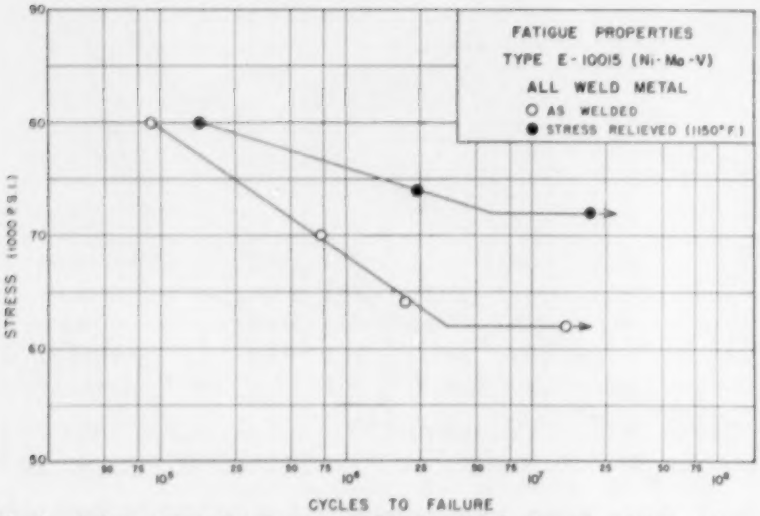

Fig. 3 Fatigue properties of type E-10015 (Ni-Mo-V) all-weld-metal deposit

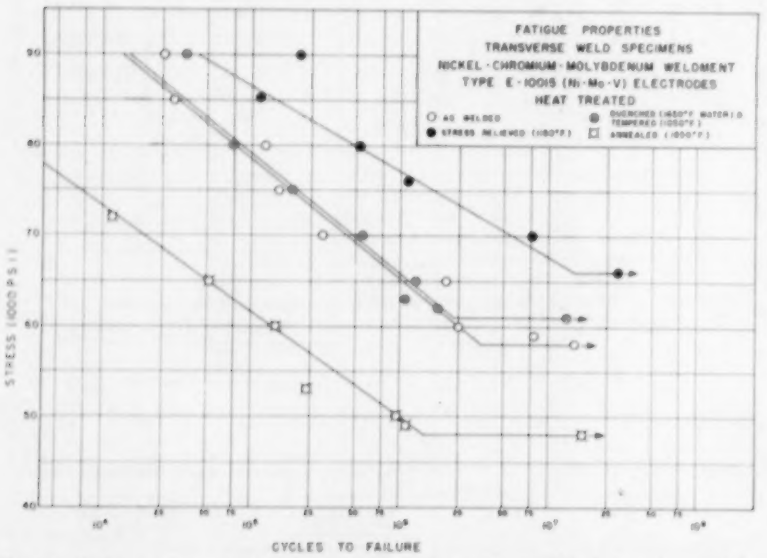

Fig. 4 Fatigue properties of transverse weld specimens; nickel-chromium-molybdenum weldment; type E-10015 (Ni-Mo-V) electrodes; heat treated

absorbed. In addition, it was observed that at the lowest test temperature for both conditions, the broken impact specimens showed partially ductile fractures with a small amount of deformation. In no instance did the crystalline area on the surfaces of fracture exceed 50%. Of particular interest is the spread of impact values between the several thermal treatments for any one test temperature at or above 0° F. The high values obtained for specimens in the fully annealed condition might indicate that when fully relaxed, the weld metal will absorb considerable energy in the presence of notches down to quite low temperatures. In the quenched and tempered condition, the weld metal closely approaches but is still somewhat superior to that of the as-welded material insofar as energy absorbed is concerned.

As shown in the summary presented in Table 5, the temperatures at which failure occurred under 15 ft-lb impact vary from +40° F for the stress-relieved material to below −80° F for the annealed material. This would indicate that the notch sensitivity of the weld metal is greatly influenced by thermal treatments and that after stress relieving at 1150° F, the notch sensitivity is greatly increased. However, it is believed that it is not uncommon to observe similar degradation in notch sensitivity of some wrought low-alloy steels when subjected to a stress-relieving treatment at 1150° F.[1]

The all-weld-metal fatigue properties illustrated in Fig. 3 indicate that the material in either the as-welded or stress-relieved condition has good resistance to failure when subjected to cycles of alternating stress. It is unfortunate that so few specimens were available to determine the slopes of the curves. However, from the information available, it is interesting to note the higher fatigue strength of the stress-relieved material when compared with the as-welded material. Also, that the slope of the fatigue curve for the stress-relieved material is less than that for the as-welded material. The endurance

Fig. 5 Gear blanks fabricated with E-10015 (Ni-Mo-V) electrodes

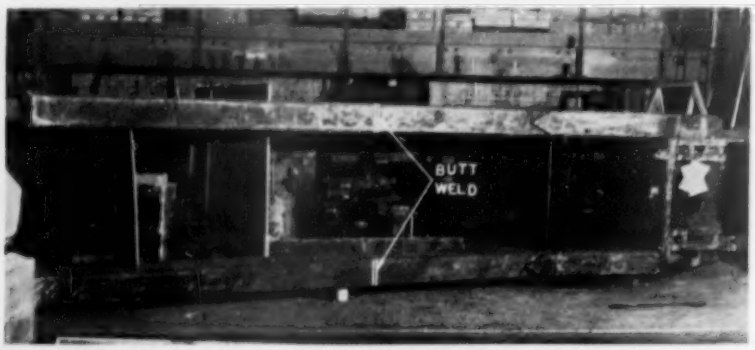

Fig. 6 Large dipper stick assembly with butt welded cover plate

limits established for the undiluted weld metal in the as-welded and stress-relieved conditions approximates 62,000 and 72,000 psi, respectively.

The fatigue data for the transverse-weld specimens presented in Fig. 4 indicate that the endurance limit for the as-welded material is somewhat lower than that shown in Fig. 3 for the same condition. Also, the slope of the curve for the as-welded transverse specimens is somewhat more severe. It is believed that the change in slope and lower endurance limit reflect the effect of residual stress developed transverse the weld during fabrication of the assembly. Of particular interest is the close proximity of the fatigue curve for the quenched and tempered transverse weld specimens to that of the as-welded transverse weld specimens. On stress relief, there appears to be definite improvement in the fatigue characteristics of the transverse weld specimens. As indicated in Fig. 4, the slope of the curve for the stress-relieved material is less severe than that for the as-welded material. However, in the annealed condition, there is considerable reduction in the fatigue life and endurance limit when compared with the as-welded condition.

The endurance limits determined from the results of the fatigue tests are presented in Table 5. Also included therein are the endurance limit-tensile strength ratios for the several conditions of test. As indicated, the longitudinal all-weld-metal ratios in the as-welded and stress-relieved conditions are 0.585 and 0.648, respectively. In addition, the transverse-weld-metal ratios for the several conditions vary from 0.586 to 0.687. These endurance limit-tensile

Table 3—Fatigue Properties Type E-10015 Weld Deposits and Nickel-Chromium Molybdenum Weldments

CALCULATED MAX. FIBER STRESS P.S.I.	ALL WELD METAL		TRANSVERSE WELD (1)			
	AS WELDED	STRESS RELIEVED (2)	AS WELDED	STRESS RELIEVED (2)	ANNEALED (3)	QUENCHED & TEMPERED (4)
	CYCLES TO FAILURE					
90,000			26,000	222,800		36,100
85,000			30,500	112,500		
80,000	89,800	165,200	120,300	538,700	1,500	75,600
77,000				8,685,200		
76,000				1,130,300		
75,000			154,000	17,796,400 (5)		186,700
74,000		2,428,500				
72,000		20,507,500 (5)			11,600	
70,000	740,800	14,502,400 (5)	302,000	7,926,400		568,500
66,000				29,754,300 (5)		
65,000			2,085,200		53,000	1,025,300
64,000	2,090,100					
63,000						1,008,600
62,000	14,862,000 (5)					1,802,600
61,000						13,177,300 (5)
60,000	17,388,200 (5)	17,319,000 (5)	2,523,300		147,400	
59,000			8,294,400			
58,000			15,235,300 (5)			
55,000					1,800,500	
53,000					238,400	
50,000					978,600	
49,000					1,105,800	
48,000					17,297,700 (5)	
45,000					14,956,100 (5)	

NOTES - (1) TRANSVERSE WELD SPECIMENS OBTAINED FROM NICKEL - CHROMIUM - MOLYBDENUM WELDMENT.
(2) HEATED AT 100°F. MAX. PER HOUR TO 1150°F. HELD 2 HOURS AND FURNACE COOLED AT 100°F. MAX. PER HOUR.
(3) HEATED TO 1650°F. HELD ONE HOUR AND FURNACE COOLED.
(4) HEATED TO 1650°F. HELD ONE HOUR, QUENCHED IN WATER TO ROOM TEMPERATURE
TEMPERED ONE HOUR AT 1050°F. FOLLOWED BY AIR COOLING TO ROOM TEMPERATURE.
(5) SPECIMEN DID NOT FAIL. TEST TERMINATED

Table 4—Tensile Properties of Type E-10015 Weld Deposits and Nickel-Chromium-Molybdenum Weldments

TYPE SPECIMEN	HEAT TREATMENT	YIELD STRENGTH POUNDS PER SQUARE INCH	TENSILE STRENGTH POUNDS PER SQUARE INCH	ELONGATION % IN 2"	REDUCTION IN AREA %	LOCATION OF FRACTURE
ALL WELD METAL	STRESS RELIEVED (1)	106,800	111,000	20	57	—
ALL WELD METAL	ANNEALED (2)	57,000	81,000	35	73	—
ALL WELD METAL	QUENCHED & TEMPERED (3)	77,000	90,000	30	69	—
TRANSVERSE	AS WELDED	77,000	94,000	18	61	BASE METAL
TRANSVERSE	STRESS RELIEVED (1)	74,000	96,000	17	62	BASE METAL
TRANSVERSE	ANNEALED (2)	50,000	75,000	26	61	BASE METAL
TRANSVERSE	QUENCHED & TEMPERED (3)	91,500	105,000	18	62	WELD METAL

NOTES - (1) HEATED AT 100°F. MAX. PER HOUR TO 1150°F. HELD 2 HOURS AND FURNACE COOLED AT 100°F MAX. PER HOUR TO BELOW 500°F.
(2) HEATED TO 1650°F. HELD ONE HOUR AND FURNACE COOLED.
(3) HEATED TO 1650°F. HELD ONE HOUR, QUENCHED IN WATER TO ROOM TEMPERATURE, TEMPERED FOR ONE HOUR AT 1050°F. FOLLOWED BY AIR COOLING TO ROOM TEMPERATURE.

Table 5—Summary of Impact, Fatigue and Tensile Results

HEAT TREATMENT	TYPE SPECIMEN	TEMP OF FRACTURE AT 15 FT-LBS IMPACT	ENDURANCE LIMIT POUNDS PER SQUARE INCH	TENSILE STRENGTH POUNDS PER SQUARE INCH	RATIO END L / T S
AS WELDED	ALL WELD METAL	–	62,000	106,000	0.585
	TRANSVERSE	-60°F	58,000	94,000	0.617
					0.547 (4)
STRESS RELIEVED (1)	ALL WELD METAL	–	72,000	111,000	0.648
	TRANSVERSE	+40°F	66,000	96,000	0.687
					0.595 (4)
ANNEALED (2)	ALL WELD METAL	–	–	81,000	–
	TRANSVERSE	(-80°F	48,000	75,000	0.640
					0.593 (4)
QUENCHED & TEMPERED (3)	ALL WELD METAL	–	–	90,000	–
	TRANSVERSE	-55°F	61,000	105,000	0.581
					0.678 (4)

NOTES - (1) HEATED AT 100°F MAX. PER HOUR TO 1150°F. HELD 2 HOURS AND FURNACE COOLED AT 100°F. MAX. PER HOUR.
(2) HEATED TO 1650°F. HELD ONE HOUR AND FURNACE COOLED.
(3) HEATED TO 1650°F HELD ONE HOUR QUENCHED IN WATER TO ROOM TEMPERATURE
TEMPERED ONE HOUR AT 1050°F FOLLOWED BY AIR COOLING TO ROOM TEMPERATURE.
(4) RATIO CALCULATED USING TRANSVERSE WELD ENDURANCE LIMIT AND ALL WELD METAL TENSILE STRENGTH

strength ratios are considered exceptionally high when compared with the endurance ratio of 0.40 generally accepted for good quality cast-ferrous metals. They likewise approximate the endurance ratios determined by Dolan and Yen[3] for wrought SAE 3140 and SAE 2340 steels which ranged from 0.56 to 0.61.

Of particular interest is the endurance limit determined for the stress-relieved weldment. This limit was indicated to be 66,000 psi with an endurance ratio of 0.687. The results indicate that this thermal treatment had no adverse effect on the fatigue properties of the weldment. This observation is in agreement with investigations reported by R. D. Chapman and W. E. Jominy[2] and by T. J. Dolan and C. S. Yen.[3] Both investigations indicate that temper brittleness has no adverse effect on the endurance limits of steel.

However, in the presence of sharp notches it might be expected that the endurance limit of a notch-sensitive steel (as determined by impact tests) would be adversely affected. According to Dolan and Yen[3] a functional relationship does not exist between the concepts of notch sensitivity in a fatigue test and the notch sensitivity evidenced in a Charpy impact test. Chapman and Jominy[2] state that in engineering applications where a temper-embrittled steel is used, they believe the endurance limit of the part will be unaffected, even at temperatures below the transition temperature. In view of the work of these investigators, it was not considered necessary to extend this study to include the endurance limit of notched specimens, particularly after having been subjected to thermal stress-relief treatments which would cause increased notch sensitivity in the Charpy impact test.

In general, the response of the AWS E10015 (Ni-Mo-V) deposit to heat treatment is considered satisfactory. However, due to low carbon content (0.06% avg), liquid-quenching treatments will not develop high hardness in the deposit. Therefore, the weld deposit should be used in the as-welded or stress-relieved condition unless such other thermal treatments do not develop strength levels in the base metal in excess of that expected for the weld metal after such treatment.

Applications

Several manufacturers have used the AWS E10015 (Ni-Mo-V) electrode to good advantage in the fabrication of machinery parts, particularly in applications that require subsequent thermal treatment. One application in current production is the fabrication of gear blanks as shown in Fig. 5. Highly stressed gears having dished webs are fabricated with SAE 8630H rim stock, mild-steel web material and forged SAE 1035 hub material. The fillet welds used to join rim stock to web and web to hub were deposited with AWS E10015 (Ni-Mo-V) electrodes. Gears were thermally treated by water quenching from 1600° F followed by tempering at 1050° F.

Another application employs AWS E10015 (Ni-Mo-V) electrodes to butt weld a $1^1/_4$-in. thick cover plate on a large dipper stick assembly. Figure

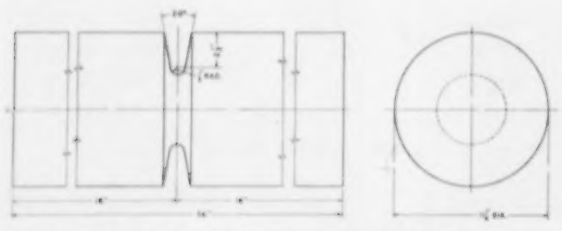

Fig. 7 Joint design for welding nickel-molybdenum steel forging billet

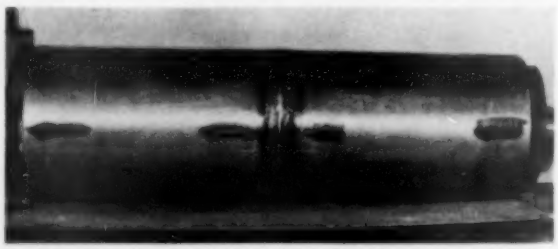

Fig. 8 Completed weld in nickel-molybdenum steel forging billet

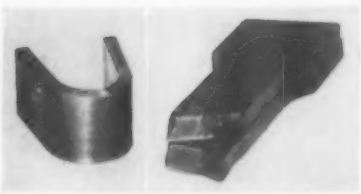

Fig. 9 Guided bend and tensile removed from nickel-molybdenum forging billet

Fig. 10 Macrograph of section removed from weld in nickel-molybdenum forging billet.

6 shows the completed assembly in which a butt weld was made in the center section of the built-up longitudinal members. The weld was ground flush to provide a smooth sliding surface. The entire weldment was normalized at 1600° F upon completion.

To further demonstrate the adaptability of the AWS E10015 (Ni-Mo-V) electrodes for machinery applications, an alloy-steel forging billet approximately 11 in. in diameter by 36 in. long was welded in a manner simulating a shafting repair. This billet was a nickel-molybdenum alloy steel of the following chemical composition: C 0.31%, Mn 0.66%, Si 0.33%, Ni 3.00% and Mo 0.33%. The billet was mounted in a lathe and a circumferential groove, the details of which are shown in Fig. 7, was cut at mid-length. Tram marks were placed 90° apart on circumferences at distances 3 and 18-in. either side of the weld centerline to facilitate warpage measurements. The welding was performed with the billet mounted in the lathe so that by rotation, the weld metal would be deposited in the downhand position. Using a quadrant technique, the weld was deposited with $^{3}/_{16}$- and $^{7}/_{32}$-in. diam electrodes at a preheat of 200° F and a controlled interpass temperature ranging from 150 to 250° F. Upon completion of the weld, measurements indicated maximum warpage did not exceed 0.004-in. and this was located at the tail stock end of the billet 18 in. removed from the weld centerline.

After the entire welded section of billet was stress relieved at 1150° F for 6 hr, it was sectioned to provide one flat transverse tensile specimen of 8-x 2- x $^{1}/_{2}$-in. gage, one transverse 0.505-in. diam tensile specimen, one transverse side-bend specimen, and one transverse macrospecimen. The following results were obtained from the transverse tensile specimens:

Type of Specimen	*Flat*	*0.505 in. Diam*
Yield strength, psi	96,200	107,500
Tensile strength, psi	114,600	113,500
Elongation, %	11.2[1]	19.0[2]
Reduction in area, %	29.0	50.9

[1] Elongation in 8-in. gage length.
[2] Elongation in 2-in. gage length.

The guided-side-bend specimen satisfactorily bent around a 2T radius to 180 deg without any indication of flaws. Figure 9 shows the guided-bend specimen and the fractured flat tensile specimen upon completion of test. Figure 10 presents a photomacrograph of a transverse section of the weld.

It is concluded that the AWS E10015-16 (Ni-Mo-V) electrodes as described herein offer considerable promise for use in machinery applications. The weld deposits are of good quality, have excellent ductility and show exceptional endurance limits under cycles of reversed stress in both the as-welded and heat-treated conditions. Under conditions of alternating loads, the performance of such weldments should be comparable to that of wrought-alloy steel of the same strength level.

Acknowledgments

The authors wish to express their appreciation for the encouragement and advice received from J. E. McCambridge, Superintendent of the Industrial Test Laboratory, Philadelphia Naval Shipyard, in the preparation of this paper. Acknowledgment is also expressed to T. N. Armstrong, Research and Development Division, International Nickel Co., for assistance in conducting the fatigue tests; and to H. Addison, J. Hare, J. Angeny, R. Beyer and other members of the Metals Section, Industrial Test Laboratory for their diligence in obtaining and illustrating the test data. Also, thanks is expressed to D. C. Smith, Harnischfeger Corp., for supplying photographs of shop applications.

References

1. Pellini, W. S., and Queneau, B. R., "Development of Temper Brittleness in Alloy Steels," *Trans. ASM*, **39**, 139, (1947).
2. Dolan, T. J., and Yen, C. S., "Some Aspects of the Effect of Metallurgical Structure on Fatigue Strength and Notch Sensitivity of Steel," *Proc. ASTM*, **48**, 664 (1948).
3. Chapman, R. D., and Jominy, W. E., "The Endurance Limit of Temper-Brittle Steel," *Trans. ASM*, **45**, 710, (1953).

RESEARCH NEWS

(*Continued from page 290-s*)

catalyst to the other. At −195° C, the liquid nitrogen freezes the oxygen. This creates a vacuum in front of the remaining gaseous oxygen and thus acts as a pump.

The steel samples to be analyzed consist of small chips and shavings. These are carefully weighed and then placed in a glass rack containing a number of pockets to hold several different types of samples. The rack is sealed into the vacuum system and mounted directly over the combustion chamber. Samples are drawn into the combustion chamber by a magnet applied by the operator to the outside of the glass.

The combustion chamber is a platinum crucible lined with aluminum oxide. It is induction heated to about 1700° C. At this temperature the steel sample is burned in the presence of a controlled amount of purified oxygen. The gas CO_2 is generated along with other gases.

These mixed gases then pass through another freezing trap containing dry ice and acetone to maintain a temperature of −80° C. At this temperature, the CO_2 passes through as a gas, the interfering gases remain frozen in the trap. The CO_2 is then frozen out in liquid nitrogen and released into a pressure gage. Since the carbon dioxide formation depends entirely on the amount of carbon in the steel sample, the gas pressure can then be translated

(*Continued on page 307-s*)

FATIGUE STRENGTH OF WELDS IN LOW- ALLOY STRUCTURAL STEELS

Experimental program shows that, for all types of specimens tested, there is little difference in the fatigue strengths of the several low-alloy steels

BY J. E. STALLMEYER, G. E. NORDMARK, W. H. MUNSE AND N. M. NEWMARK

SUMMARY. Fatigue tests have been conducted on full-scale butt welds and fillet welds in low-alloy steel plates with the stress applied either parallel to or perpendicular to the direction of welding. Several different steels meeting the ASTM designation A-242 were used in this investigation to study the uniformity of results of different steels meeting this specification.

The fatigue strengths of steels meeting the requirements of ASTM designation A-242 do not differ appreciably in spite of the comparatively wide variations in their chemical compositions. Further, the presence of the weld in the steel reduced the magnitude of the variations between the average fatigue strengths of the different alloy steels.

A comparison of the fatigue strengths of joints in the low-alloy steels with the fatigue strengths of similar joints prepared from A-7 steel with E7016 electrodes is also included in the paper.

Introduction

Object and Scope of Investigation

Since the introduction of low-alloy steels for structural purposes, the question has often been asked—on what physical property or properties should the design stress for these steels be based? The answer depends, of course, on the type of loading applied to the material when it is assembled into members and structures and also the factor of safety desired against the possible modes of failure. Originally there was some contention that all design stresses should be based on the yield point of the material; however, investigations have proved that under some conditions, such designs might have an extremely low factor of safety against failure. Such may be the case when members are subjected to repeated loads for it has been shown that the endurance limit of a steel member is not necessarily related directly to the yield point of that steel. Further, Professor W. M. Wilson [1-3] found that the presence of a welded or riveted joint in a steel having a high yield point might reduce the fatigue strength of the joint so that it is little, if any, greater than that of ordinary A-7 steel. The susceptibility of low-alloy steel to fatigue failures has, in many instances, precluded the use of this material for structures which are subjected to repeated loadings.

Relatively few fatigue tests have been conducted on welded joints in steels other than those meeting ASTM Specification A-7. The results of the tests by Wilson indicated that butt-welded joints in one low-alloy steel had a fatigue strength about 20% higher than similar joints in A-7 steel whereas the difference in yield points was about 50%. With advances in welding techniques and materials, such as the development of the low-hydrogen electrode, and also improvements in the properties of the low-alloy steels, it is desirable to determine if the fatigue strength of welded joints in low-alloy steel might have been improved enough to make the use of such materials economical in structures subjected to repeated loadings.

Description of Steels

The steel plates used in this investigation were ordered to comply with the ASTM Specification for A-242 steel. The chemical analyses and physical properties of the different steels are given in Tables 1 and 2. According to the mill tests, steel P and steel T also meet the military specification for Mil (S) 12505, Grade 1 and steel Q meets the military specification for Mil (S) 12505, Grade 5.

The tensile coupons from steel T

Table 1—Chemical Composition of Steel Plate

Steel	*Chemical content, %**								
	C	*Mn*	*P*	*S*	*Si*	*Cu*	*Ni*	*Cr*	*Vq*
A-7	0.17	0.68	0.016	0.039	0.03	...	...	...	...
P	0.12	0.56	0.106	0.043	0.32	0.45	0.46	0.61	...
T	0.20	1.08	0.010	0.025	0.10	0.38	0.60	...	...
Q	0.19	1.10	0.022	0.028	0.25	0.43	...	...	0.04

* Check analysis.

Table 2—Physical Properties of Steel Plate, Standard 8-In. Gage Length Tensile Coupon

Steel	*Yield strength, psi*	*Tensile strength, psi*	*Elongation in 8 in., %*	*Reduction of area, %*
A-7 (Average)	33,300	57,400	33	62
P (Average)	56,800	76,700	25	53
(Mill report)	57,600	81,700	24	...
T (Average)	47,800	73,600	27	58
(Mill report)	51,300	76,900	26.5	...
Q (Average)	53,100	77,600	26	49
(Mill report)	55,300	82,900	24.5	...

J. E. Stallmeyer, G. E. Nordmark, W. H. Munse and N. M. Newmark are, respectively, Research Assistant Prof. of Civil Engineering; formerly Research Associate in Civil Engineering, Research Professor of Civil Engineering and Research Professor of Structural Engineering at the University of Illinois.

Presented at the 1955 AWS National Fall Meeting held in Philadelphia, Pa., Oct. 17-21.

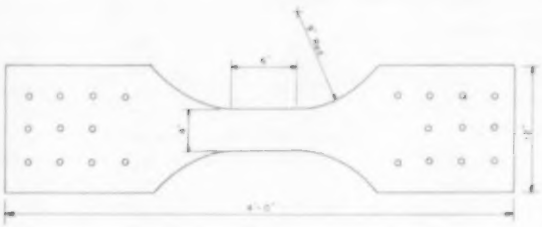

a PLAIN PLATE

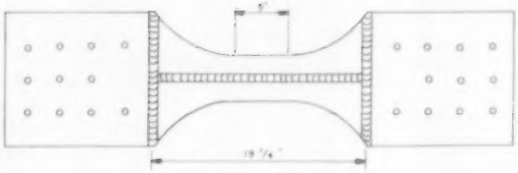

b LONGITUDINAL BUTT WELD

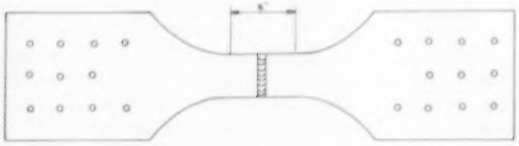

c TRANSVERSE BUTT WELD

Fig. 1 Details of butt-welded joints

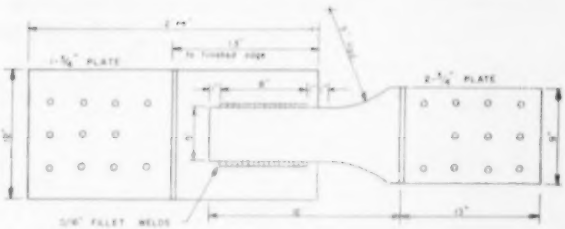

a LONGITUDINAL FILLET-WELDED JOINT

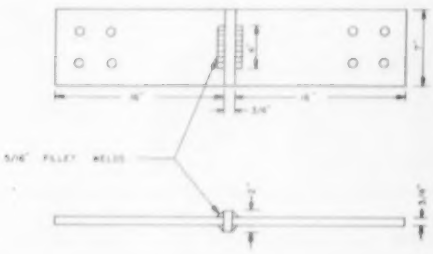

b TEE FILLET-WELDED JOINT

Fig. 2 Details of fillet-welded joints

did not meet the minimum requirements for yield point, 50,000 psi, although the mill tests indicated an acceptable strength. Steels P and Q met both the physical and chemical requirements.

Preparation of Butt-Welded Joints and Plain Plate Specimens

Typical dimensions of the plain plate specimens and the butt-welded joints are shown in Fig. 1. For all of these specimens the test section was 4 in. wide but the test section varied in length for the different materials. This variation in length of the straight section was necessary because of the limited amount of material available and the resulting necessity of welding heads of other steel to the test section of the low-alloy steel. The weld joining the test section to the heads had to be large enough to prevent failure in this weld.

The plates for the transverse butt welds were flame cut from the parent plate with an increased width at the joint to enable the start and the end of the weld to be removed from the specimen later by machining. In preparation for welding, the plate was saw-cut at the joint and the joint machined in a shaper to provide for a double-V butt weld having an included angle of 60°.

In order that each of the six weld passes could be deposited in the flat position, the two plates were securely clamped to a welding jig, as shown in Fig. 3, which could be rotated about a horizontal axis. Before the clamps of the jig were tightened, the root opening was set at $\frac{1}{8}$ in. The first two passes were deposited with $\frac{5}{32}$ in. diam electrodes and all remaining passes with $\frac{3}{16}$ in. diam electrodes. Mil 180 electrodes were used for the T and Q steels whereas E7016 electrodes were used for the P steel. In previous tests it had been found that the slag was much easier to remove from welds produced with the Mil 180 electrode.

After deposition of the first pass, the weld was back chipped to expose sound base metal. Ten minutes of air cooling was allowed between the first and second passes for the transverse butt welds and 15 min for the longitudinal butt welds. Cooling periods of 5 min were used between succeeding passes. The specimens were air cooled after deposition of the last pass. The welding sequence was such that a change of electrode occurred in the test section in each pass of the weld, adjacent passes were welded in opposite directions, and changes of electrode in adjacent passes did not occur one over the other. The

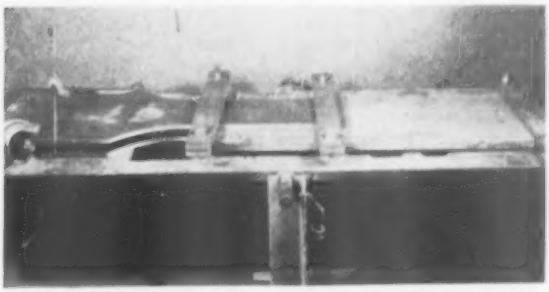

(a) Jig in position for second pass, longitudinal fillet weld

(b) Jig in position for second pass, longitudinal butt weld

Fig. 3 Welding jigs for welded joints

Table 3—Welding Procedures

Pass	Steel	Electrode	Diam., in.	Open circuit voltage, V	Current, amp	Voltage, V	Burn off rate, ipm.	Rate of travel, ipm
			Longitudinal fillet welds					
All	P	E7016	5/16	73	190	21	8.4	6.1
			Tee fillet welds					
All	P	E7016	5/16	73	185	20	4.8	9.1
			Longitudinal butt welds					
1	P	E7016	5/16	73	170	20	7.9	4.6
2-6	P	E7016	5/16	73	185	20	8.6	5.7
1	T, Q	Mil 180	5/32	72	135	20	9.0	3.5
2	T, Q	Mil 180	5/32	72	160	21	9.7	4.8
3, 4	T, Q	Mil 180	5/16	72	210	22	9.8	6.6
5, 6	T, Q	Mil 180	5/16	72	200	22	9.6	6.1
			Transverse butt welds					
1	P	E7016	5/16	72	160	20	7.7	4.2
2-6	P	E7016	5/16	72	180	20	8.4	4.0
1	T, Q	Mil 180	5/32	73	140	20	9.3	3.0
2	T, Q	Mil 180	5/32	73	160	21	9.5	4.2
3, 4	T, Q	Mil 180	5/16	73	210	22	10.0	6.4
5, 6	T, Q	Mil 180	5/16	73	200	22	9.2	5.0

welding power was supplied by a 200-amp d-c rectifier-type welder. The electrodes were operated at the current and voltage levels, given in Table 3, which were measured on portable meters connected as close to the arc as possible. After completion of the welding, the specimens were machined to the dimensions shown in Fig. 1 and the edges were draw filed.

For those specimens tested with the weld reinforcement and mill scale removed, a portable grinder was employed to remove the reinforcement, mill scale, and surface defects. The grinding was started with a 36 grit wheel and finished with a 120 grit wheel in such a manner that the final scratches were parallel to the direction of loading.

The preparation of the longitudinal butt welds was in all respects similar to that used for the transverse weld specimens except that the test weld was prepared first for the longitudinal specimen. This test section was then prepared to provide for a double-V butt weld which joined the test section to the pull heads. As a part of this process the start and the finish of the test weld was removed from the completed specimen. This precaution was taken to reduce the possibility of failure in the transverse weld.

Preparation of Tee Fillet-Welded Joints

The tee-fillet specimens were composed of two 7- x 3/8- x 16-in. longitudinal plates which were welded to a 2- x 3/8- x 7-in. transverse tee plate. To prepare the longitudinal plates for welding, one end of each plate was machined perpendicular to the plane of the plate and the mill scale was ground off the areas of the plate where the weld was to be deposited. In order to remove the mill scale and surface irregularities, each face of the tee plate was machined to a depth of 0.025 in. Uniform spacing between the longitudinal plates was maintained by the use of paper spacers consisting of eight thicknesses (0.027 in.) of No. 20 bond paper.

A 4-in. long, single pass, 5/16-in. fillet weld was manually deposited in each intersection of the joint using the welding procedures given in Table 3. Each weld was deposited with a single E7016 electrode and the direction of welding was alternated for succeeding welds. A cooling period was allowed between welds to secure an interpass temperature of less than 200° F.

Preparation of Longitudinal Fillet-Welded Joints

As shown in Fig. 2, the test section of this specimen consisted of a 12-in. x 3/8-in. x 2-ft. 3-in. center plate joined by two 5-in. x 3/8-in. x 2-ft. 7-in. outside plates with four 8-in. long, single pass, 5/16-in. fillet welds. The design stresses were approximately equal for the weld and outside plates; a stress of 12,800 psi in the outside plates corresponding to a stress of 13,600 psi on the throat of the weld.

The 8 in. length of the single-pass fillet weld required a change of electrode which was made at the mid-point of the weld. The direction of the welds was different for the two welds on one face of the specimen. During the 45-sec interval between the deposition of each electrode on one face of the specimen, the end of the weld was cleaned. A 15-min cooling period was used before welding was initiated on the second face in order that the temperature of the weldment would be 150° F or less. After completion of the welds, the specimen was allowed to air cool for at least 10 min before being removed from the welding jig.

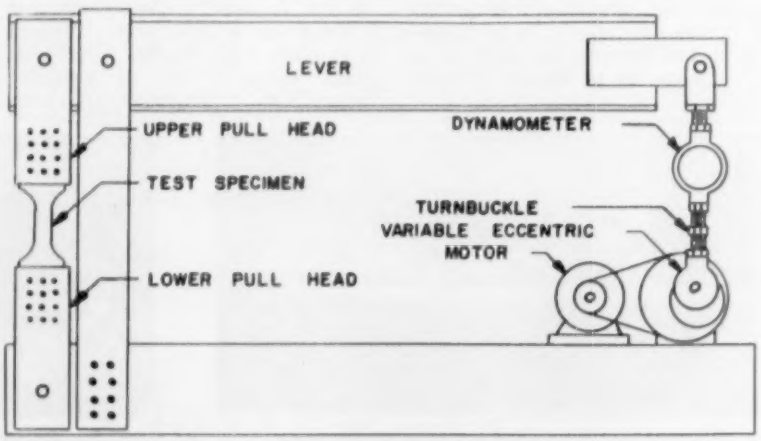

Fig. 4 Schematic diagram of Wilson fatigue testing machine

Test Procedures

The fatigue tests were performed at room temperature in two 200,000-lb capacity W. M. Wilson lever-type fatigue machines which operate at a speed of approximately 200 cpm. Because one of the machines was not equipped to apply a compressive load, it was necessary that a tension be applied to the specimen at all times to insure that the bearings would be properly seated throughout the tests. Accordingly, the stress cycle employed in the present tests was one which varied from a low tension of about 6000 lb to a maximum tension; however, this loading will be referred to as a zero-tension cycle.

The essential features of the machine, shown in Fig. 4, are a variable throw eccentric which transmits force through a dynamometer (for determining the load on the specimen) to a lever which in turn transmits the load to the upper pull head at a multiplication ratio of approximately 15 to 1. The double throw eccentric is adjusted to give the desired range of load before the test is begun. The maximum load is set by means of an adjustable turnbuckle mounted between the eccentric and the dynamometer. The stress is determined by a mechanical dial which indicates the vertical deflection across the throat of the dynamometer to the nearest 0.001 in.

After a specimen had been bolted in the fatigue machine, a stress equal to the maximum desired stress was first statically applied to the specimen. Plastic straining occurred for those specimens to be tested above their yield points. For these specimens it was necessary to allow sufficient time for the specimens to strain under the maximum load before the load could be maintained under repeated loadings.

The fatigue machines were run continuously. A microswitch stopped the machine when the maximum deformation of the specimen increased. The load was checked frequently at the start of the test, but later only as often as necessary to maintain the desired load. Failure is defined as having occurred when the fatigue crack was large enough to actuate the microswitch and stop the machine. This was generally found to be a crack about 1 1/2 in. long.

One specimen of each type was tested statically in a 600,000-lb Riehle testing machine at a strain rate of 0.10 ipm for the plain plate and butt-weld specimens and 0.05 ipm for the longitudinal fillet-welded joint.

Evaluation of Fatigue Tests

In order to numerically compare the results of fatigue tests of specimens tested at different stress levels, fatigue strengths corresponding to failure at

Table 4—Results of Fatigue Tests of Plain Plate Specimens

Specimen	Stress, psi	Cycles to failure, 10^3	—Fatigue strength— $f_{100,000}$, psi	$f_{2,000,000}$, psi	k
		A-7 Steel			
H10	35,500	1508.0		35,200	0.18
H46	40,000	450.3		33,000	0.18
H49	37,000	1078.3		34,100	0.18
H58	37,200	1627.2		36,200	0.18
			Avg	34,600	
		Steel P			
P2	50,000	126.4	51,300	36,900	0.11
P3	50,000	198.5	53,900	38,800	0.11
P4	50,000	249.4	55,300	39,800	0.11
		Avg	53,500	38,500	
		Steel T			
T2	45,000	1787.2		44,400	0.11
T3	50,000	409.6	58,400	42,000	0.11
T5	46,200	696.0	57,200	41,100	0.11
		Avg	57,800	42,500	
		Steel Q			
Q1	50,000	224.2	54,600		0.11
Q2	48,000	304.6	54,300	39,100	0.11
Q3	49,100	384.6	57,000	41,000	0.11
		Avg	55,300	40,000	

Table 5—Results of Fatigue Tests of Longitudinal Butt-Welded Joints

Specimen	Stress, psi	Cycles to failure, 10^3	—Fatigue strength* $f_{100,000}$, psi	$f_{2,000,000}$, psi
		A-7 Steel, E6010		
H7	40,100	86.0	39,300	...
H19	30,000	451.7	36,400	24,700
H77	30,000	417.4	36,200	24,400
H79	36,000	89.2	35,600	...
H91	29,600	304.5	34,200	23,300
H97	40,000	123.0	41,100	...
H103	36,000	180.6	38,900	...
		Avg	37,400	24,100
		A-7 Steel, E7016		
H9	40,000	184.0	43,400	...
H74	29,500	751.1	...	26,000
H88	30,000	447.3	36,700	24,800
H90	39,500	177.3	42,600	...
H98	30,000	1223.7	...	28,200
H100	40,000	207.7	44,000	...
		Avg	41,700	26,300
		Steel P		
P12	40,000	374.0	50,700	29,600
P13	40,000	350.2	50,200	29,200
P15	41,000	186.9	45,800	...
P16	34,000	844.1	...	29,100
P17	34,000	768.0	...	28,600
P18	34,000	321.0	42,000	24,500
		Avg	47,200	28,200
		Steel T		
T12	40,000	229.2	46,500	...
T15	40,000	145.1	42,700	...
T16	40,000	216.8	46,000	...
		Avg	45,100	
		Steel Q		
Q9	40,000	145.1	42,700	...
Q10	40,000	141.1	42,600	...
Q11	41,400	118.7	41,300	...
		Avg	42,200	

* $k = 0.13$ for A-7 steel; $k = 0.18$ for steel P, T, Q.

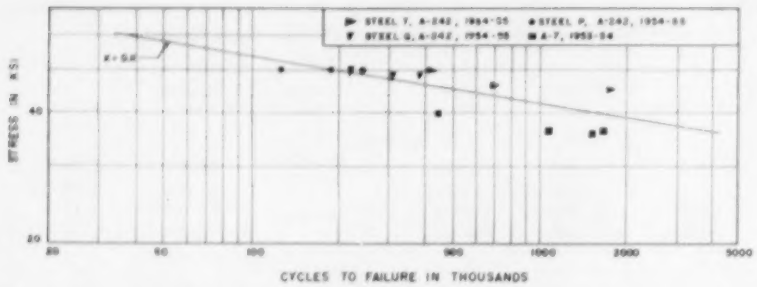

Fig. 5 Results of fatigue tests of plain plate specimens tested with the mill scale on

100,000 and 2,000,000 cycles have been computed from the formula[1] $f = S(N/n)k$, where S is the test stress at which the specimen failed after N cycles, n is the number of cycles for which the fatigue strength, f, is desired, and k is an experimental constant determined from the slope of the median plot on the S-N diagram. For those specimens having a fatigue life greater than 2,000,000 cycles, the value of S has been used as the fatigue strength at 2,000,000 cycles.

Generally, if the number of cycles to failure was less than 600,000, this data was used to compute the fatigue strength for failure at 100,000 cycles; if the value of N was greater than 300,000, the fatigue strength was computed for failure at 2,000,000 cycles. For specimens failing between 300,000 and 600,000 cycles, both fatigue strengths were computed.

Test Results

Fatigue Tests of Plain Plate Specimens

The fatigue strengths of the various alloy steels and of an A-7 steel when tested in plain plate specimens are presented in Table 4 and Fig. 5. Typical failures of plain plate specimens are shown in Fig. 6. As would be expected from the tensile coupon yield strengths, specimens T3 and T5 yielded when their maximum loads were applied statically. Although the coupon tests indicated a yield strength for the Q steel of more than 51,000 psi, specimen Q3 began yielding within the first 1000 cycles of loading. In addition, after 1,224,000 cycles of loading at a stress of 45,000 psi, specimen T2 began to yield.

The scatter of results of the Q steel was less than that of the T and P steels, and, although the scatter bands of all three steels overlap, the T specimens generally had the longer fatigue lives.

The average fatigue strengths of the T and Q specimens were about 9 and 3% higher, respectively, than that obtained from steel P. It appears that the low-alloy steels have average values of $f_{2,000,000}$ from 10 to 25% higher than the A-7 steel. However, the yield strengths of the low-alloy steels were about 45 to 75% higher.

Fatigue Tests of Longitudinal Butt Welds

The results of the fatigue tests of the longitudinal butt welds are presented in Table 5 and in Fig. 7. All of the specimens reported herein were tested in the as-welded condition. All of the failures initiated in a region where the electrode of a surface pass had been changed. Although there are some variations in the metallurgical properties at a change of electrode as a result of a short period of air cooling and the subsequent arc strike, it would appear that the cause of failure was primarily geometrical, because a notch-type discontinuity of some severity is formed perpendicular to the direction of the applied stress wherever a new electrode is started. Typical fractures of the longitudinal butt-welded specimens are shown in Fig. 8.

As may be seen in the S-N diagram,

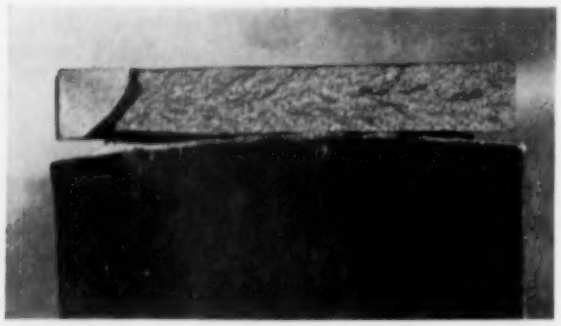

H-49

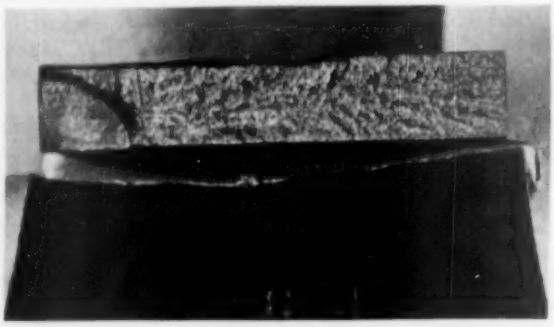

P-3

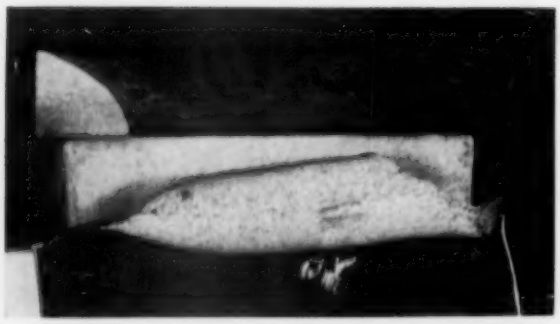

T-2

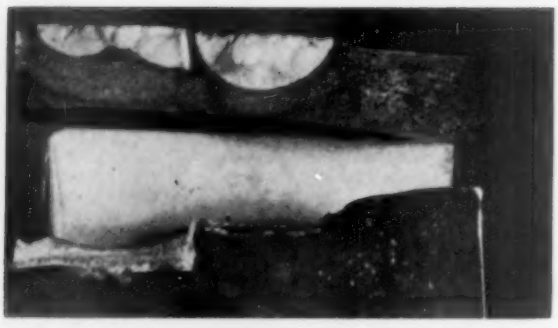

Q-3

Fig. 6 Typical failures of plain plate fatigue specimens

Fig. 7, the Q specimens exhibited very little scatter but had the lowest fatigue lives of the three low-alloy steels tested; generally, the fatigue lives of the T specimens lie between those of the Q and P specimens. These trends are also apparent in the fatigue strengths reported in Table 5. Using a value of $k = 0.18$, the average fatigue strengths of the longitudinal butt welds of steel P were 10 and 4% higher, respectively, than those of steels Q and T for $f_{100,000}$.

Fatigue data obtained from the 1953–54 series of longitudinal butt-welded joints in A-7 steel are also plotted with the results of the low-alloy steel tests in Fig. 7. The scatter bands of the A-7 specimens overlap those of the Q and T specimens and, in fact, the average fatigue strength of the A-7 steel welded with the E7016 electrode is almost as high as that of the Q steel. Accordingly, the average fatigue strengths of the longitudinal butt welds in low-alloy steel vary from 1 to 12% greater than those of the A-7 joints prepared with E7016 electrodes and 13 to 20% greater than those of the A-7 joints prepared with E6010 electrodes. Thus the use of the E7016 electrodes for the joints of A-7 steel made the advantage of the low-alloy steel negligible.

Fatigue Tests of Transverse Butt Welds

Table 6 presents the results of fatigue tests on the transverse butt-welded joints. These results are shown graphically in Fig. 9. In spite of the changes in the welding procedure [use of electrodes meeting military specification Mil-E-986-A (Mil 180), smaller diameter electrodes for the root passes, and a larger root opening], five of the six transverse butt welds of steel T failed internally from slag inclusions, or other flaws, in the weld metal. However, it was noted that fatigue cracks had also initiated at the edge of the weld of one of these specimens. One joint did fail at the edge of the weld, but after the specimen was pulled apart statically a small fatigue crack was also found in the weld metal.

For the Q specimens a higher interpass temperature was used. In spite of this fact and the more meticulous inspection of each pass for slag, one of the Q joints failed from an internal defect. Further, when the specimens were statically pulled apart, it was found that, of the two Q specimens failing at the edge of the weld, one had an internal defect visible in the fracture surface. Typical fracture surfaces of the transverse butt-welded joints are shown in Fig. 10.

The *S-N* diagram, Fig. 9, shows that the results of the tests of Q specimens did not have nearly as much scatter as those of the P and T specimens. However, the scatter bands of the three low-alloy steels overlap to a considerable extent so that there appears to be little, if any, advantage for any one of the steels. The same conclusion is apparent in the data included in Table 6. The T and Q joints had values of $f_{100,000}$ which were only 2% higher than those of the P joints.

The low-alloy steels had fatigue strengths which averaged about 12% higher than those of the previous tests of plain carbon steel when the latter specimens were welded with E6010 electrodes. However, when E7016 electrodes were used with the A-7 steel, the advantage of the A-242 joints was reduced to only 2 to 5%. This situation might be improved slightly by the use of techniques which would insure the elimination of failures in the weld metal. However, the occurrence of fatigue

Table 6—Results of Fatigue Tests of Transverse Butt-Welded Joints

Specimen	Stress, psi	Cycles to failure, 10^3	—Fatigue strength*— $f_{100,000}$, psi	$f_{2,000,000}$, psi
		A-7 Steel, E6010		
H12	29,400	537.9	36,600	24,800
H14	28,000	539.4	34,900	23,600
H22	26,000	802.2	...	23,100
H26	35,000	95.3	34,800	...
H32	26,300	984.0	...	24,000
H48	36,000	53.2	33,200	...
H54	25,000	1695.4	...	24,500
		Avg	34,900	24,000
		A-7 Steel, E7016		
H13	29,100	354.8	34,300	23,200
H17	39,000	117.8	39,800	...
H21	26,000	1097.0	...	24,000
H25	39,600	98.8	39,600	...
H31	24,200	1243.8	...	21,800
H65	25,700	3056.2	...	25,700+
		Avg	37,900	23,800+
		Steel P		
P5	37,000	73.5	35,700	...
P6	30,000	493.9	36,900	25,000
P7	29,000	556.5	36,300	24,500
P9	37,000	221.0	41,000	...
P10	36,900	349.0	43,300	29,400
		Avg	38,600	26,300
		Steel T		
T6	37,000	177.5	39,900	...
T7	37,000	113.8	37,500	...
T8	30,000	608.8	...	25,700
T9	37,000	331.2	43,200	29,300
T10	30,000	825.6	...	26,700
T11	30,000	507.1	37,000	25,100
		Avg	39,400	26,700
		Steel Q		
Q5	37,000	172.0	39,700	...
Q6	37,000	133.5	38,400	...
Q7	36,700	190.5	40,000	...
		Avg	39,400	

* $k = 0.13$.

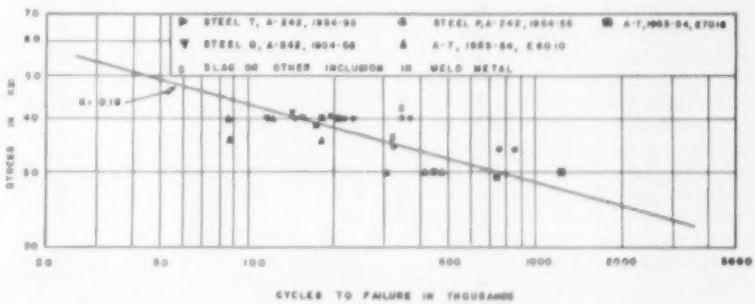

Fig. 7 Results of fatigue tests of longitudinal butt-welded joints tested in the as-welded condition

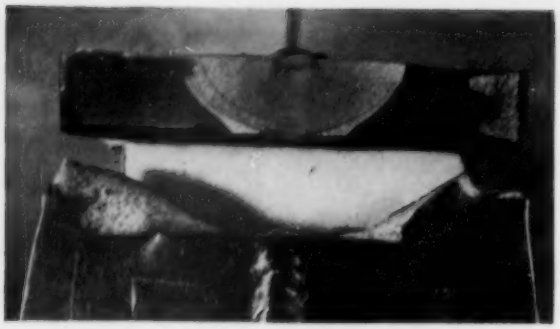

H-88

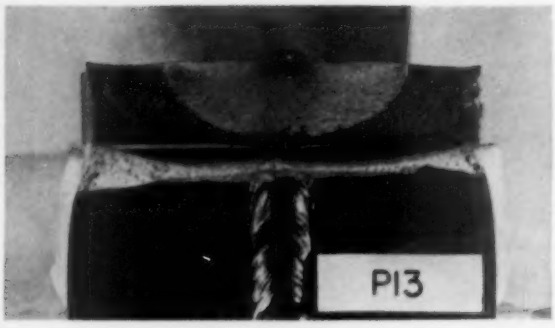

T-16

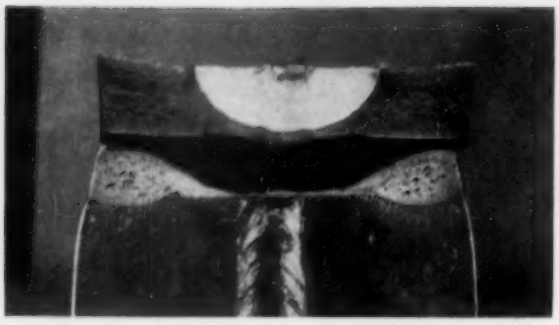

P-13

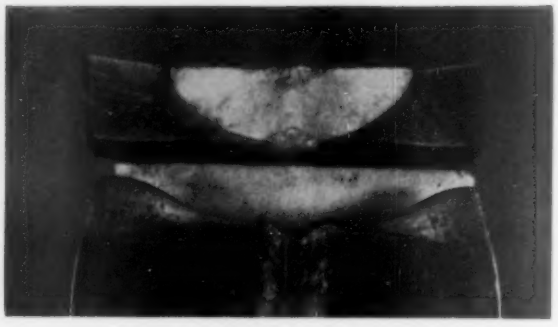

Q-9

Fig. 8 Typical fractures of longitudinal butt welds

cracks at the edge of one of the welds that failed from an internal defect, plus the fact that the specimens which failed at the edge of the weld had fatigue strengths not more than 5% greater than the joints which failed internally, makes it appear that only a negligible increase in fatigue strength would accompany the elimination of the internal failures unless such measures also improved the fatigue resistance at the edge of the weld.

It is apparent then that the A-7 transverse butt welded joints prepared with E7016 electrodes are practically as good as the joints fabricated from A-242 steel.

Fatigue Tests of Longitudinal Fillet-Welded Joints

Five of the longitudinal fillet-welded specimens, subjected to repeated loading, failed in the outside plates at the end of the weld as indicated in Fig. 11. The sixth specimen had a fatigue crack through the throat of one weld as well as a crack in the outside plate at the end of the weld on the opposite face of the specimen. However, it appears that the initial failure occurred in the plate. Four of these failures initiated in the plate from the crater end of a weld and two from the strike end.

The *S-N* diagram, Fig. 12, shows that the specimens tested on the higher stress cycle, 0–20,000 psi, exhibited negligible scatter whereas those tested with the lower stress cycle show a considerable amount of scatter. The fatigue strengths for failure at 100,000 cycles are given in Table 7.

It is difficult to make a direct comparison between the present results and those obtained in previous tests since the specimens are of different geometry. The data presented in Table 8 indicate that there were two series of tests, namely V and W, which gave extremely low values of fatigue strength. Study of the variables presented in this table reveals that these specimens differ from the others in several respects. The ratio of nominal stress in the weld to nominal stress in the plate is quite high. Also, the ratio of plate width to weld length is very high. Consequently any correlation of the fatigue strengths with nominal stresses is questionable.

It is likely that the geometry as well as the nominal stresses plays a very important role in joints of this type. More tests than are reported here are required to resolve fully this problem. However, on the basis of the available data it appears that the average fatigue strength of the low-alloy specimens may be slightly higher than would have been obtained from similar specimens of A-7 steel.

Fatigue Tests of Tee Fillet-Welded Joints

The fatigue cracks of the tee-fillet specimens occurred in the weld metal on a line approximately through, or slightly on the tee-plate side of, the throat of the weld. An examination of the fatigue cracks, after failure, and an examination of the fracture surfaces, after the specimens were pulled apart statically, indi-

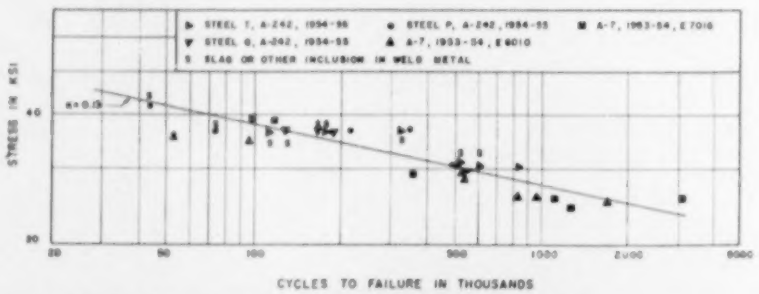

Fig. 9 Results of fatigue tests of transverse butt-welded joints

cated that most of the fatigue failures did not initiate at the ends of the weld. It is difficult to determine the point of origin of the failure in a fillet weld as the fatigue failures generally spread along the length of the weld with little indication as to the sequence of failure. Typical fatigue cracks and fracture surfaces shown in Fig. 14 indicate that the fracture surface consisted of two distinct regions; a fairly smooth, planar, surface having an angle less than 45° from the tee plate and a rough fibrous appearing surface having an angle greater than 45° from the tee plate.

In no case does the smooth portion, the region of initial fatigue fracture, extend to the surface of the weld. The rougher portion must, therefore, contain the final stages of the fatigue failure as well as the static fracture. From the similarity of the static region with part of the fatigue region, it would seem that the rate of propagation of the fatigue fracture increased when the plane of failure changed.

In the tests of A-7 steel, it was noted that many of the welds which failed in fatigue also separated slightly from the longitudinal plate. This phenomenon was especially noticeable after the welds had been pulled apart statically. However, no such separation was noted in any of the tests in the low-alloy steel. The absence of the separation in the present tests could be due to the fact that the mill scale had been removed from the longitudinal plate in the region of the weld whereas it was not in the tests of A-7 steel.

The values of stress, reported in Table 9 and Fig. 13, have been computed from the external area. As may be seen from the *S-N* diagram, both series exhibited a considerable amount of scatter.

The fatigue strengths have been computed from the test data using a value of $k = 0.25$, selected from previous tests. The average fatigue strength for failure at 2,000,000 cycles is the same for both steels but the fatigue strength for failure at 100,000 cycles is 500 psi greater for the welds in A-7 steel. It would appear that the fatigue properties of welds made with the E7016 electrode are approximately the same in either steel.

Conclusions

The following conclusions are based on the results of the experimental program discussed herein.

1. For all types of specimens tested there was little difference in the fatigue strengths of the several low-alloy steels, although the results of steel Q generally exhibited less scatter than those of steel P and T.

2. For failure at 100,000 cycles

Table 7—Results of Fatigue Tests of Longitudinal Fillet-Welded Joints

Specimen	Stress, psi	Cycles to failure, 10^3	Fatigue strength* $f_{100,000}$, psi	Fatigue strength* $f_{2,000,000}$, psi
		Steel P		
P26	20,000	175.6	23,400	...
P27	14,500	1018.3	27,800	12,000
P28	14,000	298.4	19,000	...
P29	20,000	162.8	22,900	...
P30	14,000	225.6	17,600	...
P32	20,000	185.9	23,600	...
		Avg	22,400	

* $k = 0.28$.

Table 8—Average Results of Past and Present Fatigue Tests of Longitudinal Fillet-Welded Joints Tested on a Zero to Tension Stress Cycle and Failing in the Plates

Series	Electrode	Plate width, in.	Weld length, in.	A_w Area of weld metal in.^{2}	A_{pl} Area of plate in.^{2}	$\frac{S_w}{S_{pl}}$[a]	$f_{100,000}$[b]
			A-242 Steel				
P, 1954–55[c]	E7016	5	8	7.07	7.50	1.062	22,400
			A-7 Steel				
1953–54[c]	E6010	6	7	6.19	4.50	0.728	21,500
1953–54[c]	E7016	6	7	6.19	4.50	0.728	22,700
T, Bull. 350	[d]	4	4	4.24	3.00	0.707	21,000
U, Bull. 350	[d]	6	4	4.24	4.50	1.063	20,100
V, Bull. 350	[d]	9	4	4.24	6.75	1.58	14,200
W, Bull. 350	[d]	9	4	4.24	6.75	1.58	15,300
EZ, Bull. 350	[d]	9	10½	11.13	6.75	0.690	21,600
Z, Bull. 350	[d]	9	10	10.60	6.75	0.636	18,900

[a] $\frac{S_w}{S_{pl}} = \frac{A_{pl}}{A_w}$.
[b] $k = 0.28$.
[c] See Bibliography, Reference 5.
[d] Electrode not specified.

Table 9—Results of Fatigue Tests of Tee Fillet-Welded Joints Welded with E7016 Electrodes

Specimen	Stress, psi	Cycles to failure, 10^3	Fatigue strength* $f_{100,000}$, psi	Fatigue strength* $f_{2,000,000}$, psi
		A-7 Steel		
H34	14,900	400.4	21,100	10,000
H36	20,000	280.3	25,900	...
H38	20,100	243.9	25,100	...
H66	20,000	175.4	23,000	...
H68	14,800	538.1	22,600	10,600
H80	11,900	1837.1	...	11,600
H82	20,000	780.4	...	15,700
H84	13,100	4665.3	...	13,100
H86	12,000	4319.4	...	12,000
		Avg	23,500	12,200
		Steel P		
P19	13,900	668.1	...	10,600
P20	13,000	2568.3	...	13,000+
P21	13,000	1758.2	...	12,600
P22	20,000	330.2	27,000	12,800
P32	20,000	183.1	23,300	...
P24	20,000	75.2	18,600	...
		Avg	23,000	12,300+

* $k = 0.25$.

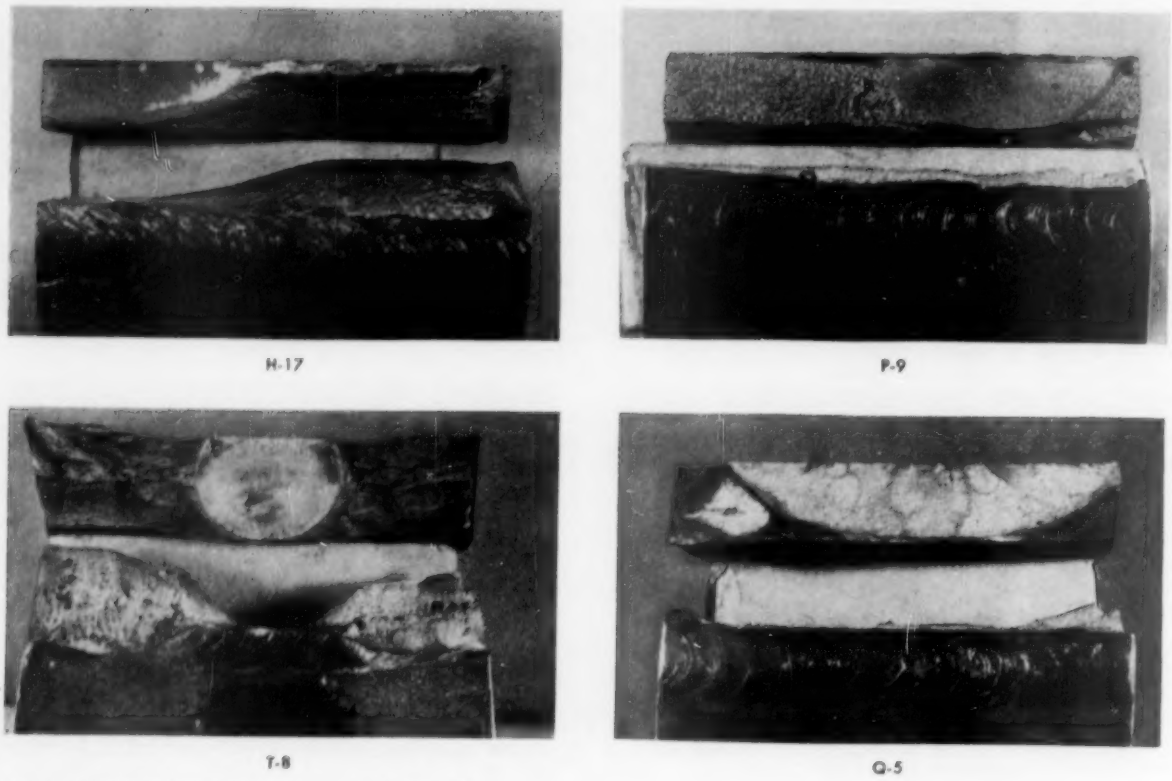

Fig. 10 Typical fractures of transverse butt welds

plain-plate specimens of the low-alloy steels exhibited an increase in fatigue strength over that of the A-7 steel of from 10 to 25%. The yield strength was, however, from 45 to 75% higher for the low-alloy steels.

3. The average fatigue strength of longitudinal butt-welded joints in the low-alloy steels were from 13 to 20% higher than those of A-7 joints prepared with the standard E6010 electrode. The use of the E7016 electrode for the

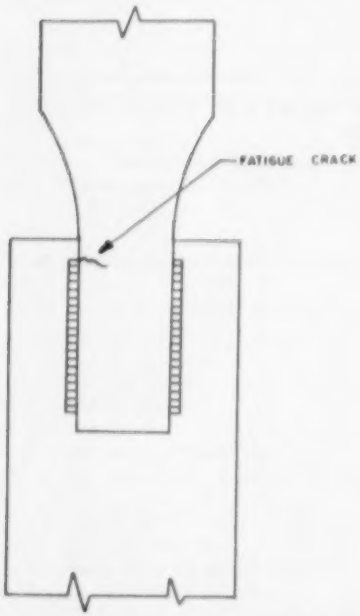

Fig. 11 Sketch of location of fatigue failure in longitudinal fillet-welded joints

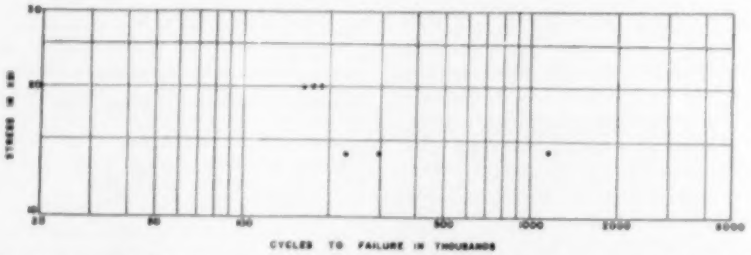

Fig. 12 Results of fatigue tests of longitudinal fillet-welded joints, Steel P, A-242

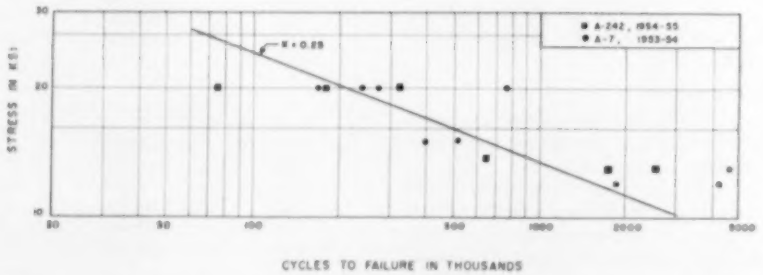

Fig. 13 Results of fatigue tests of tee fillet-welded joints welded with E7016 electrodes

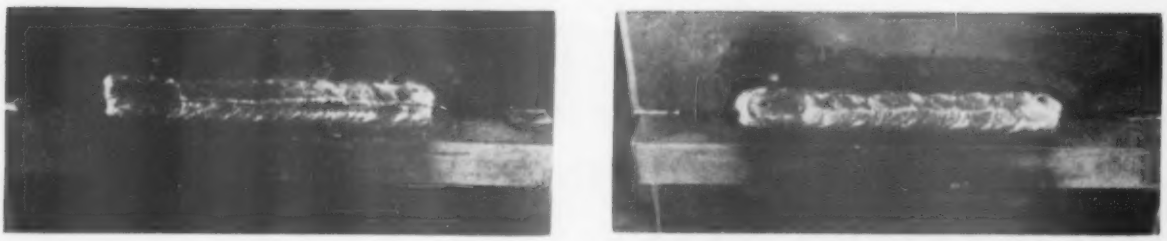

P-20 P-19

(a) Fatigue cracks

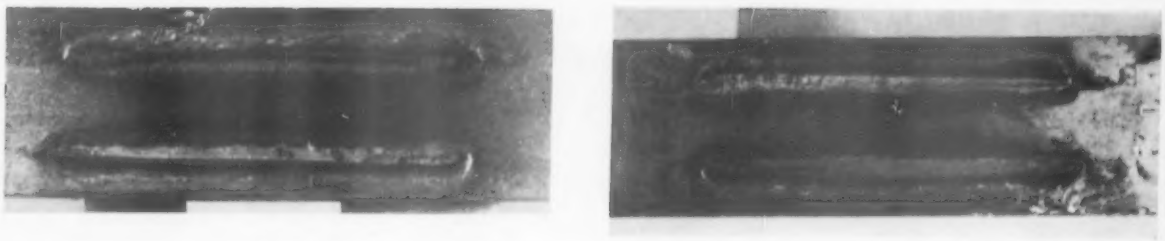

P-20 P-21

(b) Fracture surfaces

Fig. 14 Fatigue failures of tee fillet-welded joints

A-7 joints reduced the advantage of the low-alloy specimens to less than 10%.

4. For transverse butt-welded joints the advantage of the A-242 specimens was about 10% when the A-7 joints were welded with E6010 electrodes but less than 5% when E7016 electrodes were used for the A-7 joints.

5. The tests of the tee fillet specimens showed that the E7016 electrode produced weld metal having approximately the same fatigue strength when used for fillet welds in either A-7 or low-alloy steels.

Acknowledgments

The program reported herein is part of a cooperative research project conducted in the Engineering Experiment Station of the University of Illinois, Department of Civil Engineering, and sponsored by the Ohio River Division Laboratories, Corps of Engineers, U. S. Army. The work constitutes a part of the structural research program of the Department of Civil Engineering under the general direction of N. M. Newmark, Research Professor of Structural Engineering, and W. H. Munse, Research Professor of Civil Engineering.

The authors wish to acknowledge the help of L. A. Harris, former Research Associate in Civil Engineering, and Z. A. Shoukry who assisted in the laboratory work and in the compilation of the results of the past fatigue tests.

The members of the Fatigue Committee of the Welding Research Council acted in an advisory capacity in the planning of this program.

Bibliography

1. Wilson, W. M., and Thomas, F. P., "Fatigue Tests of Riveted Joints," University of Illinois Engineering Experiment Station, Bulletin Series No. 302, May 1938.

2. Wilson, W. M., Bruckner, W. H., Coombe, J. V., and Wilde, R. A., "Fatigue Tests of Welded Joints in Structural Steel Plates," University of Illinois Engineering Experiment Station, Bulletin Series No. 327, February 1941.

3. Wilson, W. M., Bruckner, W. H., Duberg, J. E., and Beede, H. C., "Fatigue Strength of Fillet-Weld and Plug-Weld Connections in Steel Structural Members," University of Illinois Engineering Experiment Station, Bulletin Series No. 350, March 1944.

4. Harris, L. A., Nordmark, G. E., and Newmark, N. M., "Fatigue Strength of Butt Welds in Structural Steels," THE WELDING JOURNAL, Research Suppl., XX, 83-s–96-s (1954).

5. Nordmark, G. E., and Harris, L. A., "Fatigue and static Tests of Fillet Welds," Report to the Ohio River Division Laboratories, Corps of Engineers, U. S. Army, Contract DA-33-017-eng-221, Civil Engineering Studies, Structural Research Series No. 82, University of Illinois, August 1954.

6. Nordmark, G. E., Stallmeyer, J. E., and Munse, W. H., "Fatigue and Static Properties of Welded Joints in Low Alloy Structural Steels," Report to the Ohio River Division Laboratories, Corps of Engineers, U. S. Army, Contract DA-33-017-eng-255, Civil Engineering Studies, Structural Research Series No. 90, University of Illinois, January 1955.

RESEARCH NEWS

(*Continued from page 297-s*)

directly into amount of carbon originally contained in the steel being tested.

Industrial Image Intensifier

A new 3-page bulletin that gives engineering data on industrial applications of a new Norelco industrial image intensifier is available from the Research & Control Instruments Division, North American Philips Co., Inc., 750 S. Fulton Ave., Mount Vernon, N. Y.

Text deals with fluoroscopic X-ray examination of steel and other metals with high density and absorption characteristics. Typical work is done in daylight using 80 kvp for 1/8 in. of steel and 150 kvp for 7/8 in. of steel with a focal spot size of 0.4 mm, constant potential.

The bulletin includes a curve showing penetrameter-sensitivity plotted against material thickness. Photos are included which show fluoroscopic detail obtained on a defective bearing block and on a faulty welded seam. Another illustration shows layout of an actual installation where electronic fluoroscopy is employed for continuous inspection of 1/2-in. steel welded pipe at 2 ips.

ALUMINUM AND ALUMINUM ALLOYS FOR PRESSURE VESSELS

Condensed version of an interpretive report prepared for the Materials Division of the Pressure Vessel Research Committee

BY MARSHALL HOLT

SYNOPSIS. This paper reviews the properties of the aluminum alloys that are especially desirable for pressure vessels and certain chemical and processing equipment. Aluminum alloys are resistant to the chemical action of many materials and, for those materials where there is some action, the resulting products are colorless; hence, they produce no discoloration. They also show remarkable resistance to atmospheric corrosion. Aluminum alloys are nonmagnetic and nonsparking. Conductivity ratings for heat and for electricity are relatively high. Commercially available alloys suitable for pressure vessels represent a wide range of tensile strength. Ten of the alloys in the form of plates covered by ASTM Specification B178-54T have specified tensile strengths in the annealed condition ranging from 9500 to 30,000 psi. Aluminum alloys do not show a decrease in ductility with depressed temperatures as does mild steel; in fact, the tensile strength, yield strength, elongation and impact resistance of most of the alloys discussed show a distinct increase as the temperature decreases to −420° F. They are readily workable and easily welded. The service record of aluminum alloys is outstandingly satisfactory. The leading producers have, as a result of many years of experimentation and experience, published much data and prepared handbooks that may be consulted for answers to specific questions.

I. Characteristics of Materials Available

The aluminum alloys described in Tables 1 and 2 possess properties and characteristics that make them suitable for the construction of pressure vessels and certain chemical and processing equipment. Alloy GS11A (6061)* and some of the cast alloys are susceptible to tempering by heat treatment. The other wrought alloys are tempered by cold working and the other casting alloys are used in the as-cast condition.

Marshall Holt is Assistant Chief, Engineering Design Division, Alcoa Research Laboratories, Aluminum Company of America, New Kensington, Pa.

The complete report is published as Bull. No. 28 in the Bulletin Series of the Welding Research Council, New York, N. Y.

The tensile strengths for the nonheat-treatable wrought alloys in the annealed condition range from 9500 to 30,000 psi.

The metal producers can give valuable assistance in the selection of a suitable alloy. This is particularly true regarding the use of Alloy GR40A (5154) for applications in which the metal will be held for a long period at temperatures near 212° F.

Since all the alloys contain relatively small amounts of alloying elements, the specific gravities, electrical and thermal conductivities and melting points are nearly the same. The specific gravity is approximately 2.7 or about one-third that of steel; the coefficient of thermal expansion is about 0.000013 or about two times that of steel. The melting points range from about 960 to 1205° F, and it should be noted that there is no change of atomic arrangement or color, such as displayed by mild steel, as the temperature is increased. The modulus of elasticity is about 10,000,000 psi or about one-third that of mild steel. The value of Poisson's ratio is about one-third, hence the modulus of rigidity is about 3,800,000 psi.

All the alloys under consideration possess a high resistance to action by most chemicals and to atmospheric corrosion. Because of the many types of commodities to be processed or stored, differences in purity and other factors, it is not practicable to present exact rules for applying aluminum alloys to the manufacture of pressure vessels and processing equipment; much specific information can be found in Aluminum Alloy Reference Sheets 28 to 33, inclusive, published by Chemical Engineering Progress.[1]

The resistance of some alloys to localized type of attack can be increased by metallurgically bonding a cladding having a solution potential higher than that of the base alloy. The compatibility with certain chemicals can sometimes be increased by special control of trace elements that are considered to be normal impurities. Alloys with these characteristics are obtained through special arrangements with the metal producer.

Electrical contact with most heavy metals or contact with fluids containing heavy-metal compounds or finely divided metal in suspension can produce galvanic corrosion of aluminum in the presence of an electrolyte. If the use of parts made of dissimilar metals cannot be avoided, the use of bushings or nipples of nonmetallic materials or aluminum protector sections or galvanized inserts may be helpful.

Fatigue data on welded butt joints are given in Fig. 1. The strengths of lap joints and butt joints with a single splice plate are inferior to those of butt joints.[2] The fatigue strength of sand cast SC51A-T6 (355-T6) at 10^8 cycles is about the same as that for the butt joints shown in Fig. 1.

In giving Charpy impact values for some of the alloys listed in Table 1, attention is called to Paragraph 2(a) of Reference 3, which says, in part, "This test was developed for the common steels and is of little significance for other metals." Reference 4, in quoting from a large number of sources, gives impact values as follows:

Alloy	*Charpy value, ft-lb*
M1A(3003)	13.5–36
GS11A-T6(6061-T6)	5.5–11
990-H16(1100-H16)	28
GR20A-F(5052-F)	25–28
MG11A-F(3004-F)	17
C4A-T6(195-T6)	2
SG70A-T6(356-T6)	1

One of the conclusions in this reference

* The ASTM designation is followed by that of The Aluminum Association in parentheses.

Table 1—Nominal Composition of Aluminum Alloys Commonly Used in Pressure Vessels and Storage Tanks

Alloy — Commercial — ASTM	Old	New*	Alloying Elements, % (Aluminum and Normal Impurities Constitute Remainder) Copper	Silicon	Manganese	Magnesium	Chromium	Titanium	Remarks (see Note)
Wrought									
996A†	CD1S	1160†							§
990A‡	2S	1100‡							§
M1A	3S	3003			1.2				§
MG11A	4S	3004			1.2	1.0			§
G1A	50S	5050				1.2			§
GS11A	61S	6061	0.25	0.6		1.0	0.25		§
GR20A	52S	5052				2.5	0.25		§
GR40A	A54S	5154				3.5	0.25	0.15	§
Cast									
C4A	19S		4.5	0.8					
GS42A	B214			1.8		3.8			
S5A	4S			5.0					
SC51A	35S		1.3	5.0		0.5			
SG70A	35S			7.0		0.3			

NOTE: Heat-treatment symbols have been omitted since composition does not vary for different heat-treatment practices.
The Alclad form consists of a core of the basic alloy and a coating of pure aluminum or a suitable alloy.
* The new commercial designations for wrought products were adopted by the Aluminum Association to become effective Oct. 1, 1954.
† 99.6% (minimum) aluminum.
‡ 99.0% (minimum) aluminum.
§ Accepted for use in ASME Code Vessels.

is that "notch sensitivity of aluminum alloys, as measured by the usual types of so-called impact tests is not adversely affected by low temperature."

The creep and stress-rupture data available indicate that, at the design stresses generally used for aluminum alloy pressure vessels, creep needs no special consideration. A few failures have been reported from this type of action where vessels have been seriously overloaded with respect to temperature and pressure. Some creep and stress-rupture data are published in Reference 5.

II. Design Rules and Problems

Design rules for pressure vessels, chemical equipment, tanks and piping have been prepared by a number of code-writing bodies, including:

1. Boiler and Pressure Vessel Code Committee of the American Society of Mechanical Engineers, Section VIII, Unfired Pressure Vessels;[6] Section IX, Welding Qualifications[7]
2. American Petroleum Institute[8]
3. American Standards Association[9]
4. Association of American Railroads[10]
5. Interstate Commerce Commission[11]

Aluminum alloy coverage differs for the specifications of these various bodies, but, in general, work is in progress to increase the coverage in every instance.

Design rules that have been developed to solve the problems of structural mechanics relating to pressure vessels are applicable, in general, to aluminum as well as to other structural materials; however, the constants relating to the mechanical properties must be given due consideration. The buckling problems of various types are encountered more frequently in the design of aluminum alloy structures than in the design of mild-steel structures, because the modulus of elasticity of the aluminum alloys is about one-third as great as that of steel. Thus, in the range of elastic stresses, the buckling strength of an aluminum alloy structure is only one-third that of a mild-steel structure of the same dimensions. However, the elastic deformations and deflections for a given set of loading conditions are three times as great in aluminum structures as in steel structures of the same dimensions.

The difference in the deflections of aluminum structures and similar ones of other common materials can be diminished by making the aluminum parts thicker. For example, in the case of simple beams of rectangular cross section, the deflection of steel and aluminum members will be equal if the thickness of the aluminum member is 1.44 times that of the steel member. Even with this added thickness, the aluminum member will weigh only about 50% as much as the steel member.

The design charts for vessels of various materials under external pressure given in Section VIII[6] of the ASME Code were all developed by the same rules, but the charts cannot be used indiscriminately because each one

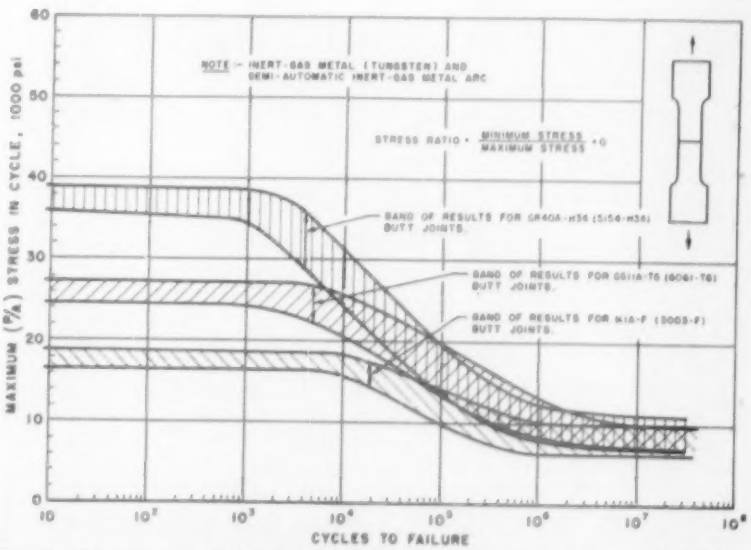

Fig. 1 Comparison of direct-stress fatigue test results for arc-welded 3/8-in. thick aluminum alloy plate

Table 2—Minimum Mechanical Properties* of Aluminum Alloys Suitable for Use in Pressure Vessels and Storage Tanks

In those cases in which the specified values vary with the thickness of plate or size of product, the value for 0.5-in.-thick product or 4-in. Schedule 40 pipe is given

Alloy ASTM	Alloy Commercial Old	Alloy Commercial New	Temper**	Tensile Strength psi	Yield Strength 0.2% Offset psi	Elong. %	Shear Strength psi	Shear Yield Strength psi	Specification Tensile Properties	Notes
WROUGHT ALLOYS										
990A	CD1S	1160	O	9 500	2 500	25	6 500	1 500	ASTM B178+	(1)
			H12	11 000	9 000	12	7 500	5 000		
			H14	12 000	10 000	10	8 000	6 000		
			H112	12 000	7 000	10	8 000	4 000		
990A	2S	1100	O	11 000	3 500	28	8 000	2 000	ASTM B178+	(2)
			H12	14 000	11 000	9	9 000	6 500		
			H14	16 000	14 000	6	10 000	9 000		
			H112	13 000	7 000	9	8 500	4 000		
M1A	3S	3003	O	14 000	5 000	23	10 000	3 000	ASTM B178+	(1)(3)(4)
			H12	17 000	12 000	7	11 000	7 000		
			H14	20 000	17 000	6	13 000	10 000		
			H112	17 000	10 000	8	11 000	6 000		
Clad M1A	Alclad 3S	Clad 3003	O	13 000	4 500	23	9 000	2 500	ASTM B178+	(1) (3)
			H12	16 000	11 000	7	10 000	6 500		
			H14	19 000	16 000	6	12 000	9 000		
			H112	16 000	9 000	8	10 000	5 000		
M11A	4S	3004	O	23 000	8 500	16	14 000	5 000	ASTM B178+	(1)
			H32	28 000	21 000	6	15 000	12 000		
			H34	32 000	25 000	5	17 000	14 000		
			H112	23 000	9 000	7	14 000	5 000		
Clad M11A	Alclad 4S	Clad 3004	O	22 000	8 000	16	14 000	4 500	ASTM B178+	
			H32	27 000	20 000	6	15 000	11 000		
			H34	31 000	24 000	5	16 000	14 000		
			H112	22 000	8 500	7	14 000	5 000		
G1A	50S	5050	O	18 000	6 000	20	12 000	3 500	ASTM B178+	(1)
			H32	22 000	16 000	6	14 000	9 000		
			H34	25 000	20 000	5	15 000	11 000		
			H112	20 000	8 000	12	13 000	4 500		
GS11A	61S	6061	T4	30 000	16 000	18	20 000	9 000	ASTM B178+	(1) (4)
			T6	42 000	35 000	10	27 000	20 000		
GR20A	52S	5052	O	25 000	9 500	18	16 000	5 500	ASTM B178+	(1)
			H32	31 000	23 000	9	19 000	13 000		
			H34	34 000	26 000	10	20 000	15 000		
			H112	28 000	16 000	7	16 000	9 000		
GR40A	A54S	5154	O	30 000	11 000	18	18 000	8 000	ASTM B178+	
			H32	36 000	26 000	12	22 000	15 000		
			H34	39 000	29 000	10	23 000	16 000		
			H112	32 000	18 000	8	18 000	8 000		
CAST ALLOYS										
C4A	19S	----	T4	29 000	13 000	6	22 000	----	ASTM B26-52T	(5)
			T6	32 000	20 000	3	24 000	----		
GS42A	B214	----	F	17 000	10 000	(a)	13 000	----	ASTM B26-52T	(5)
S5A	43	----	F	17 000	6 000	3	12 000	----	----	
SC51A	355	----	T51	25 000	18 000	(a)	19 000	----	ASTM B26-52T	(5)
			T6	32 000	20 000	2	24 000	----		
			T71	30 000	22 000	(a)	21 000	----		
SG70A	356	----	T51	23 000	16 000	(a)	17 000	----	ASTM B26-52T	(5)
			T6	30 000	20 000	3	25 000	----		
-----	XA356	----	T6	32 000	18 000	10	25 000	----	----	(6)
			T61	37 000	26 000	5	27 000	----		

* Tensile strength, yield strength and elongation are specification values, the other values would be expected for material just meeting these requirements.

** See ASTM Tentative Recommended Practice B296.

\+ See also ASME SB specification.

(a) Determination of elongation not required.

NOTES: (1) Values given are for plate, see ASTM B274 for pipe and tube. (2) Values given are for plate, see ASTM B247 for die forgings. (3) Values given are for plate, see ASTM B234 for drawn seamless tubes for condensers and heat exchangers. (4) Values given are for plate, see ASTM B273 for bars, rods and shapes. (5)Values given are for sand castings, see ASTM B108 for permanent mold castings. (6) Minor variation of SG70A, values given are tentative for permanent mold castings.

Table 3—Guide to the Selection of the Filler Metal for Welding Aluminum and Aluminum-Alloy Tanks and Vessels

Classification of filler metal		*Classification of base metal*			
		Base metal to itself		*Combination of base metals*	
ASTM-AWS	*Al Assn.*	*ASTM*	*Al Assn.*	*ASTM*	*Al Assn.*
R-996A E-996A	1160	996A	1160	...	...
R-990A E-990A	1100	990A M1A* G1A	1100 3003* 5050	990A-M1A*	1100–3003
R-G1A E-G1A	5050	M1A* G1A	3003* 5050	...	...
R-GM50A E-GM50A	5356	MG11A* GR20A GS11A GS42A	3004* 5052 6061 B214†	...	...
R-GR20A E-GR20A	5052	MG11A* GR20A	3004* 5052	...	...
R-GR40A E-GR40A	5154	MG11A* GR20A GR40A GS11A GS42A	3004* 5052 5154 6061 B214†	GR40A-GS11A	5154–6061
R-MG11A E-MG11A	3004	MG11A*	3004*	...	...
R-S5B E-S5B	4043	M1A* MG11A* G1A GR20A GS11A	3003* 3004* 5050 5052 6061	990A-M1A* M1A*-GR20A M1A*-GS11A	1100–3003* 3003*-5052 3003*-GS11A

* Clad products also.

† Commercial designation, no designation assigned by Al. Assn.

is based on the individual characteristics of a certain material or alloy.

In order to avoid the use of excessively thick aluminum flanges, steel backing rings may be used. An extreme application of this principle is an aluminum flange of the Van Stone type with a steel bolting ring.

The arrangement of supports for horizontal cylindrical shells is a compromise. To take advantage of the circumferential stiffness offered by the heads, the supports should be near the ends; but to decrease the shear stresses and longitudinal bending stresses in the shell, and thus reduce the possibility of failure caused by them, the supports should be about 22% of the length from the ends. The critical shear buckling stress for thin-walled circular cylindrical shells can be computed by formulas given in handbooks prepared by the principal material producers. The critical stresses for cylindrical shells subject to bending can be determined by the proposed new rules in Paragraph UG-23.[12]

The selection of either the design stresses or the factor of safety should involve consideration of the design procedures, manufacturing techniques and the uncertainties of operation of the equipment. The allowable stress values for the aluminum alloys in Table UNF-23[6] were determined as the smaller of two-thirds of the yield strength and one-fourth of the tensile strength in accordance with the rules in Paragraph UA-602 of the same reference. On the other hand, the allowable stress values in the AAR Specifications[10] are equal to the specified tensile strengths of the materials, the principle being that the tank will burst when the pressure reaches the design value, which is considerably larger than any reasonable operating pressure.

The yield strength of the aluminum alloys is less significant in determining the behavior of a structure than is the yield point of mild steel. This is because the yield strength of the aluminum alloys is an arbitrary point on a stress-strain curve that departs gradually from the initial straight line, whereas the yield point of mild steel represents a stress at which a strain of several percent can occur at no increase in stress. Although development of a stress equal to the yield strength of an aluminum alloy is accompanied by some permanent set, the distortion of the part is usually insignificant. Aluminum alloys work harden, and repetition of a loading that causes some permanent set will not be accompanied by another equal increment of permanent set. In other words, the material behaves elastically over a wider stress range for the second and subsequent loadings. The selection of design stresses for welded structures might also be influenced by the joint efficiency factor, or weld factor, used. For aluminum alloys in the annealed condition, the strength of a welded butt joint is usually equal to the strength of the parent plate. In fact, for all the wrought alloys listed in Table 2 except Alloy GS11A, Section IX of the ASME Code[7] requires a joint strength equal to the specified strength of the alloy in the annealed condition. For tempered material, either cold worked or heat treated, the strength of a welded butt joint may be less than that of the parent material, the difference being dependent

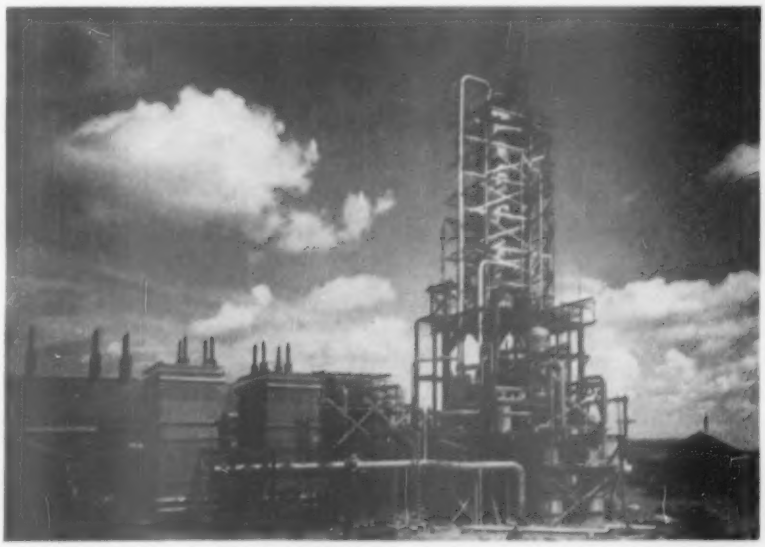

Fig. 2 Tonnage oxygen plant utilizing extensive applications of aluminum in pressure vessels and pipe fittings

Fig. 3 Aluminum test vessel employed in bursting tests

Fig. 4 Aluminum alloy tanks under construction

on the amount of heat introduced by the welding process and the length of time the material is at high temperatures. This variable is taken care of in most codes by basing design stresses on the properties of annealed material regardless of the initial temper of the material.

Although there are ASTM specifications for casting alloys,[12] none of the code-writing bodies has adopted design rules for cast parts. As noted in Table 2, the specified elongations in the tensile test are relatively low and in some cases the determination of the elongation is not required. Nevertheless, castings have been eminently successful in many applications where ductility might normally be considered an important property, such as housings, bus and aircraft wheels, commercial food handling and processing equipment, pipe fittings, pump bodies and water-cooled cylinder blocks.

III. Fabrication Processes

In general, tools for machining aluminum should have appreciably more side and top rake than are required for cutting steel; in fact, their shapes approximate more closely those used with hard woods. Lathe tools are set considerably higher on the work than is the general practice with steel. Oxygen cutting of the aluminum alloys cannot be accomplished by any of the conventional methods used on ferrous materials, and powder cutting methods have not been found suitable. A tungsten-arc cutting process using an argon-hydrogen atmosphere has recently been developed with which smooth edges and accurate dimensions can be obtained. Band saws with relatively coarse teeth and running at rather high speeds give best results for cutting.

Aluminum in the annealed condition is one of the most workable of the common metals. Except for the heat-treatable alloys, the tempering operation introduces cold work, so the degree to which forming and other operations can be carried decreases as the tempering increases.

For vessel parts involving the forming of nonheat-treatable alloys, generally the temper can be selected so that the forming operation can be completed without recourse to intermediate annealing operations. When intermediate annealing is required, the recommended treatment consists in bringing the metal to a temperature of 650° F*; the rate of cooling is not important.

Parts of Alloy GS11A in the annealed condition (for maximum formability) can be heat treated after forming.

The handbooks of the metal producers contain data that can be used as a guide in the choice of temper and forming radii.

It is important to keep machine parts that contact the aluminum clean and free of rust, scale, chips and imperfections that might mar or scratch the finished work. It is also important to avoid "heavy metal" contaminations, which might lead to serious localized corrosion.

Aluminum is drawn on the same type of equipment that is used for other metals. The tools should be so designed that the thickness changes very little during the drawing operation.

The process used for spinning aluminum does not differ essentially from that used for copper and brass, except that higher speeds are used.

Alloys listed in Tables 1 and 2 can be welded by a number of processes. Experience has shown that the combinations of filler and base alloys listed in Table 3 can be readily welded and that they give satisfactory service. The inert-gas processes have these distinct advantages: (1) no flux is required, (2) overhead welding is feasible, (3) the weld beads are relatively smooth and (4) the distortion produced by the welding heat is rather small. The principal metal producers will furnish specific information on current requirements and size of filler wire and will assist in training welders.

There have been many successful applications of aluminum in pressure vessels, chemical and oxygen-plant equipment, tank cars, highway-truck tanks, storage tanks and pipe fittings. Figures 2, 3 and 4 illustrate pressure-vessel and chemical plant applications.

* 775° F is recommended for Alloy M1A (3003) bare or clad.

Bibliography

1. Fritts, Harry W., "Aluminum Alloy Reference Sheets Nos. 28 to 33 incl.," *Chem. Engrg. Prog.*, **49** (12), 675 (1953); **50** (1), 54 (1954); **50** (2), 108 (1954); **50** (3), 146 (1954); **50** (4), 214 (1954); **50** (5), 272 (1954).

2. Hartmann, E. C., Holt, Marshall, and Zamboky, A. N., "Static and Fatigue Tests of Arc-Welded Aluminum Alloy 618-T Plate," THE WELDING JOURNAL, Research Suppl., **26** (3), 129-s to 138-s (1947).

3. Anon., "Tentative Methods of Impact Testing of Metallic Materials," ASTM, Book of Standards, Part 2, pp. 1248–1262 (1952).

4. Bogardus, K. O., Stickley, G. W., and Howell, F. M., "A Review of Information on the Mechanical Properties of Aluminum Alloys at Low Temperatures," National Advisory Committee for Aeronautics, Tech. Note No. 2082 (May 1950).

5. Dorn, J. E., and Tietz, T. E., "Creep and Stress-Rupture Investigations on Some Aluminum Alloy Sheet Metals," *Proc. ASTM*, **49**, 815–831 (1949).

Sherby, O. D., and Dorn, J. E., "The Creep Properties of Several Cold-Rolled Aluminum Alloy Sheet Metals," *Trans. ASM*, **43**, 611–634 (1951); also "The Creep Properties of Two Tempers of 63S Extruded Aluminum Alloys (63S-T5 and 63S-T6), *Proc. ASTM*, **51**, 945–953 (1951); also "Effect of Annealing on the Creep Properties of 2S-O Aluminum Alloy," *Ibid.*, **51**, 954–963 (1951).

6. Anon., "Unfired Pressure Vessels," ASME Boiler and Pressure Vessel Code, Section VIII (1952).

7. Anon., "Welding Qualifications," ASME Boiler and Pressure Vessel Code, Section IX (1953).

8. Anon., "Specification for Welded Oil Storage Tanks, Appendix F. Recommended Practice for Use of Aluminum Alloys in Construction of Tank Roofs and Top Shell Rings," API Standard 12C, Twelfth Edition (1954).

9. Anon., "American Standard Code for Pressure Piping, ASA B31.1-1951," *ASME* (1951).

10. Anon., *Manual of Recommended Practices*, Assn. Am. Railways.

11. Anon., "Interstate Commerce Commission Regulations for Shipping Containers," H. A. Campbell's Tariff No. 9 (May 12, 1954).

12. Anon., "Proposed Revisions and Addenda to Boiler and Pressure Vessel Code," *Mech. Engrg.*, **76** (12), 1039 (1954).

13. Anon., "Specifications for Aluminum-Base Alloy Sand Castings, B26," and "Specifications for Aluminum-Base Alloy Permanent-Mold Castings, B108," *ASTM*, Book of Standards, Part 2, 521–526 and 550–555 (1952).